IDENTIFICATION AND CHARACTERIZATION OF BIOACTIVE COMPOUND FROM FLAX MICROGREENS AND EVALUATION OF ITS PROTECTIVE EFFECT AGAINST TESTOSTERONE-INDUCED PROSTATE CANCER

Thesis submitted for the award of the degree of

DOCTOR OF PHILOSOPHY

in

Biochemistry

By

MUDASSIR LAWAL

Registration Number: 12204618

Supervised by

Dr. Gurmeen Rakhra (25169)

Department of Biochemistry, Bioengineering and Biosciences, Lovely Professional University, Punjab.

Co-supervised by

Dr. (Prof.) Vetriselvan Subramaniyan

Department of Medical Sciences, School of Medical and Life Sciences Sunway University, Malaysia.

Co-supervised by

Dr. (Prof.) Neeta Raj Sharma

HOS, Bioengineering and Biosciences, Lovely Professional University, Punjab.



Transforming Education Transforming India

LOVELY PROFESSIONAL UNIVERSITY PUNJAB

2025

DEDICATION

This thesis is dedicated to my beloved parent & entire family

DECLARATION

I, Mudassir Lawal hereby declared that the presented work in the thesis entitled —"Identification

and Characterization of Bioactive Compound from Flax Microgreens and Evaluation of its

Protective Effect against Testosterone-induced Prostate Cancer" in fulfilment of degree of

Doctor of Philosophy (Ph.D.) is outcome of research work carried out by me under the

supervision of **Dr. Gurmeen Rakhra** (Assistant Professor), in the Department of Biochemistry,

School of Bioengineering and Biosciences, Lovely Professional University, Punjab, India, The

research was co-supervised by Dr. (Prof) Neeta Raj Sharma (Co-supervisor I), HOS

Bioengineering and Biosciences, Lovely Professional University, Punjab, India, and Dr. (Prof)

Vetriselvan Subramaniyan (Co-supervisor II), Department of Medical Sciences, School of

Medical and Life Sciences Sunway University, Malaysia. This work has not been submitted in part

or full to any other University or Institute for the award of any degree.

Mudassir Lawal

Registration No.: 12204618

Department of Biochemistry

School of Bioengineering and Biosciences

Lovely Professional University, Punjab, India

Date: 27/10/2025

iii

CERTIFICATE

This is to certify that the work reported in the Ph.D. thesis entitled — "Identification and

Characterization of Bioactive Compound from Flax Microgreens and Evaluation of its

Protective Effect against Testosterone-induced Prostate Cancer" submitted in fulfillment of

the requirement for the award of degree of **Doctor of Philosophy (Ph.D.)** in Biochemistry, School

of Bioengineering and Biosciences, is a research work carried out by Mudassir Lawal, reg. no.:

12204618. It is bonafide record of his original work carried out under my supervision and that no

part of thesis has been submitted for any other degree, diploma or equivalent course.

Gurnes

Dr. Gurmeen Rakhra

Assistant Professor

Department of Biochemistry

School of Bioengineering and Biosciences

Lovely professional University, India

Date: 27/10/2025

iν

ACKNOWLEDGEMENTS

First and foremost, all praises are due to Allah, the Lord of all and cherisher of the universe, who in his infinite grace and mercy spared my life and bestowed me with health and capacity to carry out this research work and made the end of it a successful one. I would like to express my profound gratitude and sincere appreciation to my supervisor, Dr. Gurmeen Rakhra (Assistant Professor), Department of Biochemistry, Lovely Professional University, Jalandhar, Punjab, for her patience, tireless and unrelenting efforts in offering superb suggestions, and positive criticism throughout the research work, without which this journey may not have been successfully completed. Her profound knowledge and constant encouragement have not only shaped my research but have also inspired me to approach challenges with perseverance and determination. Her mentorship has been an immense privilege, and I cannot thank her enough for the wisdom and knowledge she has imparted during this journey. Thank you very much maam, for this great contribution.

I would like to express my sincere gratitude to my esteemed co-supervisors, **Dr.** (**Prof.**) **Neeta Raj Sharma** and **Dr.** (**Prof.**) **Vetriselvan Subramaniyan**, for their invaluable guidance, insightful suggestions, and continuous support throughout the course of my research. Their expertise, encouragement, and constructive feedback have been instrumental in shaping the direction and depth of this work. I am truly grateful for their mentorship and the opportunity to learn under their supervision.

My sincere gratitude also go to **Dr. Ashish Vyas**, Professor and Head, Department of Biochemistry and Microbiology, and **Dr. (Prof.) Neeta Raj Sharma**, HOS School of Bioengineering and Biosciences, for his unwavering support and guidance. I am also deeply thankful to **Dr. Ashok Mittal**, Chancellor, Lovely Professional University and Member of the Rajya Sabha, **Mrs. Rashmi Mittal**, Pro-Chancellor, **Dr. (Prof.) Lovi Raj Gupta**, Pro Vice-Chancellor, **Dr. Preeti Bajaj**, Vice-Chancellor, and **Dr. Monica Gulati**, Registrar, for their visionary leadership, encouragement, and continuous support, which truly embody the spirit of "**Think Big.**" I am equally thankful to the entire staff of School of Bioengineering and Biosciences, specifically the research advisory committee (RAC) members for the meaningful contributions, to make this work a wonderful one.

I would also like to express my sincere thanks to the Federal University Dutsin-Ma (FUDMA) Katsina-Nigeria for granting me study leave to pursue my postgraduate studies. This enabled me

to pursue my doctoral studies and allowing me to focus on the academic and practical aspects of my research.

I would also like to extend my heartfelt thanks to Dr. Ibrahim Hamza Kankia for his invaluable supervision and support during the animal model research. I am deeply grateful for the access he generously provided to the animal house and laboratory equipment at Umaru Musa Yaradua University, Katsina. My sincere appreciation also goes to his dedicated research team—Mr. Shamadeen Abdulkareem and Mr. Muhammad U. Mukhtar—for their assistance and collaboration, which greatly contributed to the successful completion of this part of the study.

I would like to acknowledge the contributions of my colleagues, friends, and fellow researchers at Lovely Professional University and Federal University Dutsin-Ma (FUDMA) Katsina-Nigeria who were always ready to offer their assistance, advice, and camaraderie throughout the course of this work.

Words may not be sufficient in describing the moral and financial assistance by my beloved father, **Mr. Lawal Abdu** and mother **Mrs. Amina Kasim** from the beginning of this academic journey up till now. I pray to God almighty to reward them abundantly for all they have done to me, forgive their short comings and make the paradise be their final abode.

Before I conclude, I have to deliver my heartfelt gratitude to my family and siblings for their prayers and support throughout this great academic journey.

ABSTRACT

Prostate cancer has a significant impact on men's health, and is ranked as the deadliest cancer after skin cancer. It accounts for nearly two-thirds of cancer diagnoses among men, with its prevalence increasing significantly with age, affecting nearly 60% of men over 65, according to the 2021 SEER Cancer Statistics Review. Nevertheless, the prevalence for this disease is not consistent and differs from region to region. The highest rates are observed in Northern Europe, North America, Australia/New Zealand, and the Caribbean (82.8 per 100,000), while much lower rates are seen in parts of Asia and Africa (as low as 6.4 per 100,000).

Given this global burden and variation, there is an urgent need for effective and accessible treatment strategies. While the lignans and polyphenols in flaxseeds have shown promising potential in various cancer treatments and prevention, there appears to be a lack of studies investigating the potential effects of flax microgreens specifically on prostate cancer. Previous literature proved that the flax microgreens have a high concentration of phenolic compounds, superior proteins and free amino acids, and a good fatty acid composition, making them an important plant source of components that are beneficial to health, but no research has been shown the anti-cancerous effects of flax microgreens and its bioactive compounds against prostate cancer. Therefore, this study explores the prospective use of flax microgreens and its bioactive components as a natural therapeutic source. The current work employs Gas Chromatography Mass Spectrophotometry, Ultraviolet—visible spectroscopy and High Performance Thin Layer Chromatography to identify and quantify bioactive compounds from flax microgreens and evaluate their anti-cancer effects on prostate cancer via *in silico*, *in vitro* and *in vivo* models.

The qualitative screening of the methanolic extract of flax microgreens (MEFM) revealed the presence of numerous phytochemical constituents such as alkaloids, saponins, flavonoids, steroid, cardiac glycoside, coumarins, phenolic compounds and chalcones. However, compounds such as tannins, terpenoids, and emodins were absent in the extract. MEFM exhibited significant antioxidant activity in a concentration-dependent manner. At a concentration of 1000 μg/mL, the extract exhibited strong DPPH radical scavenging activity of 84.2%. It also showed significant metal chelating activity (37% at 500 μg/mL and 38% at 1000 μg/mL) and a reducing power of 0.94% at the highest concentration tested (1000 μg/mL).

Gas Chromatography-Mass Spectrometry (GC-MS) analysis identified 60 distinct phytochemical compounds in the extract. These were confirmed based on their retention times, peak areas, peak heights, and mass spectral fragmentation patterns, matched against known profiles from the National Institute of Standards and Technology (NIST) library.

In the *in silico* phase of the study, eight key protein targets associated with prostate cancer were selected for molecular docking: Aurora A kinase (AURKA), Delta-like ligand 3 (DLL3), N-myc proto-oncogene protein (N-Myc), Cytotoxic T-lymphocyte antigen 4 (CTLA-4), 5α-Reductase (5AR), Androgen receptor (AR), Lysine-specific histone demethylase 1A (LSD1), and CD27. While structural data for most proteins were available in the Protein Data Bank (PDB), Delta-like ligand 3 (DLL3) lacked a resolved structure and was therefore modeled, analyzed, and validated using various bioinformatics tools.

Following GC-MS analysis, all identified phytocompounds were subjected to molecular docking against these eight targets. Ten compounds with a peak area greater than 2.0% and the strongest binding affinities (ranged from -4.5 to -17.1 kcal/mol) were selected for further screeing. Among these, four bioactive compounds were selected for post-docking studies based on their strong binding interactions: 4,4'-methylenebis (2,6-di-tert-butylphenol) (CID8372), 2,5-di-tert-butyl-1,4-benzoquinone (CID17161), 3,5-Dimethoxy-4-hydroxycinnamic acid (Sinapinic acid) (CID637775) and Oleanolic acid (CID10494).

Among them, **4,4'-methylenebis(2,6-di-tert-butylphenol)** (**4,4'-M(2,6-DTBP))** showed the strongest binding affinity across all eight targets (-10.5 to -17.1 kcal/mol), followed by **2,5-di-tert-butyl-1,4-benzoquinone** (**2,5-DTBQ)** (-6.8 to -11.3 kcal/mol), **Sinapinic acid** (-6.9 to -10.7 kcal/mol), and **Oleanolic acid** (-6.2 to -10.2 kcal/mol).

ADME/T (Absorption, Distribution, Metabolism, Excretion, and Toxicity) predictions revealed favorable pharmacokinetic profiles and low toxicity for all four compounds. Based on these promising results, 4,4'-M(2,6-DTBP) and 2,5-DTBQ were selected for further identification and characterization using UV-Vis spectroscopy and HPTLC, followed by validation through (*in vitro* and *in vivo*) studies. To characterize the selected compounds, 4,4'-M(2,6-DTBP) and 2,5-DTBQ methanolic extract of flax microgreens (MEFM) underwent liquid-liquid partitioning using solvents of varying polarities (*n*-hexane, ethyl acetate, *n*-butanol, and water). UV-VIS analysis revealed that both compounds were most concentrated in the non-polar fractions. Specifically,

4,4'-M(2,6-DTBP) was present at concentrations of $104.45\pm6.42~\mu g/mL$ in hexane and decreased progressively in more polar solvents. Similarly, 2,5-DTBQ showed its highest concentration in hexane ($156.36\pm2.47~\mu g/mL$) and ethyl acetate ($130.63\pm1.65~\mu g/mL$), with lower levels in butanol and aqueous fractions.

HPTLC analysis confirmed the presence and abundance of these compounds in MEFM, with 4,4'-M(2,6-DTBP) and 2,5-DTBQ accounting for 100% and 73.90% area percentages, respectively. The identity of the compounds was verified by comparing the Rf values of the extract with those of standard compounds, showing a strong match and confirming their specificity in the extract.

In vitro studies demonstrated that the methanolic extract of flax microgreens (MEFM) exhibits strong cytotoxic activity against PC-3 prostate cancer cell lines, greater than the efficacy of the standard drug, cisplatin. Among the identified bioactive compounds, 2,5-DTBQ and 4,4'-M(2,6-DTBP) both showed inhibitory effects on PC-3 cells, with 2,5-DTBQ exhibiting higher cytotoxicity than 4,4'-M(2,6-DTBP). However, their cytotoxic effects remained moderate when compared to cisplatin, a commonly used drug in prostate cancer treatment.

The IC₅₀ values were recorded as follows: MEFM (377.5 μg/mL), 2,5-DTBQ (875.4 μg/mL), 4,4'-M(2,6-DTBP) (2324.78 μg/mL), and cisplatin (273.97 μg/mL). Despite their high binding affinities in molecular docking (-11.3 kcal/mol and -17.1 kcal/mol), 2,5-DTBQ and 4,4'-M(2,6-DTBP) showed relatively weak cytotoxic effects, likely due to quick metabolism, low bioavailability, poor cellular uptake and the differences between *in silico* and *in vitro* conditions.

Apoptosis assays revealed a significant increase in cell death induced by MEFM (41.03%), 2,5-DTBQ (26.83%), and 4,4'-M(2,6-DTBP) (22.86%) as compared to untreated controls (3.92%). In early apoptotic cells, the MEFM, 2,5-DTBQ, and 4,4'-M(2,6-DTBP) demonstrated significantly higher cell death (40.9, 25.7 and 19.5%, respectively), whereas in late apoptotic cells, the cell death was found to be 0.13, 1.13, and 3.36% respectively. Although these test samples effectively induced cell death, their potency was still lower than that of cisplatin, a well-established proapoptotic drug in prostate cancer therapy.

In *in vivo* studies, wisatr rats given MEFM (5000 mg/kg) orally showed no mortality or toxicity. Therefore, the lethal dose (LD₅₀) of MEFM is considered to be greater than 5000 mg/kg. In therapeutic assessments, MEFM and its major bioactive compounds (2,5-DTBQ and 4,4'-M(2,6-

DTBP)) helped prevent body weight loss typically associated with prostate cancer (PC), with MEFM showing the most promising protective effect. Assessment of prostate weight (PW) and prostate index (PI) further highlighted MEFM's effectiveness. MEFM (200 mg/kg) dramatically decreased prostate weight to 0.89 g and prostate index to 0.37%, achieving inhibition rates of 89.46% and 94.09%, respectively, and these results were found to be closely similar to the effects of finasteride, the standard treatment. Among the selected compounds, 2,5-DTBQ (20 mg/kg) also showed strong effects, reducing prostate weight to 0.96 g (inhibition: 81.86%) and prostate index to 0.44% (inhibition: 81.2%). In contrast, 4,4'-M(2,6-DTBP) (20 mg/kg) had moderate effects, with prostate weight at 1.17 g and index at 0.52%, corresponding to inhibition rates of 60.73% and 64.62%.

Histopathological analysis of prostate tissues revealed that the disease control group exhibited significant abnormalities, including prostatic intraepithelial neoplasia (PIN) and disrupted tissue architecture. Finasteride-treated wistar rats showed a near-complete restoration of normal prostate histology. MEFM-treated wistar rats displayed notable recovery, with improved glandular structure, retained basal cell layers, and reduced intraepithelial growth, indicating partial but promising tissue restoration. Both 2,5-DTBQ and 4,4'-M(2,6-DTBP) groups showed improvements as well, with 2,5-DTBQ demonstrating better histological recovery than 4,4'-M(2,6-DTBP).

In conclusion, MEFM shows strong potential as a safe, multi-targeted, plant-derived candidate for prostate cancer prevention and treatment. Its higher effectiveness compared to isolated bioactive compounds supports the hypothesis of synergism among the various phytochemicals present in the whole extract, enhancing its overall therapeutic impact.

TABLE OF CONTENTS

DEDICATION	ii
DECLARATION	iii
CERTIFICATE	iv
ACKNOWLEDGEMENTS	v
ABSTRACT	vii
TABLE OF CONTENTS	xi
LIST OF TABLES	xvi
LIST OF FIGURES	xviii
LIST OF APPENDICES	xxi
CHAPTER ONE	1
1.0 INTRODUCTION	1
1.1 Hypothesis	6
1.2 Research aim	7
1.3 Objectives of the research	7
CHAPTER TWO	8
2.0 LITERATURE REVIEW	8
2.1 Cancer	8
2.2 Prostate cancer and its prevalence	9
2.2.1 International status	10
2.2.2 National status	10
2.3 Prostate gland	11
2.4 Types of prostate cancer	12
2.5 Etiology and risk factors of prostate cancer	
2.6 Types and treatment of prostate cancer	14
2.7 Prostate cancer target proteins	
2.7.1 Aurora A kinase (AURKA)	
2.7.2 Delta-like ligand 3 (DLL3)	16
2.7.3 N-Myc proto-oncogene protein (N-Myc)	16
2.7.4 Cytotoxic T-lymphocyte antigen 4 (CTLA-4)	17
$2.7.5 5\alpha$ -Reductase (5AR)	17

2.7.6 Androgen receptor (AR)	18
2.7.7 Lysine-specific histone demethylase 1A (LSD1)	18
2.7.8 CD27	18
2.8 Medicinal plants used as a management of prostate cancer	19
2.9 Flax	19
2.9.1. Taxonomy and genetics	20
2.9.2 Flax microgreens	20
2.9.3. Important components in flax	21
2.9.4 Major polyphenols in flax	21
2.9.4.1 Lignans	22
2.9.4.2 Phenolic acids (PAs)	22
2.9.4.3 Flavonoids	22
2.9.5 Anticancer activities of polyphenols	22
2.9.6 Identified bioactive compounds	23
2.10 Biochemistry of cell death and apoptotic signaling	25
CHAPTER THREE	27
3.0 MATERIAL AND METHODS	27
3.1 Chemicals/ reagents	27
3.2.1 Plant material and growth conditions	27
3.2.2 Collection and identification of plant materials	27
3.2.3 Extraction using the cold maceration method	28
3.3 Preliminary phytochemical screening	28
3.4 Antioxidant activity	29
3.4.1 The DPPH scavenging assay	29
3.4.2 Determination of metal chelating potential	30
3.4.3 Ferric reducing power activity	30
3.4.4 Gas chromatography–mass spectrometry analysis	30
3.5 In silico studies	31
3.5.1 Protein modeling studies of delta-like ligand 3 (DLL3)	31
3.5.1.1 Delta-like ligand 3 sequence recovery	31
3.5.1.2 Protein modeling	31
3.5.1.3 Molecular docking study	32

3.5.1.4 ADME properties and toxicity prediction	32
3.6 Isolation and identification of bioactive compounds	33
3.6.1 UV-Visible spectroscopy	33
3.6.1.1 Preparation of standard	33
3.6.1.2 Determination of maximum wavelength by UV-VIS spectroscopy	33
3.6.1.3 Preparation of standard calibration curve by UV-VIS spectroscopy	33
3.6.1.4 Preparation of test solution for UV-VIS spectroscopy	33
3.6.2 HPTLC analysis	34
3.6.2.1 Preparation of standard solution	34
3.6.2.2 Test samples (Extract) preparation	34
3.6.2.3 HPTLC setup conditions and instrumentation	34
3.7 in vitro studies	34
3.7.1 Cell viability assay	34
3.7.2 Annexin V apoptosis assay by flow cytometry	35
3.8 In vivo study	36
3.8.1. Experimental animal	36
3.8.2 Acute toxicity study of MEFM	36
3.8.3 Prostate cancer induction and experimental design	36
3.8.4 Assessment of body weight (BW), prostate weight (PW), and prostatic index (PI)	38
2.8.5 Biochemical and histological analyses	38
3.8.6 Statistical analysis	39
CHAPTER FOUR	40
4.0 RESULTS AND DISCUSSION	40
4.1 Flax Microgreens and Growth Conditions	40
4.2 Qualitative screening tests of the methanolic extract of flax microgreens	40
4.3 Antioxidant activity	41
4.3.1 DPPH scavenging activity	41
4.3.2 Metal chelating activity	42
4.3.3 Reducing power assay	43
4.4 GC-MS profiling of methanolic extract of flax microgreens	44
4.5 Molecular docking screening and bioactive compound selection process	48
2.5-Di- <i>tert</i> -butyl-1.4-benzoguinone	49

4.6 Prostate cancer target proteins	50
4.7 Protein modeling studies and sequence analysis of delta-like protein 3 (DLL3)	50
4.8 Homology modeling and validation.	55
4.9 Molecular docking analysis	58
4.9.1 Binding affinities of selected bioactive compounds (CID10494, CID17161, CID6377' and CID8372) and FDA approved drugs (Flutamide) across target proteins	
4.9.2 Half maximal inhibitory concentration (IC ₅₀) prediction (CID10494, CID17161, CID637775, CID8372) and FDA approved drugs (Flutamide)	60
4.9.3 Protein–ligand interactions of CID10494, CID17161, CID637775, CID8372 against prostate cancer target proteins	61
4.10 ADME/T properties prediction	70
4.11 UV-VIS quantification	72
4.11.1 Determination of λ_max values and linearity	72
4.11.2 Analysis of extract fractions	75
4.12 HPTLC analysis	77
4.13 In vitro Studies	81
4.13.1 Cell viability assay	81
4.13.2 Annexin apoptotic assay	84
4.14 In vivo study	86
4.14.1 Acute toxicity	86
4.14.2 Effects of MEFM and its bioactive compounds on wistar rats body weight	86
4.14.3 Effects of MEFM and its bioactive compounds on the prostate weight (PW)	87
4.14.4 Effects on serum level of testosterone and prostate specific antigen (PSA)	89
4.14.2 Histopathology results of prostate	91
CHAPTER FIVE	93
5.0 Summary, conclusion and recommendations	93
5.1 Summary	93
5.2 Conclusion	96
5.3 Recommendations	99
References	101
References	126
APPENDICES	138
Annendix-I	138

List of publications	140
List of conferences attended	
List of workshops attended	
Ethical approval certificate	148
Certificate of authentication of collected plant	149

LIST OF TABLES

Table No.	Title	Page No
2.1	Types of prostate cancer	12
2.2	Etiology and risk factors of prostate cancer	13
3.1	Phytochemical screening of MEFM	28
3.2	Animal grouping and experimental design	37
4.1	Qualitative chemical tests of the methanolic extract of flax	41
	microgreens	
4.2	Bioactive compounds found in methanolic extract of flax	45
	microgreens	
4.3	Flax microgreen's bioactive compounds with highest	49
	percentage	
4.4	The physicochemical parameters of DLL3	51
4.5	Identified domains from the sequence	51
4.6	Prosite result shows the structure, sequence position and	52
	disulfide bond between amino acids in domains	
4.7	Prediction of DLL3 secondary structure using SOPMA online	53
	tool	
4.8	Prediction of the DLL3 domain locations using deepTMHMM	54
	1.0.24	
4.9	PROCHECK tool generates a Ramachandran plot for the final	57
	DLL3 models	
4.10	PROVE analysis for the DLL3 model	58
4.11	Molecular docking result of selected bioactive compounds of	59
	flax microgreens against prostate cancer target proteins.	
4.12	Binding affinities, IC ₅₀ values, and interaction residues of 4,4'-	62
	M(2,6-DTBP) (CID8372) and FDA approved drugs	
	(Flutamide) across target proteins	

4.13	Binding affinities, IC ₅₀ values, and interaction residues of 2,5-	63
	DTBQ (CID17161) and FDA approved drugs (Flutamide)	
	across target proteins.	
4.14	Binding affinities, IC50 values, and interaction residues of	64
	Sinapinic acid (CID637775) and FDA approved drugs	
	(Flutamide) across target proteins.	
4.15	Binding affinities, IC ₅₀ values, and interaction residues of	65
	Oleanolic acid (CID10494) and FDA approved drugs	
	(Flutamide) across target proteins.	
4.16	Drug-likeness, lipophilicity and physicochemical properties	71
4.17	Toxicity prediction of CID8372, CID17161, CID637771 and	71
	CID10494 using ProTox-3.0 online tool	
4.18	λ_{Max} for 4,4'-M(2,6-DTBP) and 2,5-DTBQ in different	72
	solvents.	
4.19	UV-Visible spectroscopy linearity of 4,4'-M(2,6-DTBP) and	73
	2,5-DTBQ in different solvents	
4.20	UV-Vis quantification of 4,4'-M(2,6-DTBP) and 2,5-DTBQ	75
	from MEFM in different sub-fraction	
4.21	HPTLC peak table of 4,4'-M(2,6-DTBP) and MEFM	78
4.22	HPTLC peak table of 2,5-DTBQ and MEFM	78
4.23	IC ₅₀ and 95%CI values of cell proliferation inhibition of	83
	MEFM, 2,5-DTBQ, 4,4'-M(2,6-DTBP), and cisplatin	
4.24	Percentage of cells after MEFM, 2,5-DTBQ, and 4,4'-M(2,6-	85
	DTBP) treatment (Annexin V Apoptosis Assay)	
4.25	Effects of MEFM and its selected bioactive compounds on	87
	male wistar rats body weight	
4.26	Effects of MEFM and its selected bioactive compounds on	88
	prostate weight and relative prostate weight	

LIST OF FIGURES

Table No.	Title	Page No
1.1	Diagrammatic representation of medinal uses of flax lignans	3
1.2	Mechanism of flax bioactive compounds in cancer suppression.	4
2.1	The fifteen most prevalent cancer types for estimated new cases	9
	and deaths by sex in the United States, 2024	
2.2	Total number of prostate cancers registered with incidence rate	11
	≥ 5 per 100,000 for 28 population-based cancer registries under	
	the National Cancer Registry Programme 2012–2019	
2.3	Anatomical structure of the prostate gland in the male	12
	reproductive system	
2.4	Flaxseeds and flax microgreens	21
2.5	Structure of 4,4'-methylenebis (2,6-di-tert-butylphenol)	24
2.6	Structure of 2,5-di-tert-butyl-1,4-benzoquinone	24
2.7	Apoptotic signaling pathway	26
4.1	Well grown flax microgreens under controlled conditions in Hi-	40
	tech polyhouse facility.	
4.2	DPPH scavenging activity of MEFM compared to ascorbic acid	42
	control.	
4.3	Metal chelating activity of MEFM compared to EDTA as	43
	control.	
4.4	Reducing power assay of MEFM compared to ascorbic acid	44
	control	
4.5	GC-MS chromatogram of methanolic extract of flax	48
	microgreens (Linum usitatissimum L.)	
4.6	Molecular docking screening and bioactive compound selection	49
	process	
4.7	Sequence Logo for DLL-3 domain	52
4.8	Prediction of DLL3 secondary structure using SOPMA online	54
	tool	

4.9	Transmembrane helix prediction of DLL-3 using	55
	DeepTMHMM (1.0.24)	
4.10	Aligment between human DLL3 and delta-like protein 1(DLL1)	56
4.11	Homology modeled structure of human DLL3	56
4.12	Ramachandran map of Q9NYJ7 (Query sequence) and template	57
	sequence model	
4.13	ERRAT Plot for each loop (chain A & B) modelled structure.	58
4.14	3D Docking pose interactions of DLL3 with bioactive	66
	compounds viz; (A) CID8372, (B) CID10494, (C) CID17161,	
	and (D) CID637771.	
4.15	3D Docking pose interactions of CTLA-4 with bioactive	66
	compounds viz; (A) CID8372, (B) CID10494, (C) CID17161,	
	and (D) CID637771.	
4.16	3D Docking pose interactions of AURKA with bioactive	67
	compounds viz; (A) CID8372, (B) CID10494, (C) CID17161,	
	and (D) CID637771.	
4.17	3D Docking pose interactions of LSD1 with bioactive	67
	compounds viz; (A) CID8372, (B) CID10494, (C) CID17161,	
	and (D) CID637771.	
4.18	3D Docking pose interactions of N-Myc with bioactive	68
	compounds viz; (A) CID8372, (B) CID10494, (C) CID17161,	
	and (D) CID637771.	
4.19	3D Docking pose interactions of 5AR with bioactive	68
	compounds viz; (A) CID8372, (B) CID10494, (C) CID17161,	
	and (D) CID637771.	
4.20	3D Docking pose interactions of AR with bioactive compounds	69
	viz; (A) CID8372, (B) CID10494, (C) CID17161, and (D)	
	CID637771.	
	1	<u> </u>

4.21	3D Docking pose interactions of CD27 with bioactive	69
	compounds viz; (A) CID8372, (B) CID10494, (C) CID17161,	
	and (D) CID637771.	
4.22	UV-VIS linearity graph for 4,4'-M(2,6-DTBP) in (A) Hexane,	74
	(B) Ethyl acetate, (C) Butanol, and (D) Water	
4.23	UV-VIS linearity graph for 2,5-DTBQ in (A) Hexane, (B) Ethyl	74
	acetate, (C) Butanol, and (D) Water	
4.24	(A) UV-Vis absorption spectra of 2,5-DTBQ at the same	76
	concentration in different solvent fractions—(A) Hexane, (B)	
	Ethyl acetate, (C) Butanol, and (D) Water.	
4.25	(A) UV-Vis absorption spectra of 2,5-DTBQ at the same	76
	concentration in different solvent fractions—(A) Hexane, (B)	
	Ethyl acetate, (C) Butanol, and (D) Water	
4.26	HPTLC fingerprinting of (A) 4,4'-M(2,6-DTBP) and (B) 2,5-	79
	DTBQ from MEFM	
4.27	Densitometry graph showing isolation of 4,4'-M(2,6-DTBP)	79
	from MEFM	
4.28	(A) 3D Chromatogram of 4,4'-M(2,6-DTBP) from extract and	80
	standard. (B) Overlay of HPTLC chromatogram of all tracks.	
4.29	Densitometry graph showing isolation of 2,5-DTBQ from	80
	MEFM	
4.30	(A) 3D Chromatogram of 2,5-DTBQ from extract and standard.	81
	(B) Overlay of HPTLC chromatogram of all tracks.	
4.31	MTT cell viability assay. Plot shows the percentage viability of	83
	PC-3 cells treated with (A) MEFM, (B) 2,5-DTBQ (C) 4,4'-	
	M(2,6-DTBP), and (D) cisplatin (standard).	
4.32	Morphological changes in PC-3 cell lines at 24 h of treatment.	84
	(A) Untreated, (B) MEFM, (C) 2,5-DTBQ (D) 4,4'-M(2,6-	
	DTBP), and (E) cisplatin. CS cellular shrinkage, BL membrane	
	blebbing.	

4.33	Annexin V apoptosis assay conducted on PC-3 cells under	86
	different treatment conditions: (A) Untreated control, (B)	
	MEFM-treated, (C) 2,5-DTBQ-treated, and (D) 4,4'-M(2,6-	
	DTBP)-treated cells	
4.34	Effect of MEFM and its bioactive compounds on serum	90
	testosterone level in testosterone-induced PC wistar rats.	
4.35	Effect of MEFM and its bioactive compounds on prostate	91
	specific antigen (PSA) level in testosterone-induced PC wistar	
	rats.	
4.36	Prostate tissue histopathological analysis	92
5.1	Summary of the thesis workflow and findings	85
5.2	Flowchart showing the thesis structure	98

LIST OF APPENDICES

Table No.	Title	Page No
Appendix-I	Molecular docking result of flax microgreens bioactive	138
	compounds against prostate cancer target proteins.	

CHAPTER ONE

1.0 INTRODUCTION

Cancer is a complex group of diseases characterized by uncontrolled growth of cells and the ability of those abnormal cells to spread and invade to nearby tissues and distant parts of the body. This spreading, called metastasis, is a significant contributor to high mortality rates associated with many types of cancer (Atmaca *et al.*, 2022). Metastasis make cancer treatment more challenging, therefore early detection and effective therapy to prevent metastasis is very significant (Rojas-Armas *et al.*, 2020). Notably, cancer has not only inflicted extensive health significances but also stands as the 2nd most common cause of morbidity worldwide (Salehi *et al.*, 2019; Siegel *et al.*, 2021). The 2024 reports by the National Center for Health Statistics show that the United States had 2,001,140 new cancer cases and 611,720 cancer-related deaths. Not all the tumors are cancerous; some of them are benign and do not invade surrounding tissues or metastasize (Bisoyi, 2022).

Prostate cancer (PCa) is a hereditary disease, and its prevalence rate is more common in men aged 70 years and above. PCa stands out as one of the most prevalent malignancies and the second most common cancer among men followed by lung cancer in terms of fatality (Ahmed et al., 2024). To date, the main risk factors concerning prostate cancer are age, family history of the disease, and ethnicity (Graham et al., 2024). Testosterone controls the normal function of a prostate and its active stimulation for long time can lead to initiation and promotion of prostate cancer development (Mukherjee & Gopalakrishnan, 2024). Previous studies have indicated that the gradual increase in testosterone levels with an increase in age as a significant cause of the development of BPH (benign prostatic hyperplasia) and even prostate cancer (Xia et al., 2021; Welén & Damber, 2022). Hospital-based studies have reported prevalence rates ranging from 14% to 46.4%, with mortality between 15.6% and 64.0% within 6 months to 3 years of diagnosis (Osegbe et al., 2024). An autopsy-based study also estimated a crude prevalence of 8.8% for subclinical prostate cancer among Nigerian men aged 40 years and above, increasing with age (Akinremi et al., 2021). Many obstacles have been placed in the way of the search for an etiological cause of PCa by the heterogeneity of the gland itself (Mazurakova et al., 2022). There are several animal models of prostate cancer that are being tested that may be relevant to some stages of the

carcinogenesis or to certain subtypes of prostate cancer with particular genetic defects or biological abnormalities (Kaushal *et al.*, 2024; Adamiecki *et al.*, 2022).

Globally, medicinal plants are now widely used, and in current years, they have become crucial in the treatment of various ailments (Nnadi et al., 2021). The side effects of cancer medications have been traditionally minimized using different plant extracts due to their cost effectiveness, efficacy, easy accessibility, and preparation. Currently, several anti-cancer drugs have been developed from plants such as paclitaxel and taxol from Taxus brevifolia, vincristine and vinblastine from Catharanthus roseus and docetaxel (Taxotere) from Taxus baccata (Matowa et al., 2020). Over the past decade, considerable attention has been directed toward the use of medicinal plants in prostate cancer management, and a systematic review of 75 preclinical studies revealed that numerous plant-derived compounds exert anti-prostate cancer effects by modulating androgen receptor (AR) and estrogen receptor (ER) signaling, inhibiting cell proliferation, inducing apoptosis, and causing cell cycle arrest (Mazumder et al., 2022). In West Africa, extracts from Vernonia amygdalina, Zingiber officinale, and Azadirachta indica have demonstrated cytotoxic effects against PC-3 and DU-145 prostate cancer cells, further reinforcing the potential of ethnomedicinal plants as anticancer agents (Kwakye et al., 2025).

Flax is a multipurpose crop in the *Linaceae* family. The scientific name of flax "usitatissimum" originated from Latin which means "the most useful" one (Stavropoulos et al., 2023). The health benefits of flax/flaxseed have drawn the researcher's attention (Figure 1.1), which include cancer treatment and prevention (Morris, 2007). The seeds are abundant in lignans, dietary fiber, and essential fatty acids, and have been demonstrated to have anti-cancerous effects (Kauser et al., 2024). Secoisolariciresinol glycoside (SDG) is the most prevalent lignan of flax, which when consumed, will be metabolized by the gut microbiota and is known to produce two mammalian lignans, enterodiol and enterolactone (Chhillar et al., 2021). Other lignans include isolariciresinol, anhydrosecoisolariciresinol, matairesinol pinoresinol, and pinoresinol diglucoside (Mueed et al., 2024). Several experimental studies in the past have documented the importance of flax/flaxseeds and their phytoconstituents in retarding the progression of different cancers (Chera et al., 2022; Zare et al., 2022). In addition to flax, microgreens, the young seedlings of vegetables and herbs, are also rich in vitamins, minerals, polyphenols, and antioxidants, often exceeding the levels found in mature plants (Kyriacou et al., 2024). Recent studies highlight their anticancer potential, with

green pea, broccoli, and radish microgreens demonstrating the ability to inhibit proliferation, induce apoptosis, and exert cancer-preventive effects (Pinto *et al.*, 2021; Choe *et al.*, 2023).

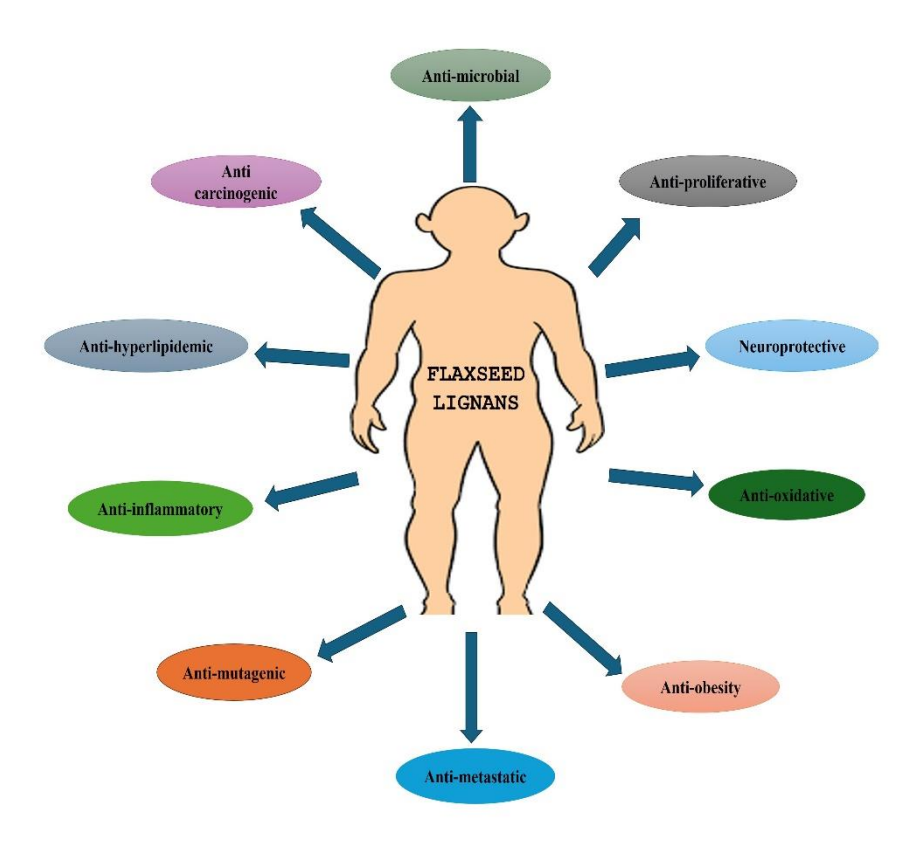


Figure 1.1: Diagrammatic representation of medinal uses of flax lignans

Previous studies have shown that the flaxseeds in the diet reduce the risk of PCa by significantly decreasing the proliferation effect and the levels of prostate-specific antigen in Wistar rats (Said *et al.*, 2015; Amorim *et al.*, 2017). According to Johnsson *et al.* (2009), the flax meal diet supplemented with seeds of flax showed anti-cancerous activity on colon cancer in rats. It has also been reported that flax extract containing enterolignans significantly reduced the risk of breast cancer in subjects. Moreover, research findings by Islam *et al.* (2023) and Viveky *et al.* (2015) also revealed that flaxseed consumption led to a reduction in tumor growth rate in ovarian cancer subjects thereby exhibiting an anti-proliferative effect. Many lignans found in flaxseed suppress the important regulatory proteins and alter apoptotic pathways to specifically target cancer cells (Mueed *et al.*, 2023).

The class of cysteine proteases known as caspases (cysteine aspartyl-specific proteases) cleaves target proteins to cause apoptosis (Khurana *et al.*, 2024). When apoptotic control is lost, cancer cells are able to live longer and accumulate, this can lead to angiogenesis, an increase in tumor growth as well as cell proliferation and differentiation derangement (Haake *et al.*, 2024). Progress through the four important stages of the cell cycle—G0/G1, S, G2, and M—is necessary for proliferation. These phases are controlled by a number of cyclin-dependent kinases, which function in complex with their cyclin partners to maintain genetic material duplication and cell division. The cell cycle derangement caused by abnormal expression of key regulatory proteins is closely linked to the development of tumors (Otto & Sicinski, 2017).

Although lignans and polyphenols in flaxseeds have demonstrated potentiality in the prevention and treatment of various cancers, research specifically investigating the effects of flax microgreens on prostate cancer is limited. Previous literature proved that the flax microgreens have a high content of polyphenols, free amino acids, fatty acid and proteins, making them an important plant source of components that are beneficial to health (Santin *et al.*, 2022), but no research has been shown the anti-cancerous effects of flax microgreens and its bioactive compounds against prostate cancer. Therefore, this study is designed to identify and characterize phytocompounds from flax microgreen and evaluate their anti-prostate cancer properties. **Figure 1.2** illustrates the mechanism of flax bioactive compounds in cancer suppression.

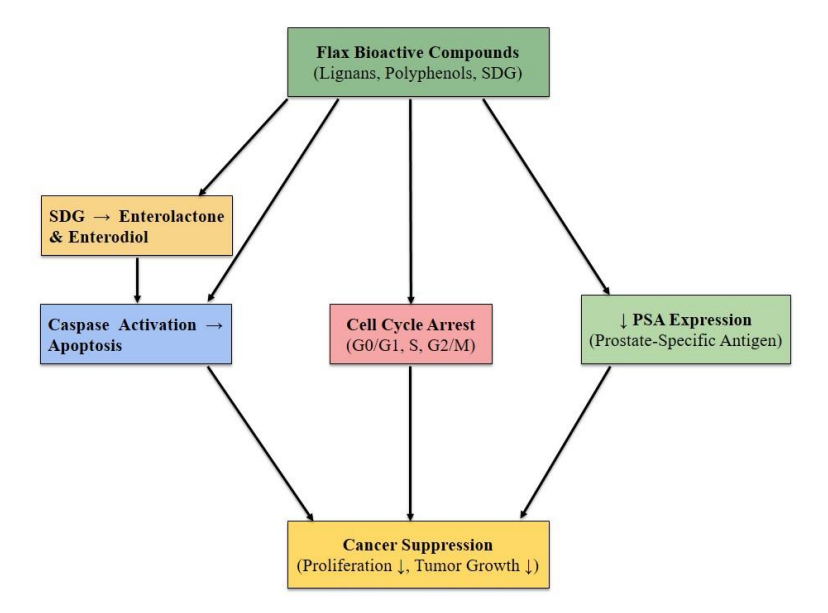


Figure 1.2: Mechanism of flax bioactive compounds in cancer suppression

In this study, virtual screening through molecular docking, molecular interaction studies, ADMET and toxicity prediction analysis were utilized aiming to screen the phytocompounds from the flax microgreens with the inhibitory activity against the target receptors were carried out as previously described by Feng *et al.*, (2021). Flax microgreens were subjected to extraction with methanol using the cold maceration method, which is a safe, efficient, and cost-effective method for extracting compounds. Qualitative phytochemical screening of methanolic extract of flax microgreens were done to determine the phytoconstituents of plant. Antioxidant activity such as DPPH Scavenging assay, metal chelating potential, and ferric reducing power activity were evaluated for the plant extracts. A validated GC-MS, UV-Vis, and HPTLC approach was used for the identification and characterization of the selected compounds. Hence, a fast sample preparation and a verified identification and quantification method using GC-MS, UV-Vis, and HPTLC were established.

Additionally, an *in vitro* approach was used to assess the anti-prostate cancer efficacy of the extracts, and bioactive compounds on the PC-3 cell lines. The cytotoxicity effects were evaluated using the MTT assay, and the IC₅₀ values were generated from dose-response curve studies. The Annexin V apoptosis assay was evaluated to understand their mechanism of action.

Furthermore, an *in vivo* approach was used to evaluate the anticarcinogenic effects of bioactive compounds and flax microgreens extract on testosterone-induced prostate cancer wistar rats. Finally, after the assessment of the anticancer efficacy of the methanolic extract of flax microgreens and its selected bioactive compounds, they may serve as one of the potential solutions to the current issue of prostate cancer, aligning with the United Nations Sustainable Development Goals (UNSDGs) 3, 9, 12, and 15 which focus on plant-based cancer therapy, development and scientific innovation, promoting sustainable production of nutraceuticals and ecological significance of medicinal plants.

1.1 Hypothesis

- 1. The herbal formulation made from the **flax microgreens** exhibit no cytotoxicity against prostate cancer.
- 2. The phytoconstituents of **flax microgreens** exhibit no cytotoxicity against prostate cancer.
- 3. The identified bioactive compounds from flax microgreens exhibit no cytotoxic effects against prostate cancer.

1.2 Research aim

This research focuses on identification and characterization of a bioactive compound from flax microgreens and evaluation of its protective effect against testosterone-induced prostate cancer.

1.3 Objectives of the research

- To assess the effects of bioactive compounds from flax microgreens on druggable target proteins of prostate cancer via *in silico* study.
- To identify and characterize the bioactive compound with anti-cancer activity from flax microgreens.
- To evaluate the anti-prostate cancer effects of bioactive compound and flax microgreens extract using *in vitro* approaches.
- To evaluate the anticarcinogenic effects of bioactive compound and flax microgreens extract on testosterone-induced prostate cancer wistar rats.

CHAPTER TWO

2.0 LITERATURE REVIEW

2.1 Cancer

Cancer refers to a disease where cells start to grow wildly and invade neighboring tissues. These cells can even spread to other body parts through the blood and lymph systems. The human body is made up of trillions of cells, and cancer can begin from any part of the body due to loss of control in cell growth (Islami *et al.*, 2021). Normally, our cells grow and split in a highly controlled manner to create new ones as needed. When cells become aged or damaged, they undergo cell death and are replaced by new, healthy cells. Cell cycle regulation fails in cancer cells, leading to uncontrolled cell division and tumor formation. Cancer cells can also affect nearby normal cells and blood vessels, helping to feed the tumor, which exists in what we call the microenvironment. This microenvironment includes blood vessels, fibroblasts, lymphocytes, and other elements that promote the growth of the cancer. For a tumor to grow and become dangerous, it needs to develop four specific features which include ability to; (a) survive in blood, (b) move, (c) degrade the extracellular matrix, and (d) establish a new tissue environment for itself (Wang *et al.*, 2018).

Cancer is the second most common cause of mortality rates worldwide annually, followed by cardiovascular diseases. It remains an obstacle towards increased average life expectancy across the global countries. Each and every year, a new estimate is published by the American Cancer Society regarding the number of cases and fatalities from the cancer that are likely to happen within the United States. Also, the most recent records of cancer incidence, mortality, and survival rates are obtained from SEER, CDC, NPCR, and the North American Central Cancer Registries (**Figure 2.1**) (Siegal *et al.*, 2024).

National Center for Health Statistics responsible for mortality data collection. **Figure 2.1** explains that in the United States, there were **2,001,140** new cancer cases and **611,720** deaths caused by cancer in the year of 2024. From 2009 to 2012, the data collected from the thirteen oldest SEER registries, there has been a steady increase in overall cancer cases in women while an overall increase of 3.1% in men was observed due to the increased rate of prostate cancer diagnosis. Since 1991, the rate of death caused by cancer has reduced significantly by more than twenty-three percent, which can be translated into over 1.7 million lives saved until 2012. However, mortality

rates continue to rise in cancers of the prostate, pancreas, liver, and uterine corpus (Siegel *et al.*, 2024).

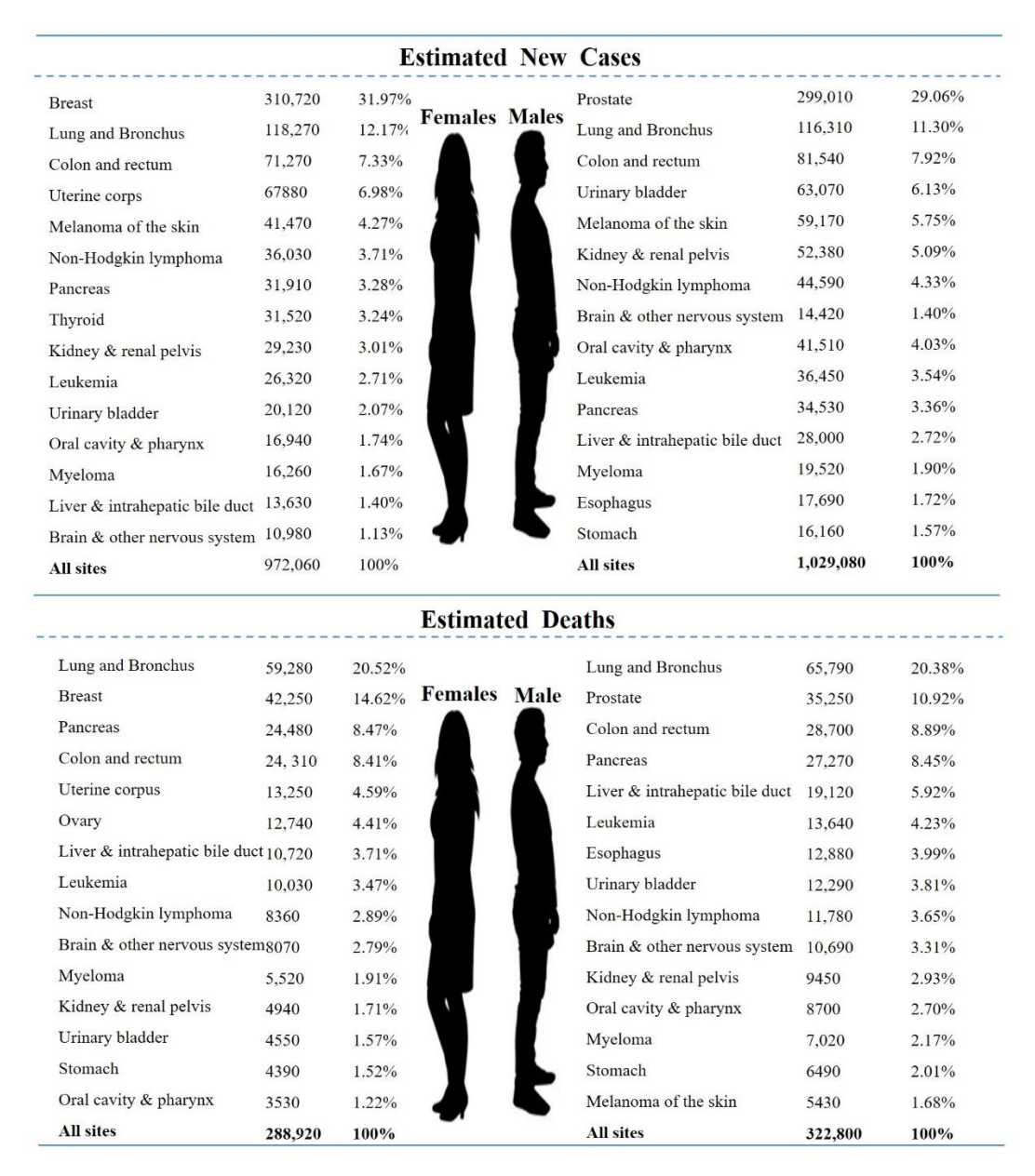


Figure 2.1: The fifteen most prevalent cancer types for estimated new cases and deaths by sex in the United States, 2024 (Siegel *et al.*, 2024). Estimates are rounded to the nearest ten. Excludes basal cell and squamous cell skin cancers and in situ carcinomas, except for urinary bladder.

2.2 Prostate cancer and its prevalence

Prostate cancer means the existence of cancer within the prostate gland, which is a part of the male reproductive system. It is also called carcinoma of the prostate. There are various types of prostate

cancer ranges from slow-growing to relatively fast-growing cancer (Mbah-Omeje *et al.*, 2022). Prostate cancer frequently metastasizes to the bones and lymph nodes, a progression that significantly contributes to disease severity and poor clinical outcomes (Samaržija, 2021). Mostly prostate cancer shows no symptoms in the earlier stages, but late on it may cause symptoms like blood in the urine, trouble urinating, and back or pelvic pain. Benign prostatic hyperplasia is one of the conditions that has the potential to show some of these signs. Other advanced symptoms include weakness due to low levels of red blood cells (Stewart and Wild, 2014). The majority of prostate cancer patients are diagnosed exclusively on the basis of increased PSA concentration in plasma (PSA>4ng/mL). PSA is a glycoprotein that is produced in the prostate tissue. It is advised that patients undergo a tissue biopsy to confirm if the cancer is present because some men were found to have elevated PSA levels but not cancer.

2.2.1 International status

According to the SEER Cancer Statistics Review 2018, prostate cancer is the cancer with highest rate of diagnosis in men, with frequent cases around 2 out of 3 men across the globe, which is 118 out of 185 of the total countries in the world. The occurrence rates of the disease are almost 60% in men aged 65 and older (Siegel *et al.*, 2018). The prevalence for this disease however is not consistent and differs from region to region. In particular, Northern Europe, Australia/New Zealand, the Caribbean, and Northern America have the highest rates of prostate cancer at 82.8 per 100,000 population. In contrast, some parts of Asia and Africa saw the lowest rate of just 6.4 per 100,000. Prostate cancer mortality rate vary significantly worldwide (Ferlay *et al.*, 2019). According to Ferlay *et al.* (2019), the lowest cancer incidence rates were observed in Asia, specifically in Northern Africa (5.8), South-Central Asia (3.3), East Asia (4.7), and Southeast Asia (5.4). An International Agency for Research on Cancer projected that, the aging and growing global population will cause the burden of prostate cancer (PCa) to increase to 1.7 million new cases and 499000 new deaths by 2030.

2.2.2 National status

One of the most common malignancies identified among Indian men living in cities is prostate cancer. Between 2012 and 2016, 11,340 cases of prostate cancer were documented across 28 Population-Based Cancer Registries (PBCRs). Urban registries accounted for 77.5% of these cases, while mixed registries with over 40% urban population contributed approximately 17.2%.

Notably, the Age-Adjusted Incidence Rates (AAR) per 100,000 males were highest in Delhi (11.8), followed by Kamrup Urban (10.9), and Mumbai (9.7) (**Figure 2.2**). Northeastern registries with the exception of Kamrup urban had an AAR that was lower than the rest of the regions. Regarding prostate cancer development risk, the ratio is 1 in 42 for the cumulative risk for Delhi and 1 in 47 for 'Kamrup Urban.' Whereas, in West Arunachal, this ratio stood at 1 in 462, which is significantly lower (Sankarapillai *et al.*, 2024).

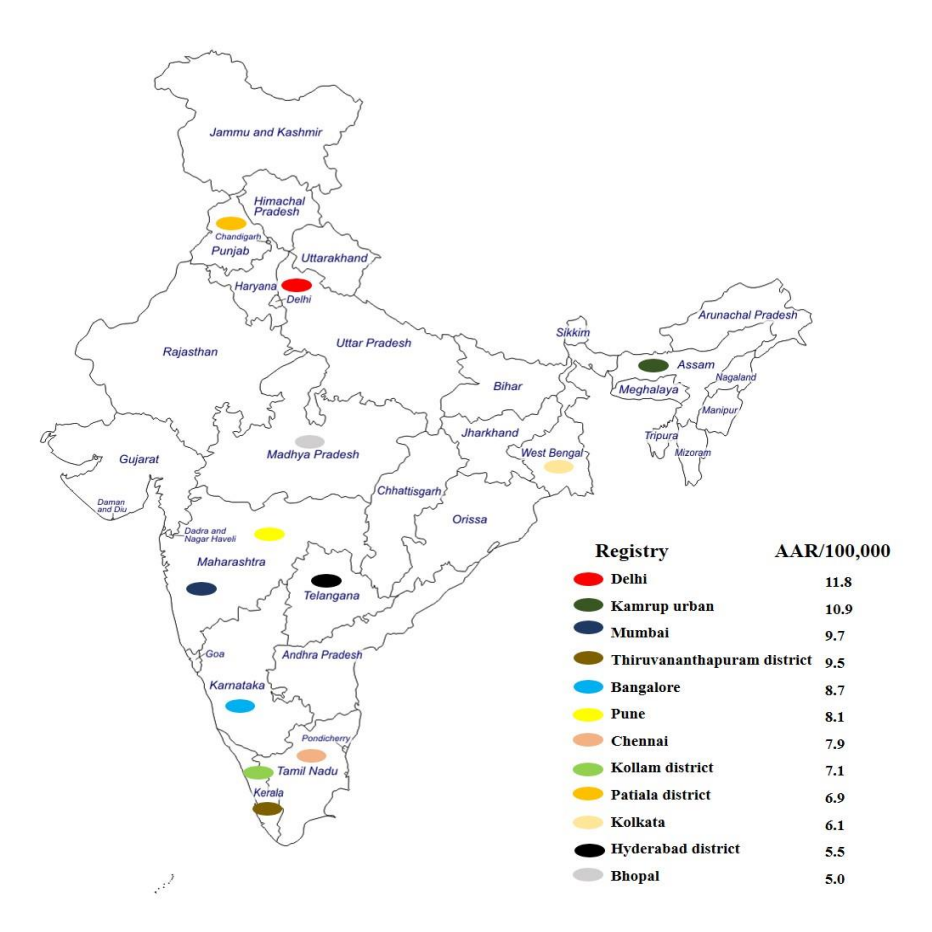


Figure 2.2: Total number of prostate cancer cases registered with an incidence rate of ≥ 5 per 100,000 across 28 Population-Based Cancer Registries (PBCRs) under the National Cancer Registry Programme from 2012 to 2016. AAR = Age-Adjusted Incidence Rate.

2.3 Prostate gland

The prostate gland, a vital component of the male reproductive system, is shaped like a walnut (**Figure 2.3**). The average weight of the prostate in adult men usually ranges between 7 to 16 grams, while its mean weight is standardized at 11 grams. In a prostate exam, this gland can be felt

underneath the urinary bladder (Leissner & Tisell, 1979; Thompson, 2022). The main function of the prostate is to secrete prostatic fluid, which is an important component of semen. The prostatic fluid is what makes a man fertile so it becomes extremely essential in terms of reproduction. The gland responsible for this surrounds the urethra at the bladder neck which connects to the bladder and completes the lower urinary tract (Young *et al.*, 2013; Vásquez, 2014; Al-Ankoshy *et al.*, 2021).

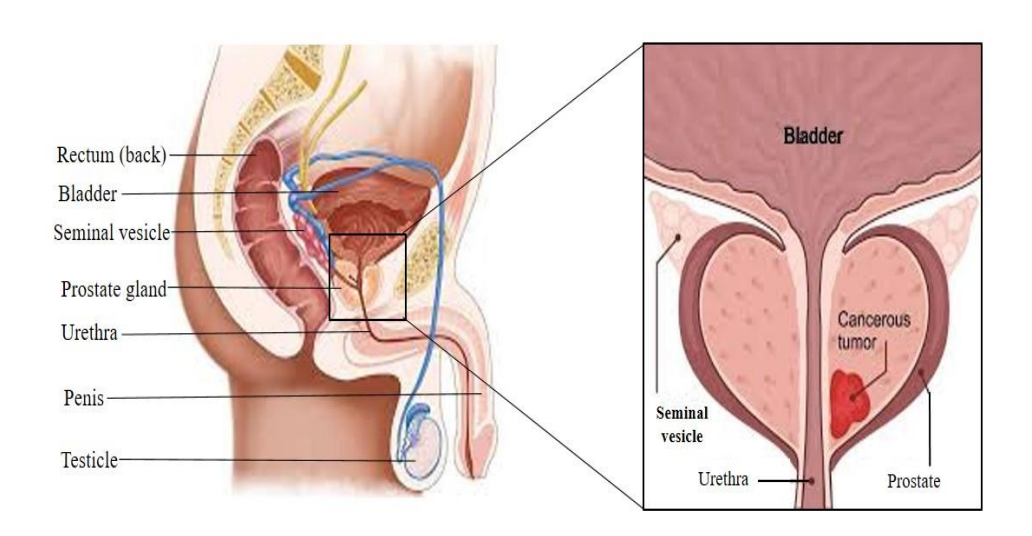


Figure 2.3: Anatomical Structure of the Prostate Gland in the Male Reproductive System (adapted and drawn by the author from [Sharma *et al.*, 2017; Obukohwo *et al.*, 2021]).

2.4 Types of prostate cancer

Prostate cancer primarily originates in the glandular cells and exhibits a wide range of behaviors, from slow-growing to highly aggressive types. The main types are the summarized in the **Table 2.1** below:

Table 2.1: Types of prostate cancer

Type of Prostate	Description	Reference(s)
Cancer		
Prostatic	Most common type (90–95% of cases); originates in the	Siripurapu et al. (2023)
Adenocarcinoma	peripheral zone. Grows slowly, often curable if detected	
	early.	

Small Cell Carcinoma	Aggressive, PSA levels remain unchanged, made of small	Furtado et al. (2011);
	round cells. Hard to detect, can only found at advanced	Abusnina et al. (2018)
	stages.	
Squamous Cell	Aggressive non-glandular type; does not raise PSA levels.	Nadal et al. (2014); Palmieri
Carcinoma	Rare and similar to small cell carcinoma.	et al. (2022)
Prostatic Sarcomas	Very rare (<0.1% of cases); affects men aged 35-60.	Cancer Research Society
	Originates from connective, lymphatic, or vascular tissue	(2016); Erul et al. (2026)
	in the prostate.	
Transitional Cell	Rare type; arises from tumors originating in the urethra or	Ifeanyi (2018); Manini &
Carcinomas	bladder.	López (2020)

2.5 Etiology and risk factors of prostate cancer

Prostate cancer incidence and prevalence among the male population are continuously rising around the globe. Its precise cause (etiology) is not known, but like other types of cancer, it has a genetic, environmental, and lifestyle basis. As it is for most common cancers, the cause of PC is still not clear despite extensive and ongoing research efforts to elucidate its underlying mechanisms. Old age, family history, hereditary factors, and ethnicity are particularly understood associated risks for prostate cancer (Ng, 2021). Epidemiological studies have linked the onset of prostate cancer to factors such as diet, lifestyle, obesity, inflammation, high blood sugar levels, infections, and being exposed to chemicals or ionizing agents (radiation). (Siemińska & Baran, 2022; Ko *et al.*, 2025). The etiology and risk factors of prostate cancer are summarize in the **Table 2.2** below:

Table 2.2: Etiology and risk factors of prostate cancer

Etiological Factor	Description	References
/ Risk Factor		
Age	PC is most common in elderly men; risk increases after	Rawla (2019)
	40 in Black men and for white men without family	
	history, it rises beyond age 50.	
Ethnicity	Higher incidence in African-American men; attributed	Rawla (2019); Rebbeck (2017)
	to both biological and socioeconomic factors.	

Family History	20% of PC patients have a family history; genetic	Mohler et al. (2016); Rawla
	background may account for 5% of cases. Risk	(2019); Muller et al. (2013)
	increases with high-penetrance alleles.	
Genetic Mutations	Heritable mutations contribute ~10% of PC cases.	Eeles et al. (2008); Rawla (2019);
	Notable genes: HPC1, HOXB13, BRCA1/2, PALB2,	Chen et al. (2003); Gallagher et al.
	CHEK2, RAD51D, ATM, MLH1, MSH2, MSH6,	(2010); Camp & Tavtigian (2002).
	PMS2 (Lynch Syndrome).	
Diet – General	High consumption of saturated fat from animals is	Narita et al. (2019); Aronson et al.
	linked to an elevated risk of PC via metabolic and	(2010); Rawla (2019)
	hormonal pathways.	
	High dairy/calcium intake (>2000 mg/day) linked to	Zhao et al. (2023); Koh et al.
	increased PC risk.	(2016); Rawla (2019)
	Processed/red meat intake correlates with PC	Koh et al. (2016); Nouri-Majd et
	incidence and mortality.	al. (2022); Rohrmann et al. (2007)
	Cruciferous vegetables reduce PC risk due to their	Watson et al. (2013); Singh et al.
	abundance of phytochemicals with anticancer activity.	(2005); Rawla (2019)
	Lycopene, the major carotenoid in tomatoes, acts as a	Liu et al. (2008); Ivanenkov et al.
	potent antioxidant and plays a significant role in	(2014); Liadi (2024)
	suppressing molecular pathways associated with	
	carcinogenesis.	

2.6 Types and treatment of prostate cancer

Prostate cancer treatment involves a range of approaches based on the cancer stage, patient health, and personal preferences, which include **Active surveillance**, suitable for low-risk, localized prostate cancers and involves routine monitoring through PSA tests and biopsies (UCLA Health system, 2009; Bott *et al.*, 2003). **Surgery** is employed to remove the prostate and surrounding tissues, with incontinence (stress, overflow, and urge) being a common postoperative issue (Silva *et al.*, 2014; American Cancer society, 2023). **Radiation therapy** includes radiation from external beam and brachytherapy, both targeting cancer cells by damaging their DNA (Song *et al.*, 2022; Kazemi *et al.*, 2023). **Hormone therapy**, which blocks or lowers testosterone, includes methods like orchiectomy, LHRH agonists and antagonists, androgen receptor inhibitors, and androgen synthesis inhibitors. These slow tumor growth, with some drugs offering reversible options or fewer cardiac side effects (Cancer Research UK, 2014; Desai *et al.*, 2021; Kumar *et al.*, 2023).

Chemotherapy is often used when prostate cancer spreads and becomes resistant to hormone therapy, delivering drugs systemically to kill cancer cells (Charalambous & Kouta, 2016; Nader *et al.*, 2018). **Immunotherapy**, which is typically saved for more advanced instances, strengthens the immune system to target cancer cells, although it might have negative side effects like fever and exhaustion (Silva *et al.*, 2020; Okwundu *et al.*, 2021). Phytocompounds also show promise for decreasing the side effects and improving treatment efficacy.

2.7 Prostate cancer target proteins

A druggable target refers to a biomolecule that acts as a key regulator in the metabolic pathway. It regulates the key regulatory step and it is usually specific for that disease. Interactions that typically happens between protein-protein and protein-nucleic acid interactions, which leads to the amplification of signals and/or alteration of metabolic processes, has a major impact on how an illness develops (Mandal & Mandal, 2009). It may be possible to stop or slow the spread of prostate cancer to other areas of the body by targeting a particular protein that is frequently overexpressed in the disease. The important prostate cancer target proteins include Aurora A kinase (AURKA) (Otto *et al.*, 2009), delta-like ligand 3 (DLL3) (Rudin *et al.*, 2017), N-myc proto-oncogene protein (N-Myc) (Gustafson *et al.*, 2014), Cytotoxic T-lymphocyte antigen 4 (CTLA-4) (Yu *et al.*, 2011), 5α-Reductase (5AR) (Aggarwal *et al.*, 2010; Schmidt & Tindall, 2011; Robitaille & Langlois, 2020), Lysine-specific histone demethylase 1A (LSD1) (Niwa *et al.*, 2020), Androgen receptor (AR) (Liss & Thompson, 2018), and CD27 (Liu *et al.*, 2021).

2.7.1 Aurora A kinase (AURKA)

Aurora A kinase (AURKA) functions as a serine/threonine protein phosphorylating enzyme for cell cycle control, predominantly, in mitotic spindle assembly and centrosome maturation (Nikonova *et al.*, 2013). AURKA dysregulation demonstrates a link to different types of cancer with prostate cancer among them. AURKA overexpression in cells leads to worsening cancer features which results in faster metastasis and lower life expectancy. Because of its function in oncogenesis, this makes it a compelling therapeutic target for the treatment of prostate cancer. By facilitating the G2/M transition and mitotic spindle assembly, AURKA contributes to the uncontrolled proliferation of cancer cells. Also, AURKA interacts with the AR pathway, an important driver in the progress to castration-resistant prostate cancer (CRPC). This interaction

underscores the potential of AURKA as therapeutic target in CRPC (Zerdan et al., 2025; Du et al., 2021).

A selective AURKA inhibitor such as **Alisertib (MLN8237) and VX-680 (Tozasertib)** have shown promising preclinical and clinical activity by inducing apoptosis and cell cycle arrest. Identifying newly bioactive compounds that demonstrate anti-tumor effects by targeting AURKA-mediated pathways will be of great importance (Durlacher *et al.*, 2016; Khushbu, 2024).

2.7.2 Delta-like ligand 3 (DLL3)

The Notch signaling pathway inhibition through Delta-like ligand 3 (DLL3) triggers its activity to neuroendocrine tumors (Chou *et al.*, 2023). Recent evidence shows that Delta-like ligand 3 (DLL3) plays a role in aggressive prostate cancer where it affects neuroendocrine prostate cancer (NEPC) (Patel *et al.*, 2019). Given its selective expression in tumor cells and limited presence in normal tissues, DLL3 has become a promising therapeutic target for prostate cancer. A DLL3-targeting ADC initially developed for SCLC, demonstrating cytotoxic effects by delivering a DNA-damaging payload to DLL3-positive cells (Patel *et al.*, 2023). Preclinical studies are evaluating DLL3 as a druggable target for CAR T-cell treatment in neuroendocrine tumors, including NEPC (Patel *et al.*, 2019).

2.7.3 N-Myc proto-oncogene protein (N-Myc)

MYCN gene encoded the protein called the "N-Myc proto-oncogene protein (N-Myc)" functions as one of the MYC family of transcription factors which control cell division, proliferation and apoptosis (Kouroukli *et al.*, 2024). Experts have discovered that N-Myc serves as a key factor in the development of neuroendocrine prostate cancer (NEPC) while continuing to be recognized mostly for its link to neuroblastoma (Lee *et al.*, 2016). Targeting N-Myc emerges as a modern strategy to advance the development of novel treatments for prostate cancer. Research has proven that aberrant expression of N-Myc act as an essential NEPC driver that enables cell transformations and therapeutic resistance (Dardenne *et al.*, 2016). NEPC presents increased N-Myc expression that results in loss AR dependency and allows the cancer to adapt to androgen-deprivation therapies (Chang *et al.*, 2017). The N-Myc stability results from Aurora A kinase activity which allows alisertib inhibitors to demonstrate tumor-suppressing properties. The development of combination therapies is required by integration of N-Myc inhibitors with current treatments like

chemotherapy and immunotherapy to enhance treatment success (Chang et al., 2017; Beltran et al., 2020).

2.7.4 Cytotoxic T-lymphocyte antigen 4 (CTLA-4)

Cytotoxic T-lymphocyte antigen 4 (CTLA-4) is an immune checkpoint receptor; it functions as an essential component for T-cell suppression together with maintaining the immune homeostasis (Scalapino & Daikh, 2008). CTLA-4 competes against the CD28 co-stimulatory receptor for binding with B7-1 (CD80) and B7-2 (CD86) antigens expressed by antigen-presenting cells thus reducing T-cell proliferation and immune response (Qureshi *et al.*, 2011). CTLA-4 functions as an important therapy target for cancer immunotherapy because of its immunosuppressive properties especially in prostate cancer therapy despite the barriers to immune evasion (Jafari *et al.*, 2020). Research shows that advanced prostate cancer patients with elevated CTLA-4 levels become resistant to chemotherapy and ADT (androgen deprivation therapy). The combined treatment of CTLA-4 and PD-1/PD-L1 inhibitors shows enhanced tumor immune response in prostate cancer patients (Rotte, 2019). Scientific research explores therapeutic strategies that combine immune checkpoint inhibitors with conventional prostate cancer treatments to enhance patient response (Rotte, 2019; Cheng *et al.*, 2024).

2.7.5 5α-Reductase (5AR)

5α-Reductase (5AR) serves as a significant metabolic enzyme which performs the conversion of testosterone to its more potent derivative, dihydrotestosterone (DHT) (Brito, 2016; Raith *et al.*, 2023). Studies have intensively explored 5AR as a therapeutic target for prostate cancer treatment due to its importance in prostate development and cancer progression (Hsu *et al.*, 2011). Medical researchers have proposed blocking 5AR activity as a strategy to decrease androgen stimulation because it slow down tumor progression management (Watson *et al.*, 2015; Raith *et al.*, 2023). Several 5AR inhibitors (5ARIs) were established and studied for their potential in prostate cancer:

• **Finasteride:** A selective inhibitor of 5AR type 2, shown to reduce prostate volume and lower PSA (prostate-specific antigen) levels but with limited efficacy in high-grade PC (Vaselkiv *et al.*, 2022; Yang *et al.*, 2024).

- **Dutasteride:** Inhibits both 5AR type 1 and type 2, leading to more significant suppression of DHT production compared to finasteride, with studies suggesting a retarded risk of PC development (Yang *et al.*, 2024).
- Combination Therapies: Combining 5ARIs with ADT (androgen deprivation therapy) has been explored to enhance therapeutic effects and delay progression to CRPC (Pippione *et al.*, 2011; Yang *et al.*, 2024).

2.7.6 Androgen receptor (AR)

The androgen receptor acts as a transcription factor that requires activation by ligands to control prostate cancer development. The androgen receptor relies on testosterone together with dihydrotestosterone (DHT) for activation which drives prostate cell exponential growth (Silva et al., 2024; Obinata et al., 2024). Targeting AR signaling represents a vital therapeutic approach in prostate cancer cases especially those classified as advanced as well as CRPC. Medical scientists have developed three distinct AR inhibitors that used in CRPC treatment including darolutamide, enzalutamide and apalutamide (Ferraldeschi et al., 2015; Kim et al., 2021). Additionally abiraterone acetate functions as a CYP17 inhibitor intratumoral androgen level reduction (Reid et al., 2008; Jacob et al., 2021).

2.7.7 Lysine-specific histone demethylase 1A (LSD1)

Lysine-specific histone demethylase 1A (LSD1) is a FAD-dependent enzyme that control epigenetics through dual demethylating functions on H3K4 and H3K9 (Kim *et al.*, 2021). LSD1 maintains crucial functions within biological processes which include gene transcription and chromatin remodeling and advances studies link it to treatment responses in prostate cancer, due its role in managing androgen receptor signals and tumor growth (Cucchiara *et al.*, 2017; Perillo *et al.*, 2020). The treatment of prostate cancer by inhibiting LSD1 involves the use of ORY-1001 along with GSK2879552 as small-molecule inhibitors alongside therapeutic strategies that combine the AR inhibitors such as enzalutamide and immune checkpoint inhibitors to improve results (Harris *et al.*, 2022; Maylin *et al.*, 2024).

2.7.8 CD27

CD27 functions as a member of TNFRSF7 family receptors which activates T cells and controls immune system regulation according to Starzer *et al.* (2019). Adaptive immunity depends on CD27

which exists primarily on T and B cells while natural killer cells also express this protein (Zhang et al., 2020). CD27 has established itself as a promising immunotherapeutic target in cancer treatment because of its immune regulatory functions which apply to prostate cancer (Starzer et al., 2019). CD27-targeted therapies, including agonist antibodies like varillumab, are being explored for enhancing anti-tumor immunity in prostate cancer, particularly in combination with checkpoint inhibitors, androgen deprivation therapy (ADT), and co-stimulatory pathway targeting for synergistic therapeutic effects (Li-Zhen et al., 2015; Butt et al., 2019; Starzer et al., 2019).

2.8 Medicinal plants used as a management of prostate cancer

Natural products serve as renowned origins for developing pharmaceutical compounds utilized to treat several human ailments such as cancers (Chopra & Dhingra, 2021). Approximately 11,14,000 extracts have been tested for anticancer efficacy from 35,000 plant samples obtained by the NCI (National Cancer Institute) from 20 different countries (Singh et al., 2020). Over 3025 plant species has been documented to contain antitumor properties (Hartwell, 1982; Asma et al., 2022). Natural compounds, especially those found in food serve as primary components in developing novel chemopreventive agents based on research conducted by Surh (2005) and George et al., (2021). Ethnobotanical and ethnopharmacological data can support more economical drug discovery programs because they offer better benefits in identifying prospective anticancer molecules than traditional plant species screening methods (Albuquerque et al., 2014). In instance, certain types of cancer and heart diseases can be prevented by phytochemicals. The understanding of cancer etiology has made it clear that blocking DNA damage while simultaneously promoting DNA repair through predominant cell proliferation inhibition would reduce the occurrence of cancer. There are many anticancer plants which might provide useful sources for the development of drugs which can be used in the treatment of cancer (Koklesova et al., 2020; George et al., 2021; Ashong, 2024).

2.9 Flax

Flax (*Linum usitatissimum* L.) had been grown 30,000 years ago and generally known as pale flax (Fu, 2023). It is one of the most significant crops grown and used by the ancestors. This flax has been widely used for fiber and oil production (Pavagada, 2013). Flax, as a highly branched plants, has been used to enhance flower production and thereby and thereby optimize seed yield. In animal

and human nutrition, flax has so many health-related properties and can be used to cure different

diseases (Cullis, 2019).

2.9.1. Taxonomy and genetics

Linum usitatissimum is a family of Linaceae and it has more than 200 species which includes

about 14 genera. L. usitatissimum is a herbaceous which cultivated once in a year. Flax is a self-

pollinating plant with a roughly 370 Mb genome (Ragupathy et al., 2011). The flax taxonomy is

as follows:

Kingdom: Plantae

Subkingdom: Tracheobionta

Superdivision: Spermatophyta

Division: Magnoliophyta

Class: Magnoliopsida

Subclass: Rosidae

Order: Linales

Family: Linaceae

Genus: Linum L.

Species: *Linum usitatissimum L.* (Akter et al., 2019; Pansare et al., 2020)

2.9.2 Flax microgreens

Young, delicate greens known as microgreens are taken and sold at the first true leaf stage, which

include cotyledons (seed leaves), first true leaves and stem. The cultivation of microgreens had

been increased very rapidly since late 1980s due to its health significance (Stavropoulos et al.,

2019). Microgreens can be grown from practically any type of grain, herb, or vegetable seed, even

those from untamed species. Microgreens have entered the market and gained popularity due to

their initial true leaves having higher nutrient concentrations than their mature leaf counterparts

(Samuolienė et al., 2019).

20

Additionally, it has been proven that flax microgreens are highly nutritious and attention has been paid for its consumption (Puccinelli *et al.*, 2022). Several studies have been shown that the flax microgreens contain higher antioxidant content, important micronutrients (Zn, Mn, and Fe), water-soluble vitamins, amino acid, fatty acids and proteins as compared to flaxseeds (Santin *et al.*, 2022).





Figure 2.4: Flaxseeds and flax microgreens

2.9.3. Important components in flax

Flax has nutritionally important components which include; dietary fiber, phytoestrogens, high-quality protein and high content of alpha-linolenic acid (ALA). It contains about 55 % ALA, 35 % fiber and 28–30 % protein (Kajla *et al.*, 2015; Haque *et al.*, 2024). Flaxseed is the major source of lignan-Secoisolariciresinol glycoside (SDG) and it also contains other lignans, namely lariciresinol, matairesinol, pinoresinol and yatein (Dmitriev *et al.*, 2021; Chhillar *et al.*, 2021).

2.9.4 Major polyphenols in flax

Polyphenols are naturally occurring compounds that offer various health benefits beyond their antioxidant properties (Rana *et al.*, 2022). Research indicates that diets rich in polyphenols may help prevent the development of several chronic diseases, including diabetes mellitus, cancer, neurodegenerative disorders, and cardiovascular conditions. (Gasmi *et al.*, 2022; Rudrapal *et al.*, 2022).

2.9.4.1 Lignans

Lignans are the most prevalent polyphenols in flax/flaxseed with secoisolariciresinol diglucoside (SDG) as the major lignan (Zanwar *et al.*, 2014), other lignans include isolariciresinol, matairesinol pinoresinol, pinoresinol diglucoside and anhydrosecoisolariciresinol (Sicilia *et al.*, 2003; Mueed *et al.*, 2024; Thomas *et al.*, 2024). SDG is a plant lignan metabolized by intestinal microbiota to enterodiol (ED) and enterolactone (EL), which have phytoestrogenic activity and potentially help prevent hormone-related cancers (Silva *et al.*, 2019). The level of SDG in flaxseed varies from 0.6 to 1.8 gram per 100 gram (Prasad, 2013).

2.9.4.2 Phenolic acids (PAs)

PAs, specifically hydroxycinnamic acids and hydroxybenzoic including p-coumaric acid, ferulic acid, and caffeic acid, are present in flaxseeds (Huang *et al.*, 2024). Additionally, according to research carried by Cullis, (2019) proved that flax leaf contain caffeic glucosides, ferulic, *p*-coumaric, hydroxy-3-methylglutaric acid (HMGA), herbacetin 3,8-*O*-diglucosid, sinapic acids and glucosides. These phenolic acids have high total antioxidant capacity and act as synergists alongside other antioxidants, improving the overall antioxidant capacity of flax extracts (Li *et al.*, 2019).

2.9.4.3 Flavonoids

Flax also possesses trace levels of flavonoids such as herbacetin and kaempferol derivatives (Gai *et al.*, 2023). While not as prevalent as lignans, flavonoids make up part of the anti-inflammatory and cardioprotective responses seen with consumption of flaxseed (Duarte *et al.*, 2025).

2.9.5 Anticancer activities of polyphenols

Polyphenols are bioactive compounds present in plant-based foods rich in antioxidants and having anti-inflammatory activities. These compounds are capable of scavenging free radicals which can damage various cell components leading to mutations and cancer (Zhang *et al.*, 2022). Beside having antioxidant activities, polyphenols alter important enzymes and signaling pathways involved in cellular growth and division. By changing these molecular mechanisms, polyphenols help restrain the triggering, encouraging, and advance features of cancer (Lewandowska *et al.*, 2016; Cháirez-Ramírez *et al.*, 2021).

Earlier study revealed that polyphenols like flavonoids, lignans, and phenolic acids can cause programmed cell death in certain cancer cells, prevent angiogenesis and limit the cancer's spread

(Hazafa *et al.*, 2022). For instance, flaxseed contains lignans which have shown good results in combating hormone-sensitive malignancies especially breast and prostate cancers, these characteristics suggest polyphenols could have cancer preventive properties and serve as possible complementary treatment to standard cancer therapies which would enhance the management of cancer in a more natural and non-toxic way (Briguglio *et al.*, 2020; Stepień *et al.*, 2025).

P-coumaric acid, a phenolic acid found in flax, has been shown to inhibit cell proliferation in colon cancer through its antioxidant action and ability to reduce DNA damage (Tehami *et al.*, 2023). Ferulic acid, another phenolic compound, suppresses tumor growth in breast, liver, and colon cancers by inducing apoptosis and enhancing the effects of chemotherapy (Gadelmawla *et al.*, 2022; Helmy *et al.*, 2022; Abdulal *et al.*, 2024). Caffeic acid also shows anti-proliferative properties in lung and colon cancers, mainly through inhibition of cancer-promoting signaling pathways (Chiang *et al.*, 2914; Alam *et al.*, 2022). Additionally, flavonoids like kaempferol and herbacetin inhibit proliferation and angiogenesis in cancers such as ovarian, pancreatic, and lung cancer, contributing to their potential as supportive agents in cancer treatment (Luo *et al.*, 2009; Morais *et al.*, 2024). Together, these flax-derived polyphenols offer targeted anti-proliferative effects across a range of cancer types.

2.9.6 Identified bioactive compounds

Polyphenols are naturally occurring phenols having many other health benefits apart from their antioxidant activity (Rana *et al.*, 2022). Previous studies have indicated that polyphenol-rich diets prevent the development of certain diseases, including diabetes mellitus, cancers, neurodegenerative diseases, and cardiovascular diseases (Gasmi *et al.*, 2022; Rudrapal *et al.*, 2022). A compound known as 4,4'-methylenebis (2,6-di-tert-butylphenol) [4,4'-M(2,6-DTBP)] is a member of polyphenols synthesized in plants through a shikimate/phenylpropanoid pathway, which leads to the formation of different polyphenolic compounds involved in plant defense, antioxidant activity, and other biological functions (Sharma *et al.*, 2019; Šamec *et al.*, 2021; Boyle *et al.*, 2012). A number of studies have demonstrated a vast array of biological activities of 2,4-di-tert-butyl-butyl phenol (2,4-DTBP), a derivative of 4,4'-M(2,6-DTBP), including antibacterial, anti-inflammatory, antifungal, antioxidant, and anti-cancer activities (Aravinth *et al.*, 2023; Dalawai *et al.*, 2023).

$$(CH_3)_3C$$
 $C(CH_3)_3$ CH_2 $C(CH_3)_3$ $C(CH_3)_3$ $C(CH_3)_3$

Figure 2.5: Chemical structure of 4,4′-methylenebis(2,6-di-tert-butylphenol).

Quinones are naturally occurring secondary metabolites that are found in microbes, plants, and other organisms (Thomson RH, 1997). Since ancient times, people have been using quinones for pharmaceutical applications, including antimalarial, antimicrobial, and antitumor. According to Mumtaz *et al.* (2025), these free radical scavengers can serve as protective agents against a number of illnesses, including diabetes, rheumatoid arthritis, atherosclerosis, and cancer. 2,5-DTBQ is a bioactive compound that belongs to the family of benzoquinones. It has various properties that make it of interest in phytochemistry and pharmacology (Gopal *et al.*, 2013).

$$O$$
 CH_3
 H_3C
 CH_3
 $CH_$

Figure 2.6: Chemical structure of 2,5-di-tert-butyl-1,4-benzoquinone

2.10 Biochemistry of cell death and apoptotic signaling

Cell death is essential for development, tissue maintenance, and preventing disease, with apoptosis being one of the most well characterized forms of programmed cell death, particularly relevant in cancer research. Apoptosis occurs through two main mechanisms: the intrinsic (mitochondrial) and extrinsic (death receptor) pathways (Figure 2.7). The intrinsic pathway is triggered by internal stressors such as DNA damage, oxidative stress, and oncogene activation, and is regulated by the Bcl-2 family of proteins, pro-apoptotic members like Bax and Bak promote mitochondrial outer membrane permeabilization (MOMP), while anti-apoptotic proteins such as Bcl-2 and Bcl-xL inhibit it. Once cytochrome c is released into the cytosol, it associates with Apaf-1 and procaspase-9 to assemble the apoptosome, leading to activation of caspase-9 and then the executioner caspases (caspase-3, -6, -7) (Chaudhry et al., 2022; Kari et al., 2022; Westaby et al., 2022; Mustafa et al., 2024). The extrinsic pathway is initiated by extracellular ligands such as FasL, TNF-α, or TRAIL binding to their respective death receptors (e.g., Fas/CD95, TNFR), which recruit adaptor proteins like FADD to form the death-inducing signaling complex (DISC) to activate caspase-8. Caspase-8 then directly activates executioner caspases or cleaves Bid, thereby linking to the mitochondrial pathway (Tian et al., 2024). Both pathways converge on the executioner caspases, leading to hallmark apoptotic changes: cell shrinkage, membrane blebbing, DNA fragmentation, and apoptotic body formation.

In prostate cancer (PCa), apoptotic signaling is often dysregulated. Overexpression of anti-apoptotic proteins such as Bcl-2 family members, mutations or inactivation of tumor suppressor p53, and altered death receptor signaling contribute to evasion of apoptosis and disease progression, particularly in castrate-resistant prostate cancer (CRPC) (Westaby *et al.*, 2022). Recent reviews and studies have highlighted therapeutic opportunities by targeting intrinsic pathway components, such as BH3-mimetics, modulators of Bcl-2/Bcl-xL/MCL-1, and agents restoring p53 function or enhancing mitochondrial outer membrane permeabilization to overcome resistance mechanisms (Helal *et al.*, 2023; Saddam *et al.*, 2024; Tian *et al.*, 2024). Flaxseed and its phytochemicals have also been explored for their capacity to promote apoptosis via mitochondrial pathways in prostate cancer cells, showing increased expression of Bax, caspase-3 and other pro-apoptotic factors in treated cell lines (HPLC phenolic profile study, Linum usitatissimum in LNCaP)

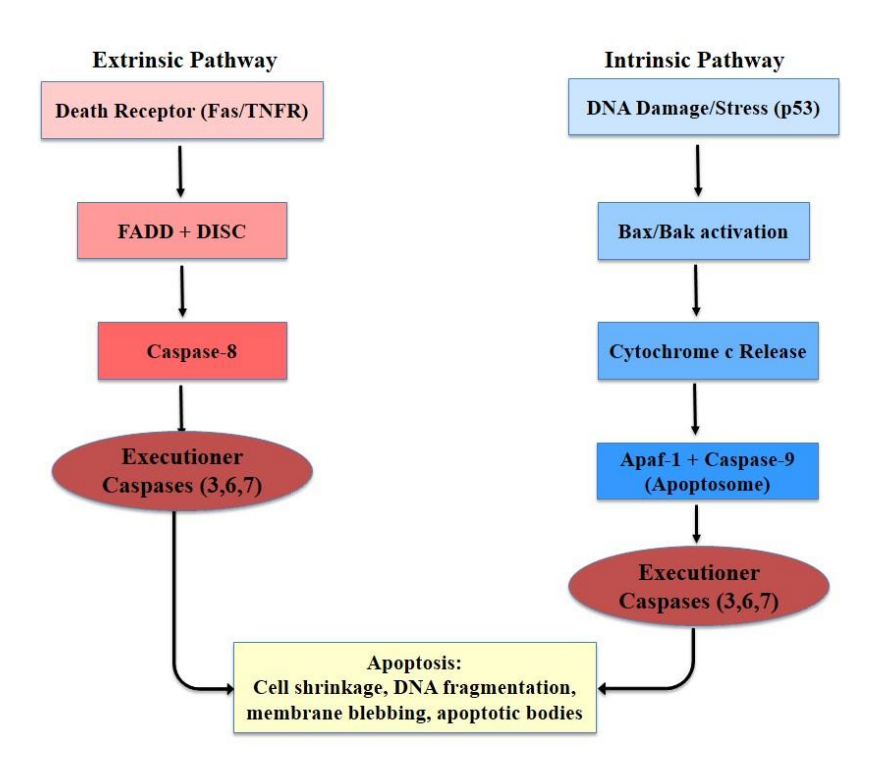


Figure 2.7: Apoptotic signaling pathways

CHAPTER THREE

3.0 MATERIAL AND METHODS

3.1 Chemicals/ reagents

4,4'-Methylenebis(2,6-di-tert-butylphenol) and 1,1-diphenyl-2-picrylhydrazyl (DPPH) were procured from Sigma-Aldrich, St. Louis, MO, USA. Dulbecco's Modified Eagle's Medium (DMEM), Fetal Bovine Serum (FBS), Phosphate Buffered Saline (DPBS), Trypsin-EDTA solution, and MTT reagent were obtained from MP Biomedicals, Germany. Dimethyl Sulfoxide (DMSO), Propidium Iodide (PI), Methanol (HPLC grade), and HPTLC Silica Gel 60 F₂₅₄ Plates were purchased from Merck, Darmstadt, Germany. The Annexin V-AbFluorTM 488 Apoptosis Detection Kit (KTA0002) was acquired from Abbkine Scientific Co., Ltd (Abbkine, Inc., USA).

3.2.1 Plant material and growth conditions

Flax seeds were purchased from a Phagwara Market, located in Phagwara, Punjab, India. The trays were filled with coco peat and the flaxseeds were sprinkled evenly and thickly over it. The flaxseeds were misted gently with plant sprayer to avoid over watering and preventing the seed from being displaced. The trays were placed in a warm and well-lit area (Hi-Tech polyhouse 26°C to 30°C during daytime and 15°C to 18°C in night) to avoid direct sunlight as it can dry out the coco peat. The coco peat's moisture level was checked daily and misted carefully to avoid overwatering. The microgreens were harvested by cutting them just above the surface of the coco peat with clean scissors.

3.2.2 Collection and identification of plant materials

Flax microgreens were collected from Hi-Tech Polyhouse (equipped with fan pad system for cooling, thermo-regulation and misting facility for maintaining humidity inside chamber), Lovely Professional University (LPU) Phagwara, Punjab-India. Its identity was authenticated by a Professor in Plant Taxonomy, Kebbi State University of Science and Technology Aliero (KSUSTA) Dr. Dharmendra Singh, with voucher specimen number (KSUSTA/PSB/H/Voucher No: 657) deposited in the herbarium of the institute. The collected microgreens were washed to make them free from cocopeat and shade dried at room temperature.

3.2.3 Extraction using the cold maceration method

50 grams of powdered flax microgreen were extracted with 250 ml of methanol using the cold maceration technique. The mixture was kept for 24 hours in a stopped container, then it was filtered using No. 1 Whatmann filter paper (Vargas-madriz *et al.*, 2020). The filtrate was concentrated using a rotary evaporator and freeze-dried using a lyophilizer. The dried methanolic extract was further extracted using solvents of different polarity (n-hexane, ethyl acetate, n-butanol, and water) (Ho *et al.*, 2019). The concentrated extracts were stored at -4 °C for subsequent analysis. The percentage yield of each extract was calculated using the following formula:

Percentage yield (%) = [Weight of solvent free extract (g)]
$$\times 100$$

Weight of dried plant (g)

3.3 Preliminary phytochemical screening

The methanolic extract of flax microgreens (MEFM) were subjected to qualitative phytochemical analysis in order to establish distinct phytoconstituent profiles, as stated by (Riaz *et al.*, 2018; Usman *et al.*, 2020). MEFM was accurately weighed and subsequently dissolved in its corresponding parent solvents to attain a concentration of 10 mg/ml, equivalent to a stock solution containing 1% extract (w/v). **Table 3.1** presents the standardized preparation facilitated the execution of various tests, each conducted independently on the MEFM.

Table 3.1: Phytochemical screening of MEFM

S/N	Test	Procedure	Positive Result Reference	
3.3.1	Alkaloids	1 mL of 1% HCl + 3 mL MEFM +	White or cream Usman et al	
	(Meyer's Test)	few drops of potassium mercuric	ercuric precipitate 2020; Rajasree et	
		iodide.		al., 2021
3.3.2	Saponins	0.5 mL MEFM + 2 mL distilled	Persistent froth > 10	Usman et al.,
		water; shaken vigorously.	mins 2020; Rajasree et	
				al., 2021
3.3.3	Tannins	2–3 mL MEFM + few drops of 5%	Dark green (condensed),	Riaz et al., 2018;
		ferric chloride.	Blue-black	Usman et al.,
			(hydrolysable)	2020
3.3.4	Flavonoids	MEFM + small amount of NaOH.	Yellow color fades with	Usman et al.,
			weak acid	2020; Rajasree et
				al., 2021

3.3.5	Steroids	500 mg MEFM + 2 mL glacial	Blue-green color	Rajasree et al.,
	(Liebermann's	acetic acid + 1 drop conc. H ₂ SO ₄ .		2021
	Test)			
3.3.6	Terpenoids	5 mL MEFM + 2 mL chloroform +	Reddish-brown layer	Velavan, 2015;
	(Salkowski Test)	3 mL conc. H ₂ SO ₄ .		Usman et al.,
				2020
3.3.7	Glycosides	osides 50 mg MEFM hydrolyzed with Red color at interface Rajasree		Rajasree et al.,
	(Borntrager's	conc. HCl (2 hrs), filtered, 2 mL		2021
	Test)	hydrolysate + 3 mL chloroform,		
		shaken; layer + 10% NH ₃ .		
3.3.8	Coumarins	2 mL MEFM + 3 mL of 10%	Yellow color	Velavan, 2015
		NaOH.		
3.3.9	Phenols (Ferric	MEFM + 3–4 drops of ferric	Bluish-black color	Riaz et al., 2018;
	Chloride Test)	chloride.		Usman et al.,
				2020
3.3.10	Chalcones	0.5 g MEFM + 2 mL ammonium	Reddish color	Velavan, 2015
		hydroxide.		
3.3.11	Emodins	MEFM + 2 mL ammonium	FM + 2 mL ammonium Red coloration Velavan, 2015	
		hydroxide + 3 mL benzene.		
3.3.12	Quinones	2 mL MEFM + conc. H ₂ SO ₄ ; shaken	Red coloration	Riaz et al., 2018;
		vigorously for 5 min.		Usman et al.,
				2020
		1	1	

3.4 Antioxidant activity

3.4.1 The DPPH scavenging assay

A DPPH scavenging assay was used to estimate the extracts' free radical scavenging activity (Reddy, 2013; Rajasree *et al.*, 2021). The methanol was used to prepare 0.1 mM DPPH solution, and 1.6 mL of methanol extract at different concentrations (62.5–1000µg/mL) was added to 2.4 mL of DPPH solution. The mixture was thoroughly vortexed and incubated in the dark at room temperature for 30 minutes. Then, its absorbance was measured at 517 nm using spectrophotometry. The following formula was to determine the % DPPH scavenging activity:

%DPPH scavenging activity = $(Absorbance of control - Absorbance of the sample) \times 100$ Absorbance of control

The IC₅₀ value was determined by plotting the percentage of inhibition against the concentration. Each concentration was tested in triplicate to ensure accuracy and reproducibility (Rajasree *et al.*, 2021).

3.4.2 Determination of metal chelating potential

The metal chelating activity of MEFM was assessed following the method described by Chew *et al.* (2009). An Fe²⁺-ferrozine complex (0.1 mM FeSO₄ and 0.25 mM of <u>ferrozine</u>) was added into 0.2 mL of the extract at different concentrations ($62.5 - 1000 \mu g/mL$). The mixture was incubated for 10 min at RT, and the absorbance was recorded at 562 nm. Positive control (EDTA).

3.4.3 Ferric reducing power activity

The reduction of iron (III) to iron (II) by the antioxidant compounds involves single electron transfer via a redox reaction mechanism and can be studied using ferric reducing power (Santos-Sánchez *et al.*, 2019). 2.5 mL of phosphate buffer (pH 6.6) was added to both extract and standard (ascorbic acid) at different concentrations of 62.5, 125, 250, 500, and 1000μg/mL each. A 2.5 mL aliquot of 1% potassium ferricyanide was added to the resulting solutions, which were then heated at 50°C for 20 min. Subsequently, TCA (2.5 mL) was added and spinned at 2,000 rpm for 10 min. After collecting the supernatant, dH₂0 (1 mL) and 0.1% FeCl₃ (250 μL) were added. The solution's absorbance (700 nm) was recorded. The color of the sample in the reducing power assay changes from yellow to green or blue depending on the antioxidant's reducing ability, with higher absorbance values indicating stronger reducing power (Koksal *et al.*, 2011; Rajasree *et al.*, 2021; Perumal *et al.*, 2024).

3.4.4 Gas chromatography-mass spectrometry analysis

The Shimadzu (GCMS-TQ8040 NX) Gas Chromatograph was used for the GC-MS study. It was connected to a Perkin Elmer Turbomass 5.1 mass detector Turbo mass gold with an Elite - 1 (100% Dimethyl poly siloxane) capillary column measuring 30 m × 0.25 mm ID × 0.25 µm. The temperature of the instrument was initially set to 50°C, and it remained there for three minutes. The oven temperature was increased at the rate of 10°C/min, rosed up to 300°C and maintained for 8 min. Injection port temperature was ensured at 250°C and helium flow rate at 1.02 ml/min. The ionization voltage was 70 eV. The split mode of injection for the samples was 10:1. The range of the mass spectral scan was 34 -600 (m/z). It kept the interface temperature at 310°C and the ion source temperature at 240°C. The MS start time was 4 min, and end time was 37 min with solvent

cut time of 4 min. The contents of phytochemicals present in the test sample were identified based on the comparison peak area, peak height, retention time (min) and mass spectral patterns with those spectral database of authentic compounds stored in the National Institute of Standards and Technology (NIST) library (Linstrom & Mallard, n.d.).

3.5 In silico studies

3.5.1 Protein modeling studies of delta-like ligand 3 (DLL3)

3.5.1.1 Delta-like ligand 3 sequence recovery

The delta-like ligand 3 (DLL3) sequence of humans was obtained in FASTA format from the UniprotKB database with sequence identity (ID: Q9NYJ7) (UniProt Consortium, 2019). The ExPASy ProtParam server were used to compute the physicochemical properties of protein sequence which include molecular weight (MW), isoelectric point (pI), instability index (II), total number of amino acids residues, grand average hydropathy (GRAVY), extinction coefficient, and aliphatic index (ai) (Sahay et al., 2020). The InterPro server and Conserved Domain Database (CDD) of the NCBI were used to confirm the protein domains and functional sites after they were identified using the Prosite database (Sigrist et al., 2012; Lu et al., 2020). PSSpred and SOPMA online tools were used to study and analyze the structural features of the Delta-Like Ligand 3 (DLL3) (Joshi et al., 2023). The protein conformation was selected viz. alpha-helix, beta-sheet, coil and turn, window width and similarity threshold were maintained at 17 and 8, respectively, whereas 50 output with used for SOPMA. The transmembrane regions were identified using TMHMM 2.0 (Luo et al., 2023). Important features like solvent accessibility, amino acid arrangement, secondary structure, and its composition were assessed using the PredictProtein server. The buried hydrophobic and exposed hydrophilic regions reflected the solvent accessibility (Yachdav et al., 2014).

3.5.1.2 Protein modeling

The SWISS-MODEL online software was used to generate 3D structure of protein target (DLL3) (Waterhouse *et al.*, 2018). Comparative protein modeling is carried out by the SWISS-MODEL using fragment-based assembly and local similarity search. Protein threading, homology modeling and *ab-initio* are the protein modeling techniques used by the SWISS-MODEL. After superimposing the two created models, a standard deviation and distance plot were produced. Ramachandran plot analysis was used to study the stereochemical characteristics of the modeled

protein (Park *et al.*, 2023). The overall structural quality of the modelled DLL3 was obtained using SAVES v6.0 server with PROCHECK, VERIFY 3D, and PROVE (Joshi *et al.*, 2023). The UCSF Chimera 1.13.1was used to generate publication-quality images and structural analysis (Pettersen *et al.*, 2004).

3.5.1.3 Molecular docking study

A molecular docking simulation was used to study the protein-ligand interaction using PyRx tool which is a virtual screening tool that employs Vina as well as Autodock 4.2 (Verma et al., 2023; Dallakyan & Olson, 2015). The phytochemicals and three FDA approved drugs in .sdf format were obtained from the PubChem database (www.pubchem.com) and converted into .pdbqt format before running docking (Lawal et al., 2020; Gulati et al., 2023). The 3D structure of target proteins was download from the protein databank (http://www.rscb.org/pdb) and using grid box analysis, the active site was manually predicted (Verma et al., 2023). Protein configurations were improved by removing extraneous water molecules and the only area essential for binding with ligands was kept. The optimal geometries for docking scenarios were obtained by ligand optimization. The docking begins as soon as the ligands and proteins are ready. In this stage, the ligands were bound into the active side of the protein and the binding affinity was measured. Through PyRx AutoDock Vina simulations, the binding affinity strengths and patterns were attained, and protein-ligand interaction were understood and identified. After docking search is completed, then Protein-Ligand interaction profiler (PLIP), PyMOL and LigPlot software were used to study protein-ligand interactions in the pdb format preparations (Spackman et al., 2021; Verma et al., 2022; Kumar et al., 2024). The ligand's binding strength were determined using a negative score (kcal/mol) (Ortiz et al., 2019):

$$K_i = e^{\Delta G/RT}$$

Where: $\Delta G = \text{Gibbs free energy}$; $R = (1.985 \text{ x } 10^{-3} \text{ kcal/mol/K})$; T = (298.15 K)

3.5.1.4 ADME properties and toxicity prediction

ADMETlab 3.0 online (https://admetlab3.scbdd.com/server/evaluationCal) (Duan *et al.*, 2023) and ProTox-3.0 online software (https://tox.charite.de/protox3/index.php?site) (Banerjee *et al.*, 2024) prediction tools were used to study the physicochemical properties, lipophilicity, water solubility, pharmacokinetics, drug-likeness and toxicity prediction, violations of Veber's rule (Veber *et al.*,

2002), violations of Lipinski's rule of five (Lipinski *et al.*, 1997), with only one violation accepted in the case of variables (Kaur *et al.*, 2022).

3.6 Isolation and identification of bioactive compounds

3.6.1 UV-Visible spectroscopy

3.6.1.1 Preparation of standard

 $100\mu g/ml$ stock solution was prepared by adding 100 ml of solvent (hexane) into 10 mg of standard in a volumetric flask. The various concentrations of 1, 2, 3, 4, 5, 6, and $7 \mu g/ml$ were prepared by withdrawing 0.1, 0.2, 0.3, 0.4, 0.5, 0.6, and 0.7 ml of solutions from the stock solution and diluting them to 10 ml with hexane. The same methodology was applied for the remaining solvents (ethyl acetate, butanol, and water) (Kadam *et al.*, 2018).

3.6.1.2 Determination of maximum wavelength by UV-VIS spectroscopy

Standard solution (5 µg/ml) was scanned at a wavelength of 200-800 nm using UV-VIS spectrophotometer. For the hexane, ethyl acetate, butanol, and water solutions, respective solvents were utilized as blanks (Behera *et al.*, 2012; Kadam *et al.*, 2018).

3.6.1.3 Preparation of standard calibration curve by UV-VIS spectroscopy

The absorbance of a standard solution prepared from stock solutions of various solvents (hexane, ethyl acetate, butanol, and water) in the concentration range of 1–7µg/ml was measured in triplicate in order to obtain the standard calibration curve. The absorbance was plotted against concentration for the calibration curve (Kadam *et al.*, 2018).

3.6.1.4 Preparation of test solution for UV-VIS spectroscopy

To prepare 10μg/ml of extract solutions, 1 mg of extract from each solvent (hexane, ethyl acetate, butanol, and water) was carefully weighed, transferred into a 100 mL conical flask, and the respective solvents were added up to the mark. The absorbance of resultant solutions was analyzed in different solvents (Kadam *et al.*, 2018).

3.6.2 HPTLC analysis

3.6.2.1 Preparation of standard solution

1 mg/mL of stock was prepared by dissolving the 6 mg of standard compound in 6 mL of methanol. Consequently, 1 mL of the stock solution was added to 10 mL of methanol to obtain 0.1 mg/mL solutions (Muhammad & Pandey, 2024).

3.6.2.2 Test samples (Extract) preparation

To achieve 1 mg/mL of methanolic extract solution, extract (10 mg) was added into methanol (10 mL). Membrane filter (0.22 mm) was used to filter the resultant solution (Muhammad & Pandey, 2024).

3.6.2.3 HPTLC setup conditions and instrumentation

HPTLC was conducted on a silica gel 60 f 254 (3.0×10 cm; Merck, Germany) HPTLC plate. The plate was kept in a mobile phase automated development chamber containing solvents in a ratio of 20:2.5:0.5:2 (ethyl acetate: methanol: formic acid: water), respectively. Using an automated spray applicator with a 100 μ L syringe, 10.0 μ L of both extract and the standard solution (4,4'-M(2,6-DTBP)) with a concentration of 1 mg/mL was applied to the plates in the form of 6.0 mm bands at the rate of 150 nl/s. The CAMAG-Linomat IV was used for sample application, and its settings were as follows: application rate of 150 nl/s, band length of 6.0 mm, distance between bands 10 mm, distance from the bottom of the plate measuring 8.0 mm, and distance from the plate side edge of 5 mm. WIN CATS program version 1.4.6.2002 was used to densitometrically evaluate the bands using CAMAG TLC Scanner 3. The following were the settings for the scanner: (Scanning rate: 20 mm/s; Slit dimension: 4.00 x 0.30 mm; Mode: absorption/reflection; monochromator band width: 30 nm at an optimum wavelength of 515). The retention factor (Rf) value was calculated by comparing the peak of the isolated component from the extract to that of the standards. The calibration curves were used to determine the target compound's concentration (Adhikari & Saha, 2022; Adhikari *et al.*, 2025).

3.7 in vitro studies

3.7.1 Cell viability assay

The PC-3 cell lines were collected from National Centre for Cell Science (NCCS), Pune. The cells were cultured in DMEM supplemented with 10% FBS, 200µl of the cell suspension (approx.

10,000 cells) was added into 96-well plates and the plate was incubated at 37°C and 5% CO₂ atmosphere for 24 h. After 24 h, the spent medium was replaced with medium containing the test samples at various concentrations (62.5–1000 μ g/ml) and incubated in CO₂ incubator at 37°C, and 5% CO₂ for 24 h.

After this incubation, the drug-containing media were aspirated, and 100 μL of MTT solution (5 mg/mL in PBS) was added to each well. The plate was then incubated at 37 °C for 4 hours. Then, DMSO (100 μL) was added to each well to solubilise formazan crystals, and the contents were mixed gently. After ensuring complete solubilization at room temperature, the absorbance was measured at 570 nm and 630 nm using a microplate reader. The percentage of cell viability was calculated using the following formula, and the IC₅₀ was calculated from the dose-response curve (Mosmann, 1983; Shastry *et al.*, 2021). The percentage cell viability was calculated using formula below:

Cell Viability (%) =
$$\frac{\text{(Abs of treated - Abs of blank)}}{\text{(Abs of treated - Abs of blank)}}$$
 X 100

3.7.2 Annexin V apoptosis assay by flow cytometry

The PC-3 cells were cultured in a 6-well plate at a density of 3×10^5 cells/2 ml and incubated in a CO₂ incubator overnight at 37°C for 24 h. The old media were removed, and the cells were washed with 1 ml 1X PBS. Fresh media containing test compounds at different concentrations were added and incubated for 24 h. One of the wells was left untreated, which served as a negative control. At the end of the treatment, the cells were harvested directly into the centrifuge tubes (5 ml) and washed with PBS (500 μ l). The PBS was removed and replaced with trypsin-EDTA solution (200 μ l). Incubate for 3-4 minutes at 37°C. The cell suspension was transferred directly into the centrifuge tubes and centrifuged at 300 × g for five minutes at 25°C. The supernatant was discarded and the cells were resuspended in 500 μ l annexin V binding buffer. After adding Annexin V-FITC (5 μ l) and PI (2 μ l), they were well combined and left to sit at room temperature in the dark for 15 minutes. After adding an additional 500 μ l of annexin V binding buffer, the samples were subjected to flow cytometry analysis (Elasbali *et al.*, 2022; Shalal & Irayyif, 2023).

3.8 *In vivo* study

The anticancer effects of 2,5-DTBQ, 4,4'-M(2,6-DTBP), and MEFM were further confirmed through animal model research using an adult male wistar rats in good health as the animal model.

3.8.1. Experimental animal

In the present study, male wistar rats weighing between 190 and 230 g were kept in cages made of polypropylene. The Committee for the Purpose of Control and Supervision of Experiments on Animals (CPCSEA) established guidelines that were followed in all experimental operations. started, Before the received ethical approval (Approval Number: study we UMYUCAUC/2024/49). For 14 days before the trial, the wistar rats were acclimated to standard laboratory conditions, which included a 12-hour photoperiodic cycle, 21-25°C, and 45-65% humidity. During the research, the wistar rats received a regular food and unrestricted access to water.

3.8.2 Acute toxicity study of MEFM

The acute toxic effects of MEFM were evaluated according to the method of Lorke (1983). In the initial phase, the wistar rats of both sexes were grouped into three, each consisting of three rats, and administered the extract orally at doses (10, 100, and 1000 mg/kg). They were observed for 24 h for any signs of toxicity. In the subsequent phase, three wistar rats per group received the same extract at higher doses (1600, 2900, and 5000 mg/kg) orally, and were monitored for 24 h for MEFM toxicity or any other signs. As no deaths were observed after both phases I and II, the LD₅₀ of MEFM was assumed to be greater than 5000 mg/kg.

3.8.3 Prostate cancer induction and experimental design

The male wistar rats were weighed before the commencement of the experiment, on the first day of treatment, and on the day of sacrifice. The wistar rats (n=5) were grouped randomly into six groups, as described in **Table 3.2**. Prostate cancer was induced by subcutaneous administration of testosterone (5 mg/kg) dissolved in corn oil for 28 days, as previously described by Joshi *et al*. (2023). The experimental groups (3–6) were administered doses orally only once in a day for 21 sequential days as follows: 10 mg/kg of finasteride, 20 mg/kg of 4,4'-M(2,6-DTBP), 20 mg/kg of 2,5-DTBQ, and 200 mg/kg of MEFM.

Table 3.2: Animal grouping and experimental design

Group	Group category	Injection of 5mg/kg of testosterone in corn oil (Joshi <i>et al.</i> , 2023; Prasad <i>et al.</i> , 2007)	Treatment (Gavage)	References
Group 1	Normal	-	Distilled water	(Joshi et al., 2023; Prasad et al., 2007)
Group 2	Disease	+	Distilled water	(Joshi et al., 2023; Prasad et al., 2007)
Group 3	Standard drug (Finasteride)	+	10 mg/kg	(Akbari <i>et al.</i> ,2021)
Group 4	Group treated with 4,4'-M(2,6-DTBP)	+	20mg/kg	(Mariko <i>et al.</i> , 2019)
Group 5	Group treated with 2,5-DTBQ	+	20mg/kg	(Matsuo et al., 1984)
Group 6	Group treated with extract (MEFM)	+	200 mg/kg	Grudzińska et al.,2023)

Key:

- **Group 1 (Normal control):** This group consisted of healthy, untreated rats that did not receive testosterone or any test compounds. They received only distilled water via gavage and served as the baseline.
- Group 2 (Disease control): Rats in this group received testosterone in corn oil to induce prostate cancer but no treatment, serving as the disease model.
- Group 3 (Standard drug Finasteride): Rats received testosterone plus 10 mg/kg finasteride to serve as the positive control.
- Groups 4–6 (Treatment groups): Rats received testosterone plus the respective test compounds: 4,4'-M(2,6-DTBP), 2,5-DTBQ, and methanolic extract of flax microgreens (MEFM) at specified doses.

3.8.4 Assessment of body weight (BW), prostate weight (PW), and prostatic index (PI)

The initial and final body weight of each individual wistar rat was recorded on the first and last day of the experiment, respectively. Prostate weights (PW) were recorded for all groups. The Prostatic Index (PI), representing the prostate weight to body weight ratio, was calculated for each group. Additionally, the percentage inhibition of prostate weight and inhibition of the prostatic index were determined using the formulas below (Hongcai *et al.*, 2018; Uroko *et al.*, 2022):

% of prostate growth inhibition =
$$100 - \frac{\text{Treatment group - Normal control}}{\text{Negative control - Normal control}} \times 100$$

2.8.5 Biochemical and histological analyses

On the 49th day of the study, Wistar rats were fasted overnight prior to sample collection. Blood was drawn from the retro-orbital plexus under appropriate anesthesia. Following blood collection, the animals were humanely sacrificed, and the prostate glands were immediately dissected, weighed, and prepared for subsequent analyses.

Biochemical analyses: Blood samples were centrifuged at $5,000 \times g$ for 20 minutes to separate the serum. The serum was then used to determine testosterone levels and prostate-specific antigen (PSA) concentrations.

Histological analyses: Prostate tissues were fixed in 10% formalin and sent to the Neuroscience and Bioinformatics Unit, Department of Human Anatomy, Ahmadu Bello University, Zaria, Nigeria. Histological sections were prepared and stained for microscopic examination. Images were analyzed and captured by an expert anatomist, Dr. Akinyemi Ademola. Evaluations were conducted under magnifications of $40\times$ (scale bar = $100~\mu m$) and $60\times$ (scale bar = $50~\mu m$), revealing structural details of the prostate tissue across experimental groups.

3.8.6 Statistical analysis

Data were expressed as Mean ± Standard deviation (SD). Evaluations between group results were performed using a one-way ANOVA test, followed by a t-test. A p-value of less than 0.05 was considered statistically significant. All statistical analyses were conducted using GraphPad Prism Software (GraphPad Software Inc., United States).

CHAPTER FOUR

4.0 RESULTS AND DISCUSSION

4.1 Flax microgreens and growth conditions

The flax microgreens were grown by sowing the flaxseeds in cocopeat at Hi-Tech Polyhouse Lovely Professional University (LPU). The flaxseeds germination time was about 8 days under controlled conditions (26°C to 30°C during daytime and 15°C to 18°C at night). **Figure 4.1** presents well grown flax microgreens in a highly controlled environment called "Hi-Tech Polyhouse" at Lovely Professional University (LPU). Following their growth, extraction of phytochemicals from flax microgreens using methanol showed good yield (33%).



Figure 4.1: Well grown flax microgreens under controlled conditions in Hi-Tech Polyhouse facility.

4.2 Qualitative screening tests of the methanolic extract of flax microgreens

The qualitative analysis of the methanolic extract of flax microgreens showed the presence of numerous phytochemical constituents such as alkaloids, saponins, flavonoids, steroid, cardiac glycoside, coumarins, phenolic compounds and chalcones whereas Tannins, Terpenoids, Emodins were absent as shown in **Table 4.1**, which agrees to the finding of Monica & Joseph (2016) and

Hanaa *et al.* (2017), who found that methanolic extracts of flaxseed contain steroids, terpenoids, tannins, alkaloids, glycosides, flavonoids, phenols anthocyanins and emodins.

Table 4.1: Qualitative chemical tests of the methanolic extract of flax microgreens

S/N	Phytochemicals Analysis	Results
1.	Alkaloids	+VE
2.	Saponins	+VE
3.	Tannins	-VE
4.	Flavonoids	+VE
5.	Steroid	+VE
6.	Terpenoids	+VE
7.	Cardiac glycoside	+VE
8.	Coumarins	+VE
9.	Phenolic compounds	+VE
10.	Chalcones	+VE
11.	Emodin	-VE

Note. +VE = present, -VE = absent

4.3 Antioxidant activity

4.3.1 DPPH scavenging activity

This is a widely used technique for determining a plant extract's potential for antioxidant activity. DPPH donates hydrogen ions to molecules in their oxidized form, acting as a free radical scavenger or an antioxidant (Monica & Joseph, 2016; Girish *et al.*, 2023). The result of the DPPH scavenging activity of MEFM is presented in **Figure 4.2**. The extracts exhibited a concentration dependent increase in scavenging activity. At $1000 \,\mu\text{g/mL}$ concentration, the MEFM exhibited higher DPPH radical scavenging activity of 84.2%. Though MEFM exhibited DPPH radical scavenging activity, it is significantly (p < 0.001) less effective than ascorbic acid at all tested concentrations. The current results agreed with the report by Alachaher *et al.* (2018), which indicates that the DPPH scavenging capacity of methanolic and butanolic extracts of *L. usitatissimum* was 93.1% and

96.2%, respectively, at 800 μ g/mL. According to the results of Hanaa *et al.* (2017), the aqueous methanol (70%) extract of flaxseeds exhibited a maximum level of inhibition of 62.10%, which is significantly higher than the current findings. This might be attributed to the fact that aqueous methanol (70%) is more polar and it can extract a good amount of phenolic compounds.

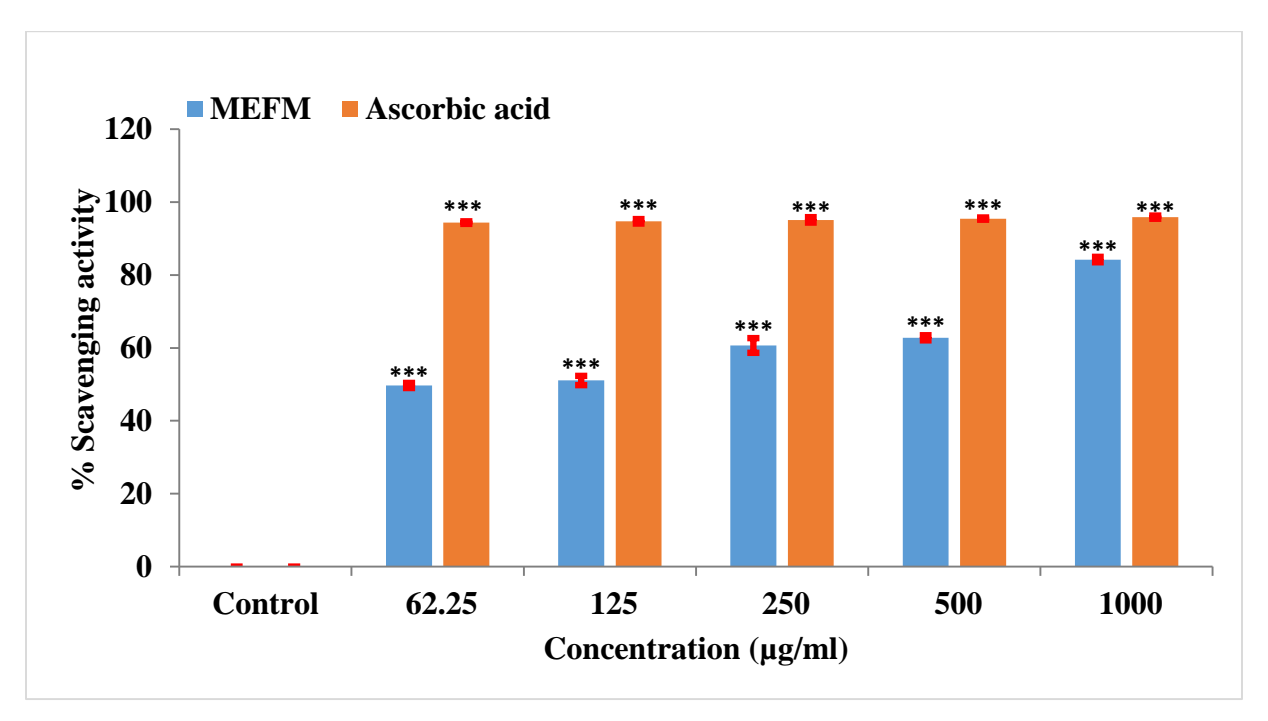


Figure 4.2: DPPH scavenging activity of MEFM compared to ascorbic acid control. Data presented as the mean and standard deviation (mean \pm SD) in triplicate. Mean values (bar graphs), Standard deviation (vertical lines), Asterisk (***) above the bars is statistically significance ($P \le 0.001$).

4.3.2 Metal chelating activity

Transient metal ion chelation is involved in the scavenging of reactive oxygen species by binding transition metals like iron and copper, thereby preventing them from catalyzing harmful ROS-generating reactions such as the Fenton reaction (Fucassi *et al.*, 2014; Zhang *et al.*, 2024). **Figure 4.3** presents the metal chelating capacity of MEFM using EDTA as the standard control. Both the standard and the extract were tested at different concentrations (62.5, 125, 250, 500, and $1000\mu g/mL$). At 500 and $1000\mu g/mL$ concentrations, the MEFM exhibited significant chelating activity of 37% and 38%, respectively. Although MEFM exhibited metal chelating activity, it is significantly (p < 0.001) less effective than EDTA at all tested concentrations. Previous research

had proven that metal chelating activity plays protective effects against oxidative damage caused by metal catalysed decomposition reactions (Gulcin & Alwasel, 2022).

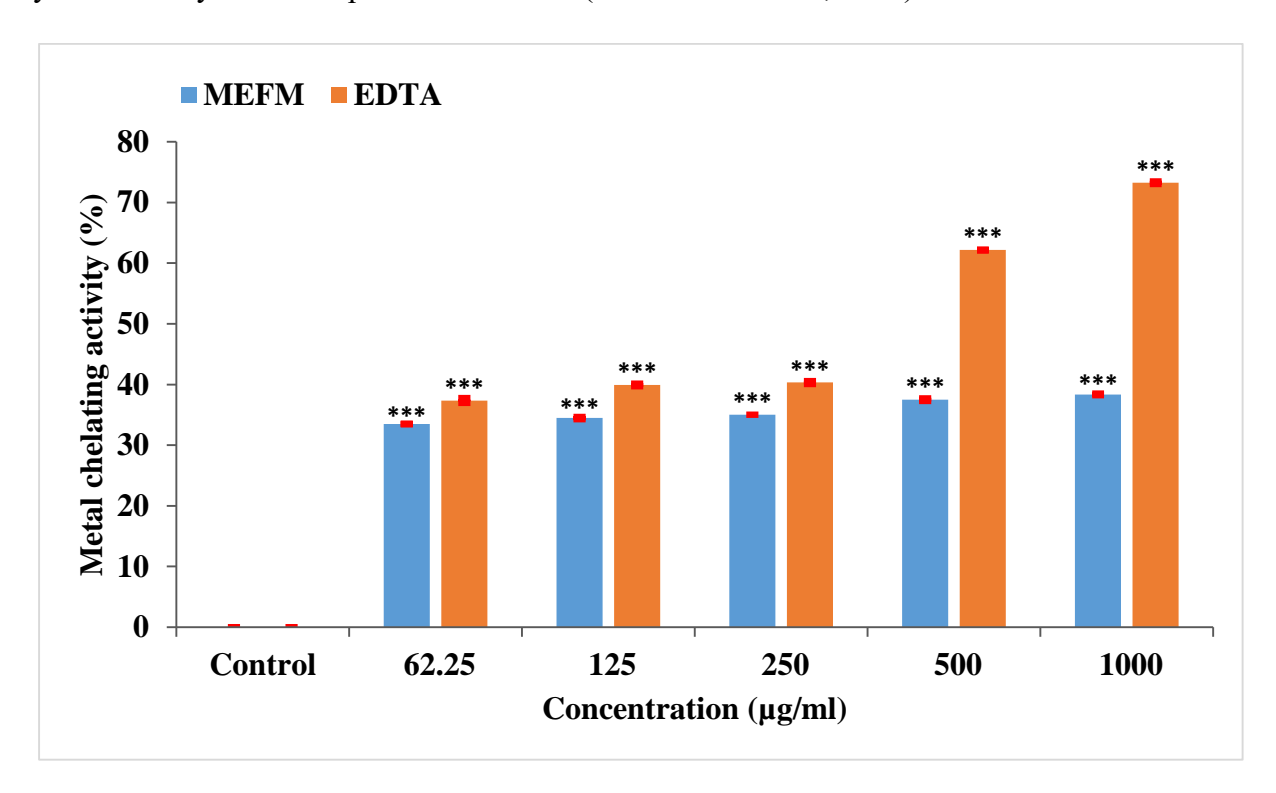


Figure 4.3: Metal chelating activity of MEFM compared to EDTA as control. Data presented as the mean and standard deviation (mean \pm SD) in triplicate. Mean values (bar graphs), Standard deviation (vertical lines), Asterisk (***) above the bars is statistically significance ($P \le 0.001$).

4.3.3 Reducing power assay

The ferric reducing antioxidant potentials of the plant extracts were represented as FRAP values (Esguerra *et al.*, 2024). **Figure 4.4** represents the reducing power assay of MEFM. The ascorbic acid standard and the extract were tested at various concentrations (62.5, 125, 250, 500, and 1000μg/mL). The extracts exhibited a concentration-dependent increase in reducing power activity. At 1000 μg/mL concentration, the MEFM exhibited reducing power activity of 0.94%. While MEFM exhibited reducing power activity, it was significantly (p < 0.001) less effective than ascorbic acid at all tested concentrations. These findings align with those of Ouis and Hariri (2023), who reported that the methanolic extract of flaxseeds demonstrated high reducing power activity, suggesting its potential applications in the food and pharmaceutical industries. Antioxidants prevent biological system damage by scavenging chelating agents, reducing agents, singlet oxygen molecules, and enhancing the activity of antioxidant enzymes (Zanwar *et al.*, 2011; Dumanović *et*

al., 2021). One of the most significant indicators of a compound's possible antioxidant activity is its capacity to reduce oxidative damage (Munteanu & Apetrei, 2021). The presence of reductones is typically linked to the reducing capacity as it was reported to inhibit the peroxide formation (Ouis & Hariri, 2023).

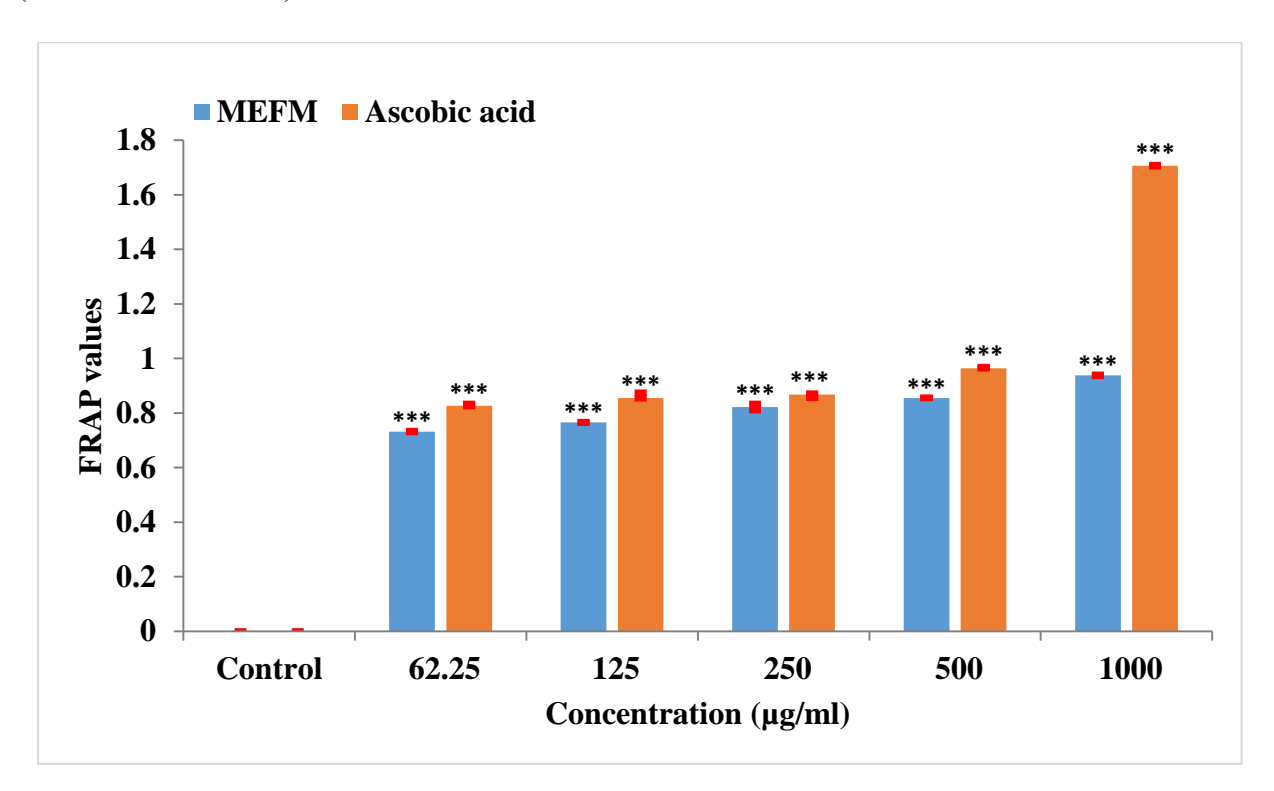


Figure 4.4: Reducing power assay of MEFM compared to ascorbic acid control. Data presented as the mean and standard deviation (mean \pm SD) in triplicate. Mean values (bar graphs), Standard deviation (vertical lines), Asterisk (***) above the bars is statistically significance ($P \le 0.001$), Asterisk (***) above the bars is statistically significance ($P \le 0.001$).

4.4 GC-MS profiling of methanolic extract of flax microgreens

A total of 60 chromatogram peaks were identified from methanolic extract of flax microgreens which correspond to the bioactive compounds and were recognized by relating their retention time, peak area (%), peak height (%) and mass spectral fragmentation patterns to that of the known compounds described by the National Institute of Standards and Technology (NIST) library. According to research conducted by Farag *et al.* (2021), 28 phytochemicals were identified from flaxseed whereas the current study revealed 60 different phytocompounds from flax microgreens. The total ion chromatogram is presented in **Figure 4.5**. **Table 4.2** presents the phytocompounds

along with their corresponding molecular formula, retention time (RT), molecular weight (MW), and peak area (%).

Table 4.2: Bioactive compounds found in methanolic extract of flax microgreens.

SN	RT	Compound	Compound names	Molecular	Molecular	Peak
		CID:		Formula	Weight	area (%)
1	4.188	534410	3-Heptafluorobutyroxypentadecane	$C_{19}H_{31}F_7O_2$	424.4	1.18
2	4.588	7976	2-Methylpyrazine	$C_5H_6N_2$	94.11	0.10
3	4.763	111244	2-Methyl-N-(2 methylpropyl)propan-1-imine	$C_8H_{17}N$	127.23	0.33
4	6.431	10413	4-Hydroxybutanoic acid	$C_4H_8O_3$	104.10	0.08
5	6.492	7938	2,6-Dimethylpyrazine	$C_6H_8N_2$	108.14	0.07
6	7.427	7974	2-Methylpiperidine	$C_6H_{13}N$	99.17	0.15
7	7.710	137584	1-(2-Methylprop-1-enyl)pyrrolidine	$C_8H_{15}N$	125.21	0.19
8	8.524	18372057	But-3-enyl (E)-2-methylbut-2-enoate	$C_9H_{14}O_2$	154.21	0.37
9	8.954	558410	1-(3-Methylbut-3-enyl)pyrrolidine	C ₉ H ₁₇ N	139.24	0.15
10	10.482	5364729	Prop-2-enyl (E)-2-methylbut-2-enoate	$C_8H_{12}O_2$	140.18	0.25
11	11.453	119838	3,5-Dihydroxy-6-methyl-2,3-dihydropyran-4-	$C_6H_8O_4$	144.12	1.03
			one			
12	11.950	5367771	[(Z)-2,5-Dimethylhex-3-enyl] formate	$C_9H_{16}O_2$	156.22	0.21
13	14.608	332	4-Ethenyl-2-methoxyphenol	$C_9H_{10}O_2$	150.17	0.37
14	15.804	83742	1,3-Bis(ethenyl)imidazolidin-2-one	$C_7H_{10}N_2O$	138.17	0.11
15	17.082	5988	Sucrose	$C_{12}H_{22}O_{11}$	342.3	1.48
16	17.255	91737510	Methyl 4-methoxy-2-trimethylsilyloxybenzoate	$C_{12}H_{18}O_4Si$	254.35	0.67
17	17.562	5373219	2-(1-Hydroxybut-2-enylidene)cyclohexanone	$C_{10}H_{14}O_2$	166.22	010
18	17.604	530729	Tridec-2-ynyl 2,6-difluorobenzoate	$C_{20}H_{26}F_2O_2$	336.4	0.13
19	17.831	7311	2,4-Ditert-butylphenol	$C_{14}H_{22}O$	206.32	0.49

20	18.183	267716	1-Methyl-4-[2-(4-methylphenyl)sulfonylethyl]piperazine	$C_{14}H_{22}N_2O_2S$	282.4	0.17
21	18.662	35960	4-Ethenyl-2,6-dimethoxyphenol	$C_{10}H_{12}O_3$	180.2	0.44
22	19.253	545303	7,9-Di-tert-butyl-1-oxaspiro[4,5]deca-6,9-diene-2,8-dione	$C_{17}H_{24}O_3$	276.4	1.99
23	19.647	91719722	2-O-Hexan-3-yl 1-O-(2-methylpropyl) benzene-1,2-dicarboxylate	$C_{18}H_{26}O_4$	306.4	0.13
24	21.275	3026	Dibutyl phthalate	$C_{16}H_{22}O_4$	278.34	0.76
25	21.340	96009	(4-Hydroxyphenyl) acetate	$C_8H_8O_3$	152.15	0.23
26	21.620	91691499	1-Propan-2-yloxyicosane	$C_{23}H_{48}O$	340.6	0.68
27	21.824	985	n-Hexadecanoic acid	$C_{16}H_{32}O_2$	256.42	4.27
28	22.890	7427	Trehalose	$C_{12}H_{22}O_{11}$	342.3	0.76
29	23.460	17161	2,5-Di-tert-butyl-1,4-benzoquinone	$C_{17}H_{24}O_3$	276.4	4.33
30	23.756	64947	(2R,3S,4S,5R,6S)-2-(hydroxymethyl)-6-methoxyoxane-3,4,5-triol	$C_7H_{14}O_6$	194.18	13.01
31	24.091	54725318	L-Ascorbic acid, 6-octadecanoate	$C_{24}H_{42}O_{7}$	442.6	5.21
32	24.375	54018957	Decyl nonyl carbonate	$C_{20}H_{40}O_3$	328.5	1.13
33	24.510	637775	3,5-Dimethoxy-4-hydroxycinnamic acid (Sinapinic acid)	$C_{11}H_{12}O_5$	224.21	3.21
34	24.815	101715	Cyclohexane-1,2,3,4,5-pentol	$C_6H_{12}O_5$	164.16	13.30
35	25.692	5281	Octadecanoic acid	$C_{18}H_{36}O_2$	284.5	1.39
36	25.770	9546746	9,12,15-Octadecatrienoic acid, methyl ester, (Z,Z,Z) 2-	C ₃₉ H ₇₂ NO ₈ P	714	1.01
37	25.911	5280435	Phytol	$C_{20}H_{40}O$	296.5	3.22
38	26.140	5280450	(9Z,12Z)-Octadeca-9,12-dienoic acid	$C_{18}H_{32}O_2$	280.4	0.51
39	26.215	5280934	(9Z,12Z,15Z)-Octadeca-9,12,15-trienoic acid	$C_{18}H_{30}O_2$	278.4	0.74
40	26.612	521846	Tetrapentacontane	$C_{54}H_{110}$	759.4	1.55

41	26.766	532617	Cyclohexyl-(3,5-dimethylphenoxy)-dimethylsilane	$C_{16}H_{26}OSi$	262.46	0.77
42	27.740	11747713	3,7,11-Trimethyl-14-propan-2-ylcyclotetradeca-1,3,6,10-tetraene	$C_{20}H_{32}$	272.5	0.72
43	27.872	10494	Oleanolic acid	$C_{30}H_{48}O_3$	456.7	2.40
44	28.787	547838	2-Methyl-1-(6-methylheptoxy)propan-2-ol	$C_{12}H_{26}O_2$	202.33	0.80
45	29.080	6230	Norethindrone	$C_{20}H_{26}O_2$	298.4	0.59
46	29.170	42956	Hexadecyl 2-ethylhexanoate	$C_{24}H_{48}O_2$	368.6	1.13
47	29.300	8343	Bis(2-ethylhexyl) phthalate	$C_{24}H_{38}O_4$	390.6	0.56
48	29.695	191964	Bis(2-propylpentyl) benzene-1,2-dicarboxylate	$C_{24}H_{38}O_4$	390.6	4.19
49	30.150	8089	Squalane	$C_{30}H_{62}$	422.8	0.35
50	30.720	11008	Dotriacontane	$C_{32}H_{66}$	450.9	0.67
51	31.038	8372	4,4'-Methylenebis (2,6-di-tert-butylphenol)	$C_{29}H_{44}O_2$	424.7	3.74
52	31.478	589198	Octadecyl octanoate	$C_{26}H_{52}O_2$	396.7	0.49
53	32.188	22932	Bis(2-ethylhexyl) benzene-1,4-dicarboxylate	$C_{24}H_{38}O_4$	390.6	1.91
54	32.326	91735525	3-O-octan-4-yl 1-O-pentyl benzene-1,3-dicarboxylate	$C_{21}H_{32}O_4$	348.5	1.13
55	32.550	117981	2-Methyl-2-(2-methylundecan-2-yldisulfanyl)undecane	$C_{24}H_{50}S_2$	402.8	0.73
56	32.875	638072	Squalene	$C_{30}H_{50}$	410.7	4.62
57	34.004	181087	4-Hydroxy-2',3',5',6'-tetrachlorobiphenyl, tert- butyl	$\underline{C}_{12}\underline{H}_{6}\underline{C}\underline{I}_{4}\underline{O}$	308.0	1.40
58	35.395	11002708	(3S,4S)-3,4-Bis(1,3-benzodioxol-5-ylmethyl)oxolan-2-one	$C_{20}H_{18}O_6$	354.4	0.22
59	35.401	290541	5-[4-(1,3-Benzodioxol-5-yl)-2,3-dimethylbutyl]-1,3-benzodioxole	$C_{20}H_{22}O_4$	326.4	0.33
60	5.860	91691425	Cholestane-3,5-diol, 5-acetate, (3beta,5alpha)-	<u>C₂₉H₅₀O₃</u>	446.7	0.52

RT: Retention Time

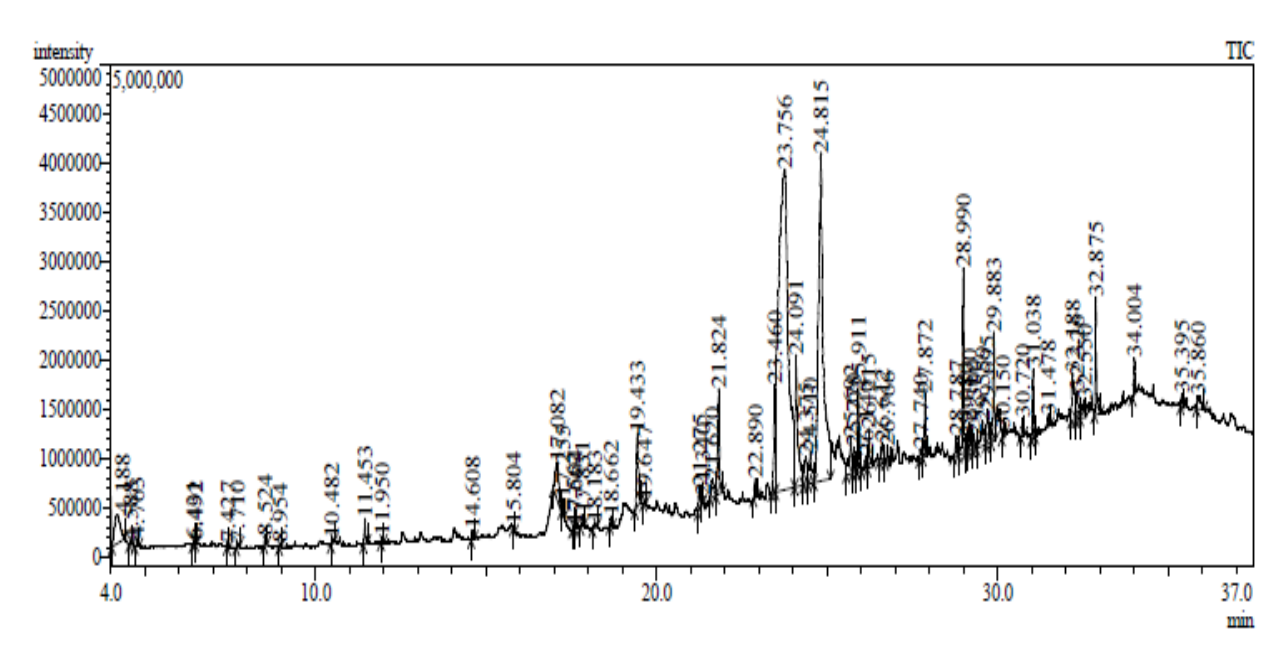


Figure 4.5: GC-MS chromatogram of methanolic extract of flax microgreens (*Linum usitatissimum L.*)

4.5 Molecular docking screening and bioactive compound selection process

GC-MS analysis result revealed that the **MEFM** contain several phytocompounds that exhibit various phytochemical activities. The prostate cancer target molecules were identified after intensive literature searches, focusing on key signaling pathways, molecular markers, and therapeutic targets associated with the disease. For pre-docking screening, all phytocompounds were docked against the eight (8) prostate cancer target proteins and their binding affinities were recorded (**Table S1**) (See appendix). **Figure 4.6** shows the molecular docking screening and selection process of bioactive compounds for further study. **Table 4.3** presents the bioactive compounds with higher peak area (higher than 2.0%) along with their corresponding molecular formula, retention time (RT), molecular weight (MW), and peak area (%).

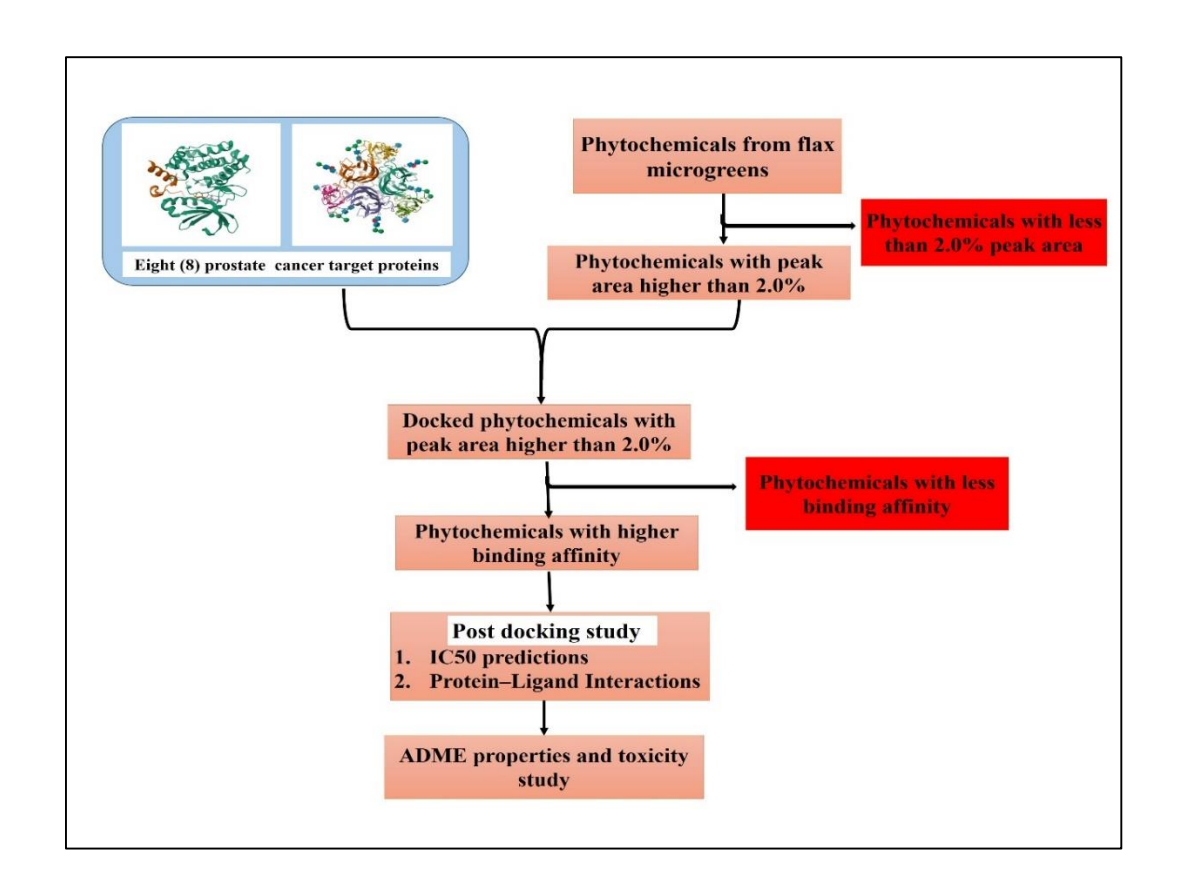


Figure 4.6: Molecular docking screening and bioactive compound selection process

Table 4.3: Flax microgreen's bioactive compounds with highest percentage.

SN	RT	Compound	Compound names	Molecular	Molecular	Peak
		CID:		Formula	Weight	area (%)
1	21.824	985	n-Hexadecanoic acid	$C_{16}H_{32}O_2$	256.42	4.27
2	23.460	17161	2,5-Di-tert-butyl-1,4-benzoquinone	$C_{17}H_{24}O_3$	276.4	4.33
3	23.756	64947	(2R,3S,4S,5R,6S)-2-(Hydroxymethyl)-6-methoxyoxane-3,4,5-triol	C ₇ H ₁₄ O ₆	194.18	13.01
4	24.091	54725318	L-Ascorbic acid, 6-octadecanoate	$C_{24}H_{42}O_{7}$	442.6	5.21
5	24.510	637775	3,5-Dimethoxy-4-hydroxycinnamic acid (Sinapinic acid)	$C_{11}H_{12}O_5$	224.21	3.21
6	25.911	5280435	Phytol	$C_{20}H_{40}O$	296.5	3.22
7	27.872	10494	Oleanolic acid	$C_{30}H_{48}O_3$	456.7	2.40

8	29.695	191964	Bis(2-propylpentyl) dicarboxylate	benzene-1,2-	$C_{24}H_{38}O_4$	390.6	4.19
9	31.038	8372	4,4'-Methylenebis (2,6-di-ter	t-butylphenol)	$C_{29}H_{44}O_2$	424.7	2.74
10	32.875	638072	Squalene		$C_{30}H_{50}$	410.7	4.62

RT: Retention time

4.6 Prostate cancer target proteins

It may be possible to stop or slow the spread of PCa to other areas of the body by targeting a particular protein that is frequently overexpressed in the disease. The important PCa target proteins include Aurora A kinase (AURKA) (Otto *et al.*, 2009), DLL3 (Rudin *et al.*, 2017), N-myc proto-oncogene protein (N-Myc) (Gustafson *et al.*, 2014), Cytotoxic T-lymphocyte antigen 4 (CTLA-4) (Yu *et al.*, 2011), 5 α -Reductase (5AR)) (Robitaille & Langlois, 2020; Schmidt & Tindall, 2011), Androgen receptor (AR) (Liss & Thompson, 2018), Lysine-specific histone demethylase 1A (LSD1) (Niwa *et al.*, 2020), and CD27 (Liu *et al.*, 2021). The structure of all the target proteins except DLL3 was available and downloaded from PDB (http://www.rscb.org/pdb). Therefore, the modeling studies, sequence analysis, selection, and validation of DLL3 were done using different bioinformatic tools.

4.7 Protein modeling studies and sequence analysis of delta-like protein 3 (DLL3)

The structure of DLL3 is not available on PDB database. Therefore, the Delta-Like Ligand 3 (DLL3) sequence of humans was retrieved in FASTA format from the protein sequence and functional information database (UniprotKB) with sequence identity (ID: Q9NYJ7). The ExPASy ProtParam server was used to compute the physicochemical properties of query sequence and tabulated in **Table 4.4**. The result shows isoelectric point (pI), Aliphatic Index (AI), Instability Index (II) and GRAVY value of query protein (DLL3) was 7.590, 66.540, 53.730 and -0.1870 respectively which corroborate with the findings of Joshi BP *et al.* (2023). The isoelectric point (pI) shows the acidity or basicity nature of the protein. With a wider temperature range, the query protein's greater Aliphatic Index (AI) demonstrates its stability. The hydrophilic nature of the protein is indicated by the negative GRAVY values for protein.

Table 4.4: The physicochemical parameters of DLL3.

DLL3
Uniprot ID: Q9NYJ7
592.0
7.590
53.730
66.540
-0.1870

The InterPro and CDD of the NCBI were used to confirm the protein domains and functional sites after they were identified using the Prosite database. **Tables (4.5 and 4.6)** present the domain, profile, and patterns found for DLL3's characteristic functionalities. Six conserved EGF-like domains were found by both Prosite, InterPro and CDD, which is in line with the DLL3's function and the body of existing literatures. **Table 4.6** also illustrates the amino acid sequences for each of the six EGF 3 domains, along with their respective disulfide bond positions. **Figure 4.7** presents the sequence logo which helps in visualizing the cysteine residue position for disulfide bond in the EGF domain.

Table 4.5: Identified Domains from the sequence.

Database	Accession number	Identified Domains
Prosite	PS50026	EGF_3
CDD	cd00054	Calcium-binding EGF-like domain (EGF_CA)
	<u>pfam07657</u>	N terminus of Notch ligand C2-like domain (MNNL)
	pfam00008	EGF-like domain (EGF).
	<u>smart00051</u>	Delta serrate ligand (DSL)
InterPro	IPR013032	EGF-like, conserved site (EGF_CS)

Table 4.6: Prosite result shows the structure, sequence position and disulfide bond between amino acids in domains.

Protein	Domain	Sequence	Amino acid sequence	Disulfide	bond
Name	Name	Position		between A	A
Delta-like	EGF_3	216-249	APLVCRAGCSPEHGFCEQPGECRCLEGW	220-231,	224-237,
ligand 3			TGPLCT	239-248	
		274-310	GPGPCDGNPCANGGSCSETPRSFECTCP	278-289,	283-298,
			RGFYGLRCE	300-309	
		312-351	SGVTCADGPCFNGGLCVGGADPDSAYIC	316-327,	321-339,
			HCPPGFQGSNCE	341-350	
		353-389	RVDRCSLQPCRNGGLCLDLGHALRCRCR	357-367,	362-377,
			AGFAGPRCE	379-388	
		391-427	DLDDCAGRACANGGTCVEGGGAHRCSC	395-406,	400-415,
			ALGFGGRDCR	417-426	
		429-465	RADPCAARPCAHGGRCYAHFSGLVCACA	433-444,	438-453,
			PGYMGARCE	455-464	

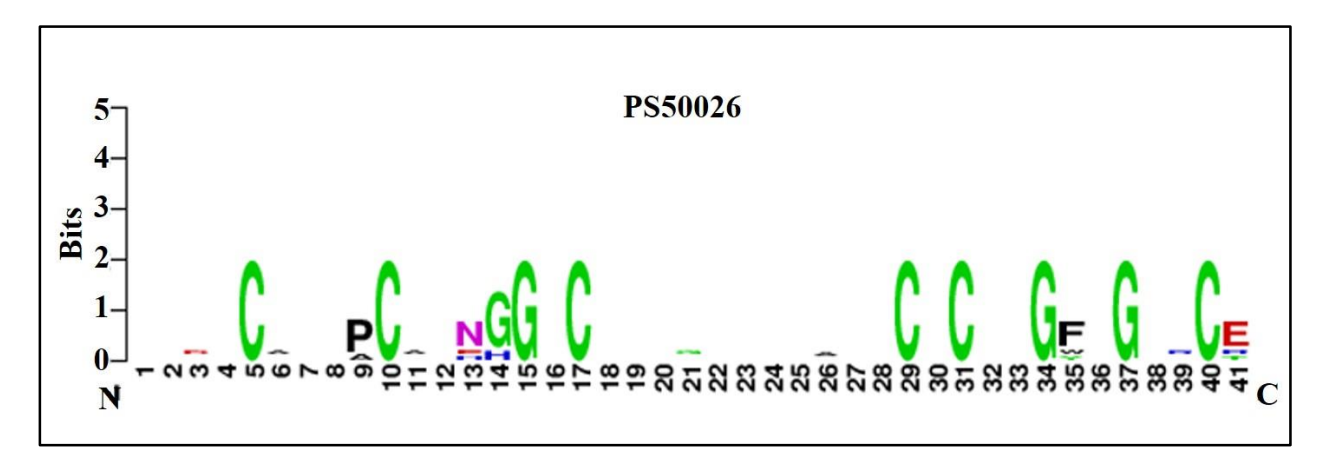


Figure 4.7: Sequence Logo for DLL-3 domain

PSSpred and SOPMA online tools were used to study and analyze the structural features of the Delta-Like Ligand 3 as shown in **Table 4.7** and **Figure 4.8**. The result of SOPMA is comparable with that of PSSpred prediction. The secondary structure of Delta-Like Ligand 3 shows the extended strands, beta turns, alpha helix, and domination of random coils. The PredictProtein server shows a very high percentage of turns and coils for Delta-Like Ligand 3 whereas the presence of strands and helix was significantly lower.

Table 4.7: Prediction of DLL3 secondary structure using SOPMA online tool.

Delta-Like Ligand 3 (Q9NYJ7)	Structural features of DLL3 (%)
α-helix	09.55
310-helix	00.00
π-helix	00.00
ß-bridge	00.00
Extended-strand	14.89
ß-turn	04.53
Bend-region	00.00
Random-coil	71.04

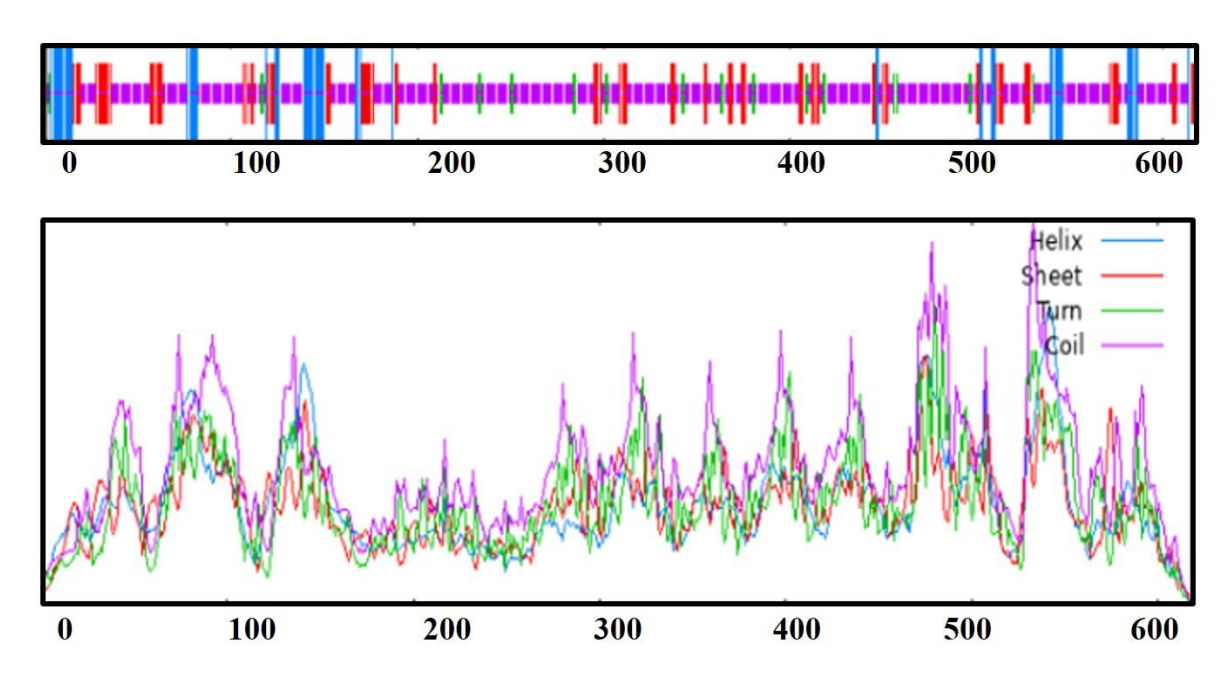


Figure 4.8: Prediction of DLL3 secondary structure using SOPMA online tool.

According to the solvent accessibility analysis, 45.31%, 41.10%, and 13.59% of DLL3 regions are buried, exposed to solvent, and intermediate regions, respectively. The result from DeepTMHMM 1.0.24 revealed that the predicted amino acids in signal, extracellular, transmembrane, and cytoplasmic regions were 1–26, 27–491, 492–513, and 514–618, respectively, (**Table 4.8 and 4.9**) which agrees with the findings of Joshi *et al.* (2023) of about 70%. This can be attributed due to DeepTMHMM 1.0.24 server updation.

Table 4.8: Prediction of the DLL3 domain locations using DeepTMHMM 1.0.24

Transmembrane prediction software	Location of domain	Sequence position
DeepTMHMM 1.0.24 prediction of the DLL3	Signal	1 – 26
domain locations	Extracellular region	27 – 491
	Transmembrane Helix region	492 – 513
	Cytoplasmic region	514 – 618

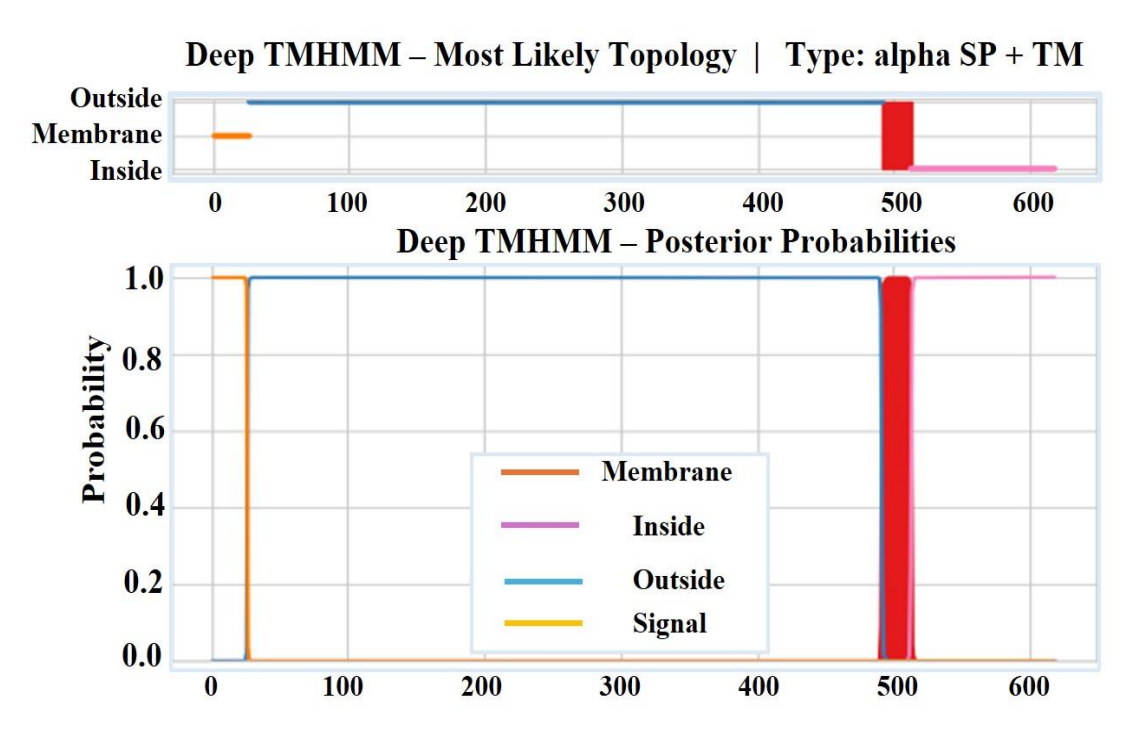


Figure 4.9: Transmembrane helix prediction of DLL-3 using DeepTMHMM (1.0.24)

4.8 Homology modeling and validation

Figure 4.10 presents the accurate prediction of the C2, DSL, and EGF domains generated from the SWISS-MODEL server. Newly modelled protein subjected to additional analysis viz; Ramachandran plot analysis, distance plot standard deviation, RMSD values, secondary structure, cytoplasmic and transmembrane helix prediction. Figure 4.10 also presents the sequence alignment between Human DLL3 and Delta-like protein 1(DLL1). The template used for modeling of Delta-like ligand 3 protein was crystal structure of Delta-like ligand (DLL1) with PDB ID (4XBM). The reliability and quality of the generated model were determined. Figure 4.11 presents the homology modeled structure of Human DLL3. The quality of built protein was further evaluated using PROVE and PROCHECK server. Protein residues are categorized using the Ramachandran plot according to their areas in the quadra plot and the φ and ψ angles of the protein backbone. Glycine is represented by triangles in the quadra plot, while other amino acids are represented by squares. The yellow and red areas represent the allowed and most allowed regions, respectively. The Ramachandran plot of both (query and template sequences) of protein which have been generated using SWISS MODEL is shown in the Figure 4.12. Red regions on the Ramachandran plot represent the most favored and allowed conformations for amino acid residues. Black dots show the actual positions of residues, indicating whether they lie within allowed or

disallowed regions. **Table 4.9** shows the 0.6% of amino acids residues were in the disallowed region. **Figure 4.13** presents ERRAT plot in chain A & B of modelled DLL3 protein. The ERRAT plot also shows some of the regions with high error, these results suggest the need for model refinement. After completion of three iterations of loop refinement there is no residue in the ERRAT plot displays high error and ~99% residues are present in generously allowed regions in the plot. The atomic calculation in form of z-score from PROVE server indicates the quality of the modelled protein structure (**Table 4.10**).

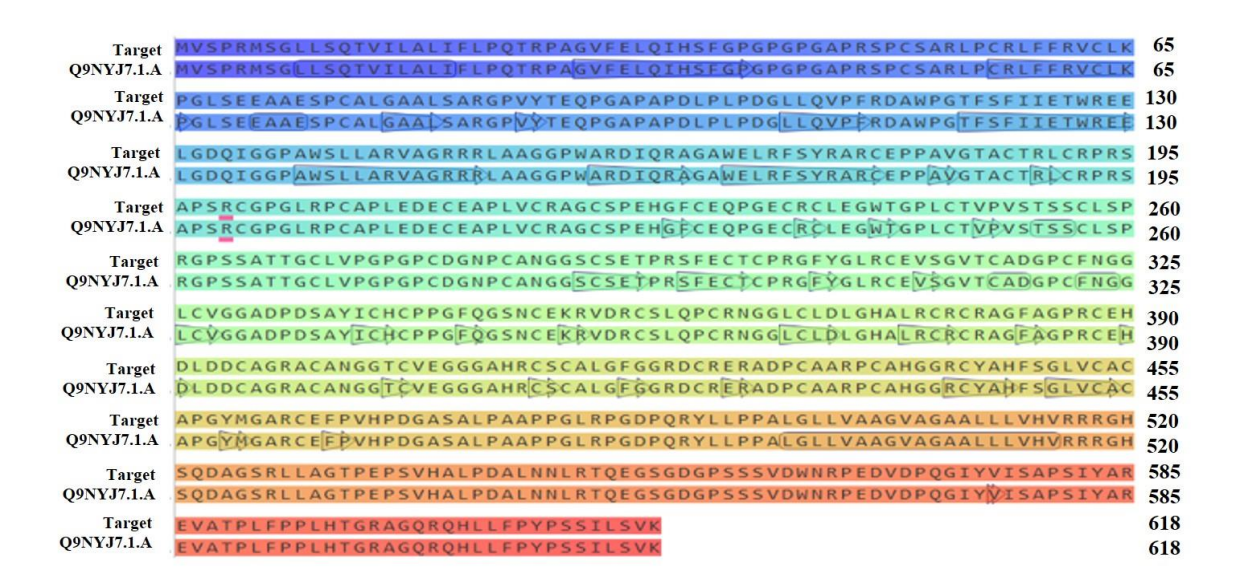


Figure 4.10: Alignment between Human DLL3 and Delta-like protein 1(DLL1)

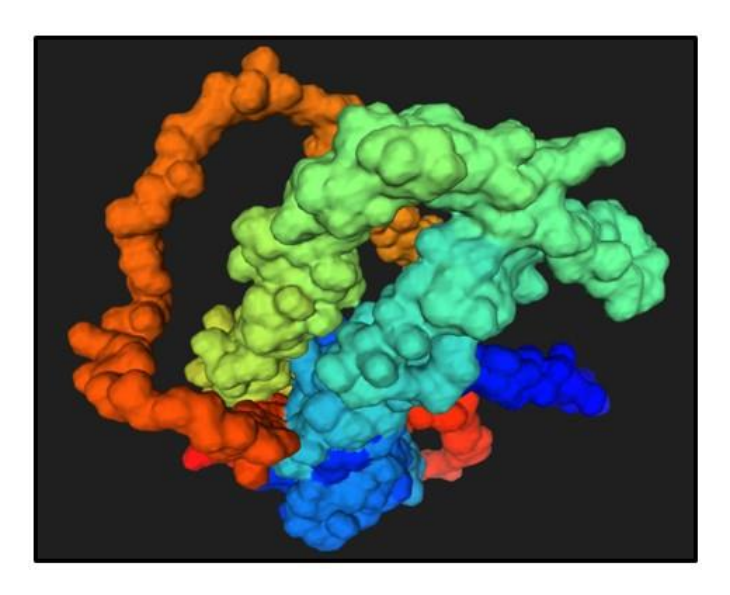
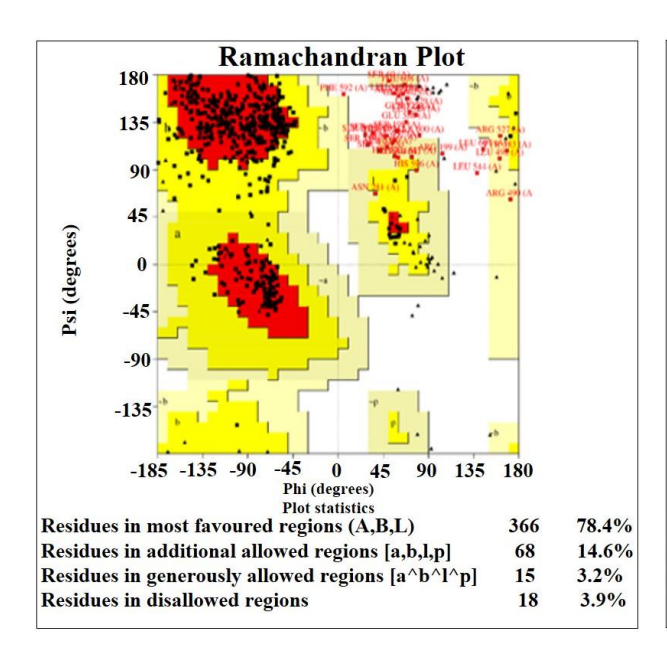


Figure 4.11: Homology modeled structure of Human DLL3



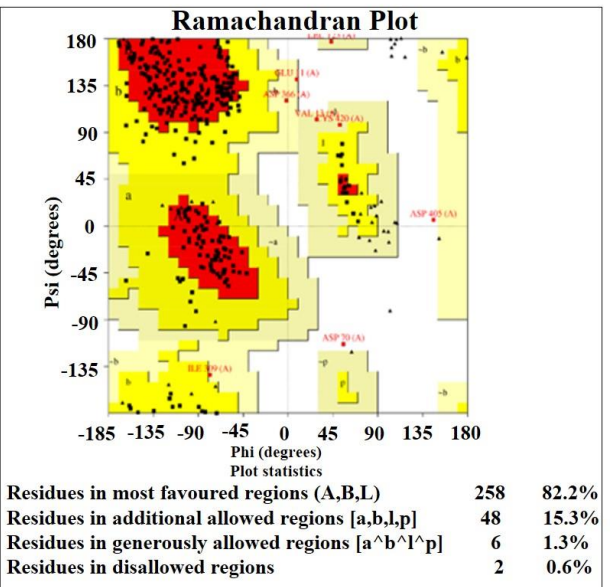


Figure 4.12: Ramachandran map of Q9NYJ7 (Query sequence) and Template sequence model

Table 4.9: PROCHECK tool generates a Ramachandran plot for the final DLL3 models.

Modeling	Protein	Accession	Regions of amino acid residues	Percentage (%)
Server	Name	Number		
Swiss Model	DLL3	Q9NYJ7	Amino acids in the most favoured region	82.20
			Amino acids in generously allowed region	1.90
			Amino acids in additionally allowed region	15.30
			Amino acids in disallowed region	0.60

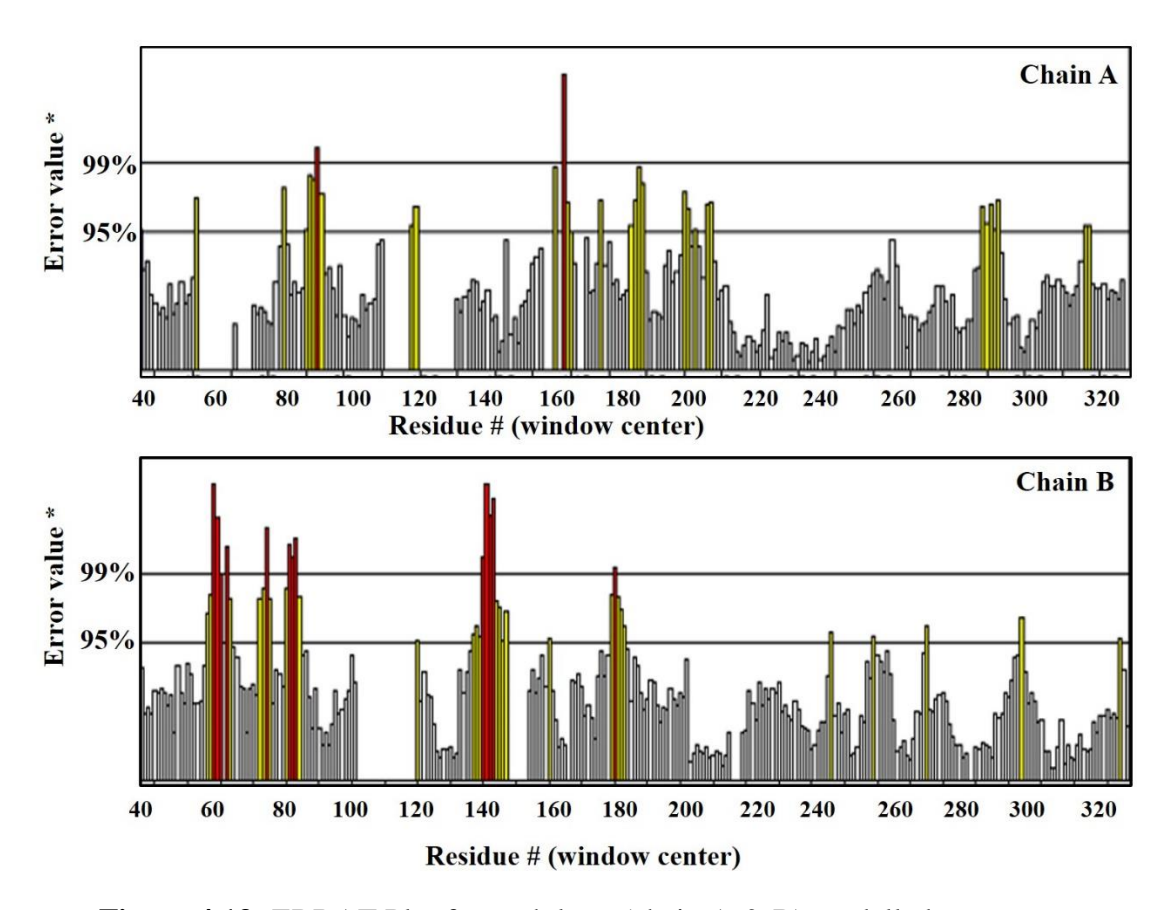


Figure 4.13: ERRAT Plot for each loop (chain A & B) modelled structure.

Table 4.10: PROVE analysis for the DLL3 model.

Protein (Accession Number)	Z-score information	Value(s)
Delta-like ligand 3 (Q9NYJ7)	Average (mean)	0.751
	Standard deviation	1.391
	Root Mean Square (RMS)	1.580

4.9 Molecular docking analysis

Eight (8) target proteins were downloaded from the PDB database (PDB id: 4XMB.2, 3OSK.1, 4J8M, 6KGM, 5G1X, 7BW1, 3L3X, and 7KX0), and using grid box analysis, the binding pocket was manually predicted (Lawal *et al.*, 2020). The phytocompounds in .sdf format were obtained from the PubChem database and converted into .pdbqt format (Gulati *et al.*, 2023). The molecular

docking screening was done using the PyRx software (Verma *et al.*, 2023; Dallakyan & Olson, 2015). **Table 4.11** presents the docking result of ten (10) bioactive compounds with peak area above 2.0% against eight (8) prostate cancer target proteins. The binding affinities ranged from –4.5 to –17.1 Kcal/mol across the docking result. Out of this ten (10) bioactive compounds only four (4) compounds with their pubchem ID (CID10494, CID17161, CID637775, CID8372) were selected for post docking study.

Table 4.11: Molecular docking result of selected bioactive compounds of flax microgreens against prostate cancer target proteins.

					Target pr	ID)			
SN	Compound CID:	DLL3 (4xmb.2)	CTLA-4 (3osk.1)	CD27 (7kxo)	AURKA (4j8m)	N-Myc (5ixo.1)	5AR (7bw1)	AR (313x)	LSD1 (6kgm)
1	10494	-6.2	-7.2	-9.1	-6.1	-6.2	-10.2	-7.1	-10.2
2	17161	-6.8	-8.2	-10.7	-8.4	-6.7	-11.3	-7.4	-9.8
3	191964	-6.6	-5.8	-6.6	-7.7	-5.9	-8.5	-7.9	-8.5
4	5280435	-6.5	-6.1	-7.9	-7.1	-6.1	-8.0	-6.7	-8.8
5	54725318	-4.7	-5.1	-5.6	-6.7	-4.0	-7.7	-6.1	-7.1
6	637775	-6.9	-7.5	-9.1	-9.3	-7.9	-10.7	-8.5	-9.8
7	638072	-4.5	-5.4	-7.0	-6.6	-4.0	-8.0	-7.8	-7.8
8	64947	-4.6	-4.9	-6.3	-6.1	-47	-6.4	-6.1	-6.5
9	8372	-11.5	-10.5	-13.3	-14.5	-10.6	-15.8	-14.9	-17.1
10	985	-5.0	-4.7	-6.0	-6.2	-4.7	-6.6	-7.0	-6.8

4.9.1 Binding affinities of selected bioactive compounds (CID10494, CID17161, CID637775, and CID8372) and FDA approved drugs (Flutamide) across target proteins

Molecular docking studies were performed to evaluate the binding affinities of four selected bioactive compounds (CID8372, CID17161, CID637775, and CID10494) against eight key prostate cancer target proteins, using Flutamide (CID3397), an FDA-approved drug, as the reference standard (Ito & Sadar, 2018). According to **Table 4.12**, CID8372 (4,4'-methylenebis(2,6-

di-tert-butylphenol)) exhibited the strongest binding affinities ranging from -10.5 to -17.1 kcal/mol. It showed particularly high binding toward LSD1 (-17.1 kcal/mol), AR (-14.9 kcal/mol), and 5AR (-15.8 kcal/mol), surpassing the binding affinity of flutamide (-10.5 kcal/mol) as well as established AR and 5AR inhibitors such as enzalutamide and finasteride (Saah et al., 2023; Rao et al., 2015). As shown in **Table 4.13**, CID17161 (2,5-di-tert-butyl-1,4-benzoquinone) also demonstrated favorable binding affinities, with the highest affinity observed for 5AR (-11.3 kcal/mol), higher than the flutamide and aligning closely with known AR inhibitors (Ito & Sadar, 2018; Saah et al., 2023). Table 4.14 presents CID637775 (Sinapinic acid), which revealed strong interaction with 5AR (-10.7 kcal/mol) and AR (-8.5 kcal/mol), indicating its potential as a competitive inhibitor relative to finasteride and enzalutamide (Rao et al., 2015; Saah et al., 2023). Lastly, **Table 4.15** shows that CID10494 (Oleanolic acid) had binding affinities ranging from -6.2 to -10.2 kcal/mol, with notable values for 5AR (-10.2 kcal/mol) and AR (-7.1 kcal/mol), which are comparable to those of flutamide and traditional prostate cancer therapies (Ito & Sadar, 2018; Rao et al., 2015). These findings highlight the promising multi-target potential of the selected bioactive compounds, particularly CID8372 as effective natural alternatives or adjuncts in prostate cancer treatment.

4.9.2 Half maximal inhibitory concentration (IC₅₀) prediction (CID10494, CID17161, CID637775, CID8372) and FDA approved drugs (Flutamide)

The IC₅₀ value prediction was done to quantitatively measure the concentration of compound required to produce half maximum inhibition to a given biological process and is universally used to symbolize the inhibitory effect of compounds (Cheng *et al.*, 2023). The predicted IC₅₀ value for the studied compound, 4,4'-M(2,6-DTBP) (CID8372), ranged from 0.0003 to 14.80 nM (**Table 4.12**). It demonstrated the strongest inhibitory potential against the LSD1 target with IC₅₀ value of just 0.0003 nM, while exhibiting the weakest inhibition against the N-Myc target protein, with an IC₅₀ of 14.80 nM. The predicted IC₅₀ value for the 2,5-DTBQ (CID17161), ranged from 0.005 to 12.49 μM (**Table 4.13**). It demonstrated the strongest inhibitory potential against the 5AR target with IC₅₀ value of 0.005 μM, while exhibiting the lowest possible inhibition against the N-Myc target protein with an IC₅₀ of 12.49 μM. The predicted IC₅₀ value for the 3,5-dimethoxy-4-hydroxycinnamic acid (CID637775), ranged from 0.015 to 9.813 μM (**Table 4.14**). It demonstrated the highest inhibitory potential against the 5AR target with an IC₅₀ value of just 0.015 μM, while exhibiting the weakest inhibition against the DLL3 target protein with an IC₅₀ of 9.813 μM. The

predicted IC₅₀ value for the oleanolic acid (CID637775) was in a range of 0.034 to 31.583 μM (**Table 4.15**). It demonstrated the highest inhibitory potential against the 5AR and LSD1 targets with an IC₅₀ of 0.034 μM, while exhibiting the lowest inhibition against AURKA target protein with 31.583 μM. In comparison to the control FDA drug (flutamide), the 4,4'-M(2,6-DTBP) shows the predicted IC₅₀ value higher than that of control FDA drugs whereas the 2,5-DTBQ, Sinapinic acid, and oleanolic acid show IC₅₀ almost same/similar to that of standard drug.

4.9.3 Protein-ligand interactions of CID10494, CID17161, CID637775, CID8372 against prostate cancer target proteins

Studying the mechanism of action through protein-ligand interactions is highly important. These interactions involve different forces, which include electrostatic, hydrogen bonding, and hydrophobic interactions. The positive results cannot be achieved from binding affinity alone (Laskowski & Swindells, 2011). However, by considering the amino acid residues involved in the protein-ligand interaction can support the docking results and enhance their overall credibility. The results show that the amino acid residues favorably interact with the 4,4'-M(2,6-DTBP), 2,5-DTBQ, sinapinic acid, and oleanolic acid compounds at the target proteins' active sites in **Tables 4.12, 4.13, 4.14 and 4.15** respectively. Hydrogen bonds and hydrophobic interactions show that this ligand positively interacts with the binding site of the enzyme; this could possibly lead to enzyme inhibition, which is necessary in drug design by targeting the specific receptor. The protein-ligand interaction stabilized the ligand to perfectly fit into the binding pocket of the target proteins. 3D representations of protein-ligand interactions are illustrated in **Figures 4.14–4.21** (PLIP online server) (Rosário-Ferreira *et al.*, 2021; Dhiani *et al.*, 2022).

Table 4.12: Binding affinities, IC₅₀ values, and interaction residues of 4,4'-M(2,6-DTBP) (CID8372) and FDA approved drugs (Flutamide) across target proteins.

Protein	CID8372	Flutamide	CID8372	Flutamide		CID8372-AA Residues
	(kcal/mol)	(kcal/mol)	IC50	IC50	H-bond	Hydrophobic interactions
DLL3 (4xmb.2)	-8.9	-6.8	306.60 nM	10.555 μΜ		GLU681A, PRO682A, VAL684A, VAL685A,
						HIS714A, VAL715A, TRP718A, LEU744A, ALA748A, ARG752A.
CTLA-4 (3osk.1)	-10.5	-6.8	15.40 nM	10.555 μΜ	PRO282A	LEU139A, VAL147A, ALA160A, LEU194A, ALA213A, LEU263A, ALA281A.
AURKA (4j8m)	-14.6	-8.4	0.021 nM	0.712 μΜ	ARG195B	PHE199B, PHE202B, TYR220B.
LSD1 (6kgm)	-17.1	-10.2	0.0003 nM	0.034 μΜ	TYR81A	PRO61A, GLU62A, TYR81A, VAL85A, GLN86A, THR89B.
N-Myc (5G1X)	-10.7	-7.5	14.80 nM	3.245 μΜ	ASP555A	VAL333A, THR335A, PHE538A, LEU659A, TYR761A, ALA809A, THR810A.
5AR (7BW1)	-15.8	-9.4	0.0027 nM	0.132 μΜ	GLU57A, ASN193A.	TYR33A, TRP53A, TYR98A, ASN193A, PHE194A, PHE216A, PHE223A, LEU224A.
AR (3L3X)	-14.9	-10.5	0.012 nM	0.021 μΜ	CLY150A, CYS151A, THR152A, ALA154C.	LEU145C, PHE147A, HIS148B, THR152AB, ILE153A, ILE153C, ALA154B, ALA154C.
CD27 (7KX0)	-13.3	-8.6	0.180 nM	0.508 μΜ	LEU12A	LEU12A, ALA86B, THR89B, ILE117B.

Table 4.13: Binding affinities, IC₅₀ values, and interaction residues of 2,5-DTBQ (CID17161) and FDA approved drugs (Flutamide) across target proteins

Protein	CID17161	Flutamide	CID17161	Flutamide		CID17161-AA Residues
	(kcal/mol)	(kcal/mol)	IC ₅₀	IC ₅₀	H-bond	Hydrophobic interactions
DLL3 (4xmb.2)	-6.8	-6.8	10.555 μΜ	10.555 μΜ	ARG195B	PHE191B, ARG193B, PHE199B, TYR220B.
CTLA-4 (3osk.1)	-8.2	-6.8	0.862 μΜ	10.555 μΜ	LEU12B	VAL10B, ALA86A, THR89A, ILE117A.
AURKA (4j8m)	-8.4	-8.4	0.712 μΜ	0.712 μΜ		ALA160A, LEU194A, LEU210A.
LSD1 (6kgm)	-9.8	-10.2	0.112 μΜ	0.034 μΜ		TYR761A, VAL811A.
N-Myc (5G1X)	-6.7	-7.5	12.490 μΜ	3.245 μΜ	ARG195B.	PHE191B, ARG193B, PHE199B, TYR220B.
5AR (7BW1)	-11.3	-9.4	0.005 μΜ	0.132 μΜ		TRP53A, TYR98A, PHE194A, PHE223A, LEU224A.
AR (3L3X)	-7.4	-10.5	3.823 μΜ	0.021 μΜ	PHE764A.	LEU701A, LEU704A, LEU707A, MET749A, PHE764A.
CD27 (7KX0)	-10.7	-8.6	0.015 μΜ	0.508 μΜ	ALA154B	LEU145C, ALA154B.

Table 4.14: Binding affinities, IC₅₀ values, and interaction residues of sinapinic acid (CID637775) and FDA approved drugs (Flutamide) across target proteins

Protein	CID637775	Flutamide	CID637775	Flutamide	CID637775-AA Residues					
	(kcal/mol)	(kcal/mol)	IC ₅₀	IC ₅₀	H-bond	Hydrophobic interactions				
DLL3 (4xmb.2)	-6.9	-6.8	9.813 μΜ	10.555 μΜ	ARG195B, ALA198 ALA198B, THR222B	В, РНЕ199В				
CTLA-4 (3osk.1)	-7.5	-6.8	3.245 μΜ	10.555 μΜ	THR89B, VAL116B, ASP118 GLU120B	B, LEU12A, ALA86B, ILE117B.				
AURKA (4j8m)	-9.3	-8.4	0.197 μΜ	0.712 μΜ	LYS162A, GLU181. GLN185A, ASP274A, PHE275					
LSD1 (6kgm)	-9.8	-10.2	0.067 μΜ	0.034 μΜ	LEU659A, TRP751. VAL811A.	A, ALA331A, TYR761A.				
N-Myc (5G1X)	-7.9	-7.5	2.982 μΜ	3.245 μΜ	ARG195B, ALA198. THR222B.	В, РНЕ199В.				
5AR (7BW1)	-10.7	-9.4	0.015 μΜ	0.132 μΜ	TYR33A, ASN160A, ASN193.	A. TRP53A, LEU224A.				
AR (3L3X)	-8.5	-10.5	0.681 μΜ	0.021 μΜ	GLY683A, ARG752A.	PRO682A, VAL715A, ALA748A, LYS808A.				
CD27 (7KX0)	-9.1	-8.6	0.219 μΜ	0.508 μΜ		HIS148B, CYS151A, THR152B, THR152C.				

Table 4.15: Binding affinities, IC_{50} values, and interaction residues of oleanolic acid (CID10494) and FDA approved drugs (Flutamide) across target proteins

Protein	CID10494	Flutamide	CID1049	Flutamide	CID10	049-AA Residues				
	(kcal/mol)	(kcal/mol)	IC ₅₀	IC ₅₀	H-bond	Hydrophobic interactions				
DLL3 (4xmb.2)	-6.2	-6.8	24.812 μΜ	10.555 μΜ	THR222B	PHE199B, TYR220B.				
CTLA-4 (3osk.1)	-7.2	-6.8	4.617 μΜ	10.555 μΜ	GLU120B	LEU12A, ILE117A.				
AURKA (4j8m)	-6.1	-8.4	31.583 μΜ	0.712 μΜ	ARG220A	VAL147A, ALA160A, LEU194A, TYP212A, THR217A, LEU263A.				
LSD1 6kgm)	-10.2	-10.2	0.034 μΜ	0.034 μΜ	MET332A, VAL333A	ALA331A, THR335A, TYR761A, THR810A.				
N-Myc (5G1X)	-6.2	-7.5	24.812 μΜ	3.245 μM		PRO61A, TYR81A, GLN86B, GLN90B.				
5AR (7BW1)	-10.2	-9.4	0.034 μΜ	0.132 μΜ	GLU57A, ARG94A, ARG114A.	TRP53A, LEU111A, ARG114A, PHE118A, PHE216A, PHE219A, PHE223A, LEU224A.				
AR (3L3X)	-7.1	-10.5	5.251 μΜ	0.021 μΜ	TRP751A	GLU681A, PRO682A, VAL715A, TRP728A, LEU744A, MET745A, ALA748A, ARG752A, PHE804A, LYS808A.				
CD27 (7KX0)	-9.1	-8.6	0.219 μΜ	0.508 μΜ	HIS148B, GLY150B, THR152B, SER155A	LEU145A, LEU145B, THR152C, ILE153B, ALA154C.				

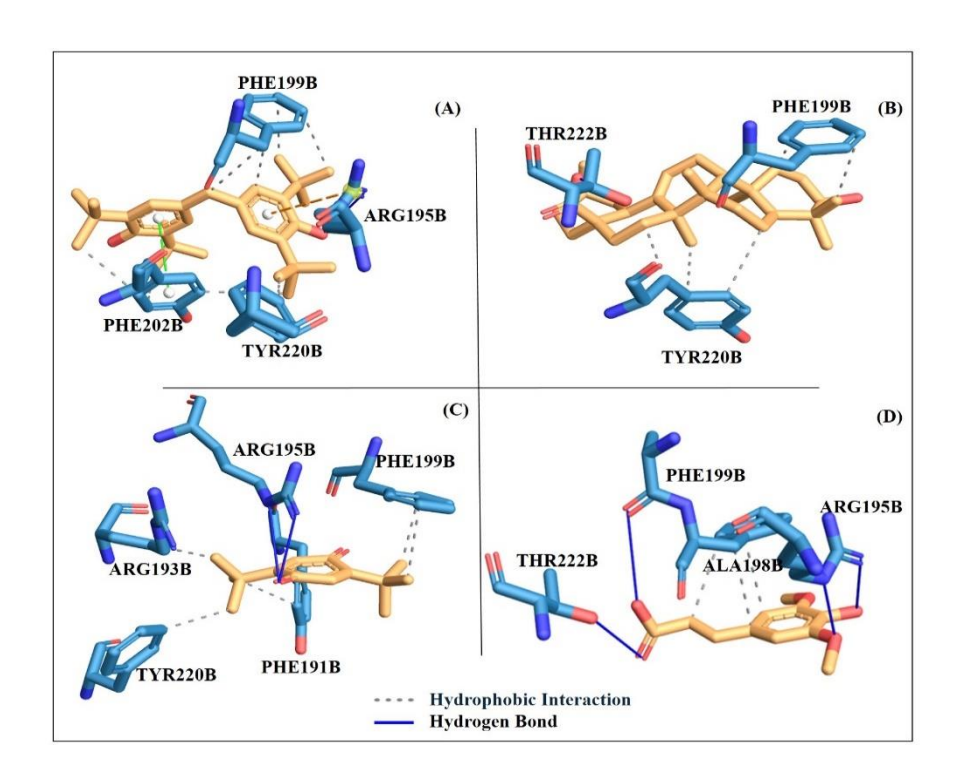


Figure 4.14: 3D Docking pose interactions of DLL3 with bioactive compounds viz; (A) CID8372, (B) CID10494, (C) CID17161, and (D) CID637771.

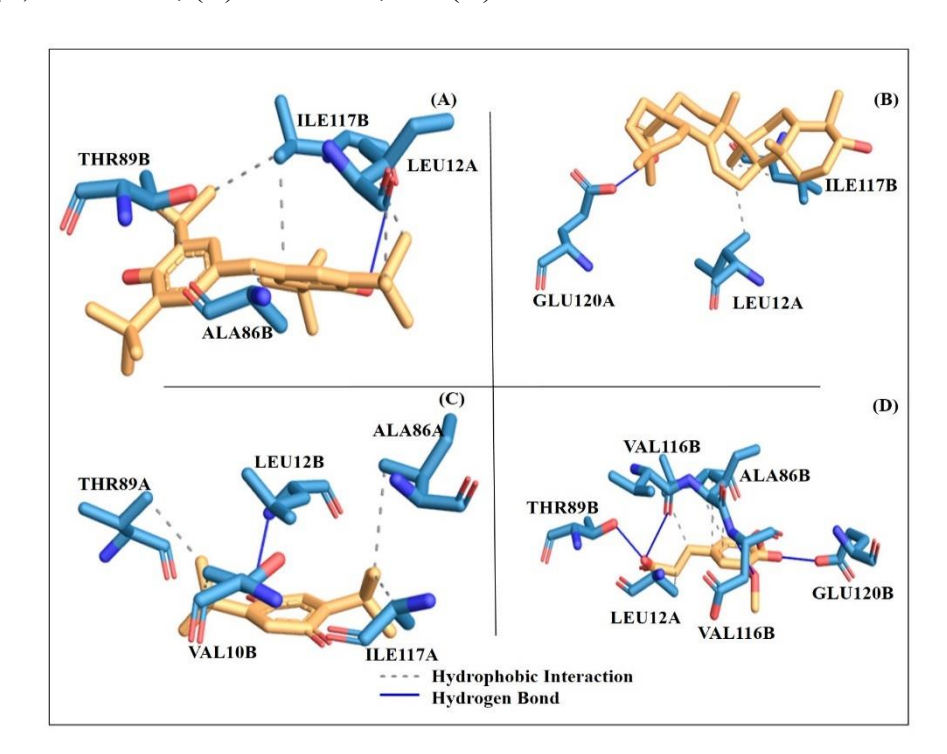


Figure 4.15: 3D Docking pose interactions of CTLA-4 with bioactive compounds viz; (A) CID8372, (B) CID10494, (C) CID17161, and (D) CID637771.

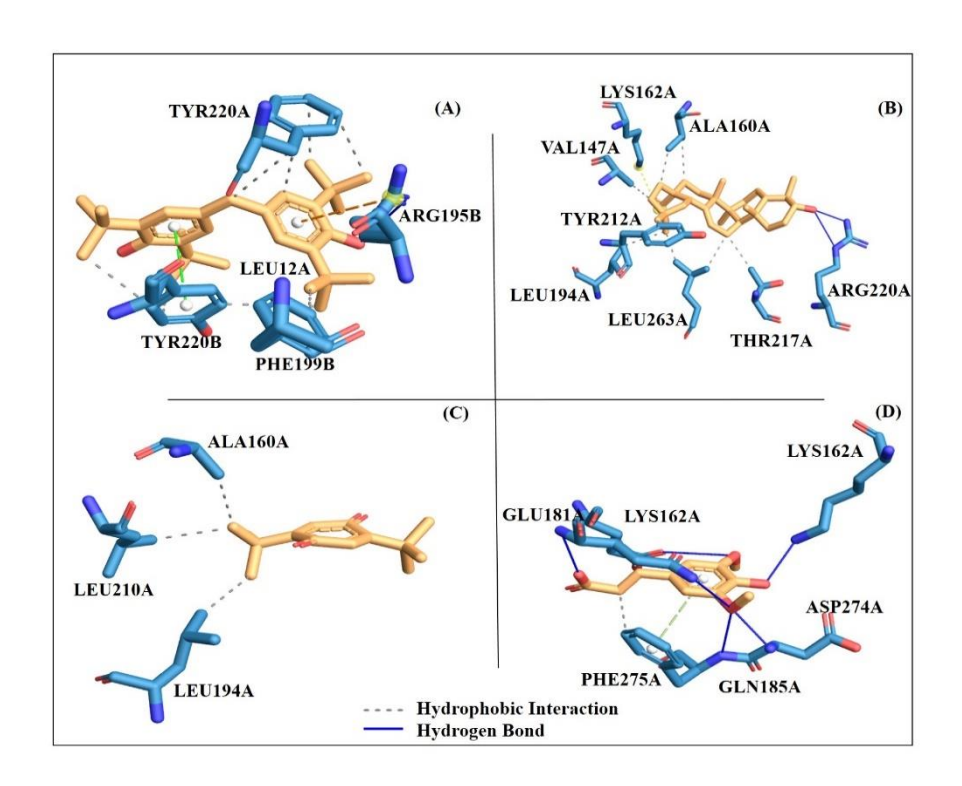


Figure 4.16: 3D Docking pose interactions of AURKA with bioactive compounds viz; (A) CID8372, (B) CID10494, (C) CID17161, and (D) CID637771.

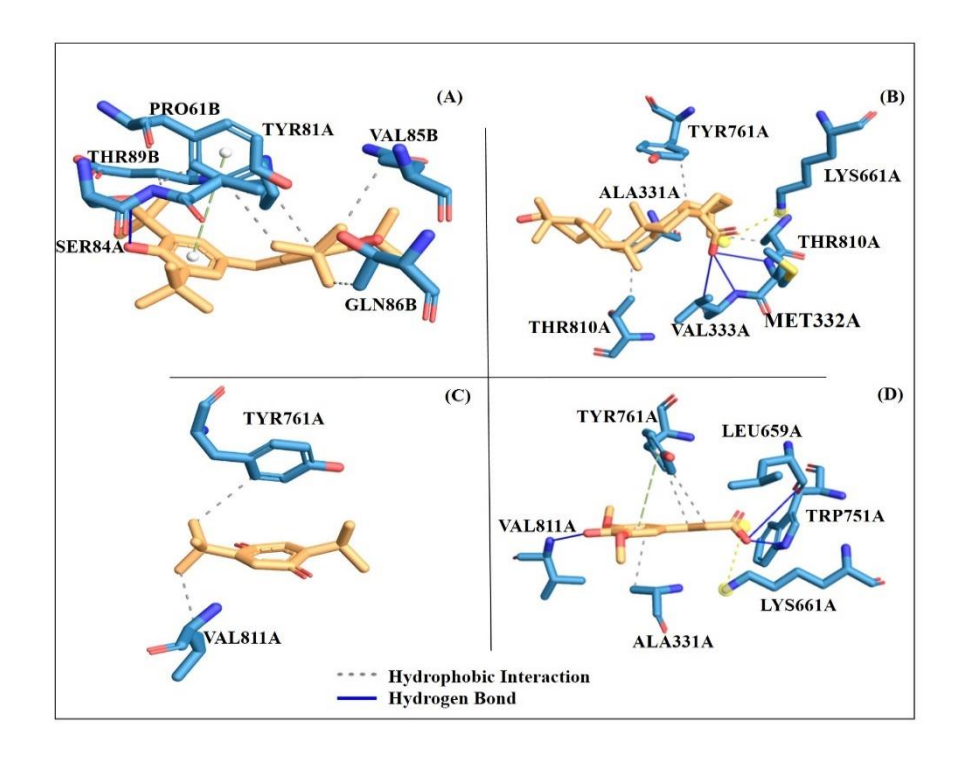


Figure 4.17: 3D Docking pose interactions of LSD1 with bioactive compounds viz; (A) CID8372, (B) CID10494, (C) CID17161, and (D) CID637771.

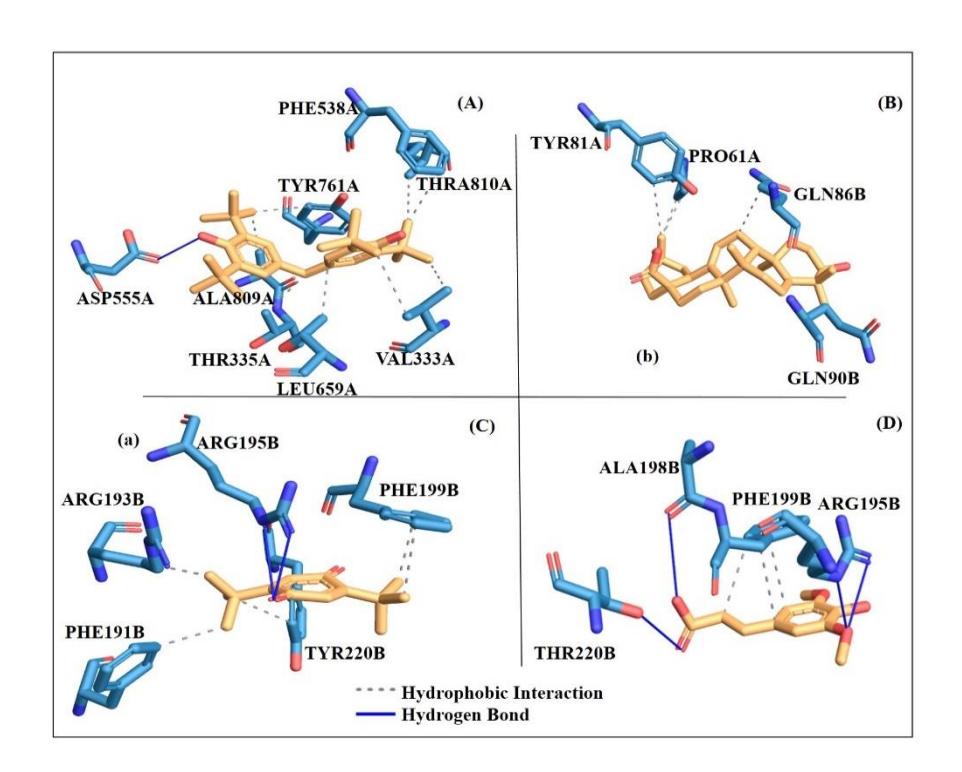


Figure 4.18: 3D Docking pose interactions of N-Myc with bioactive compounds viz; (A) CID8372, (B) CID10494, (C) CID17161, and (D) CID637771.

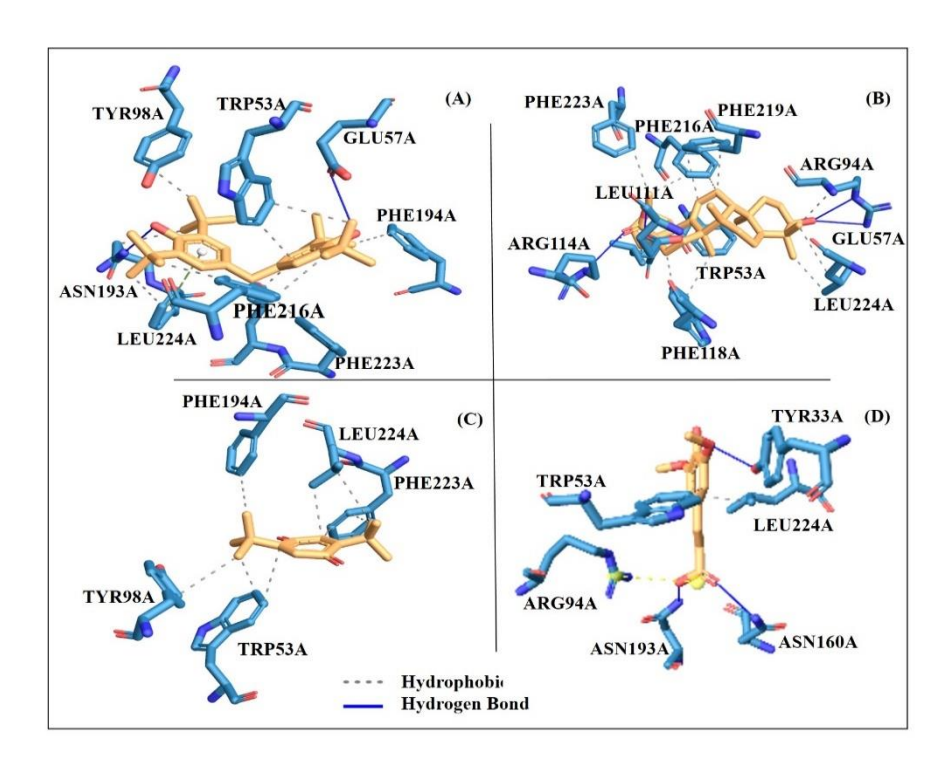


Figure 4.19: 3D Docking pose interactions of 5AR with bioactive compounds viz; (A) CID8372, (B) CID10494, (C) CID17161, and (D) CID637771.

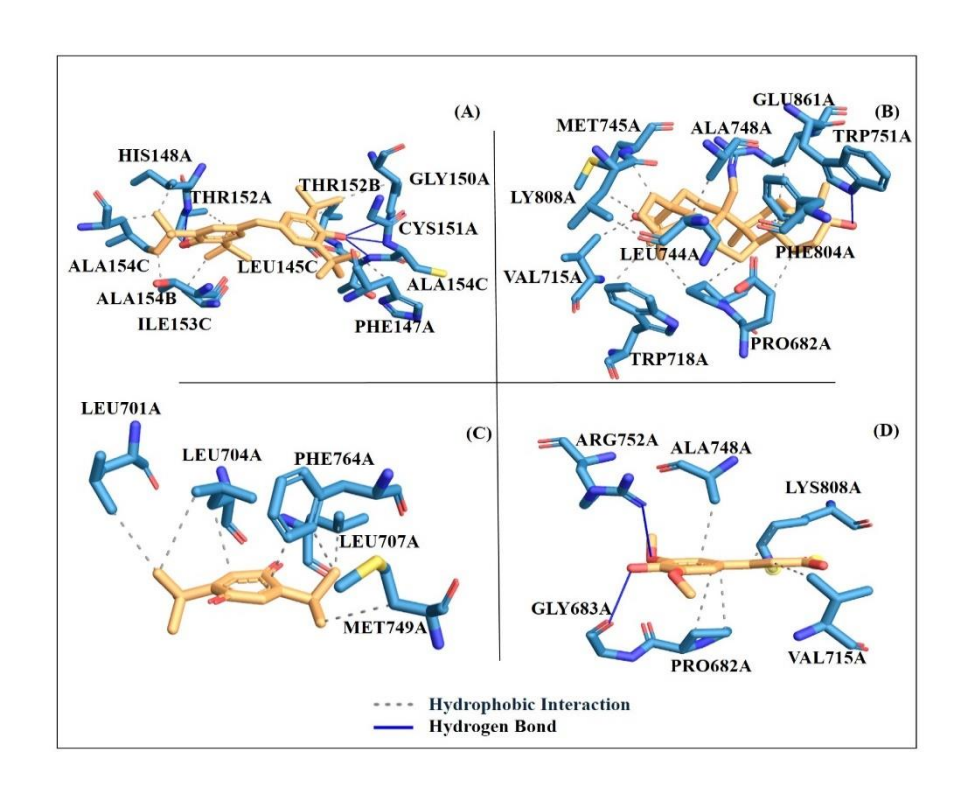


Figure 4.20: 3D Docking pose interactions of AR with bioactive compounds viz; (A) CID8372, (B) CID10494, (C) CID17161, and (D) CID637771.

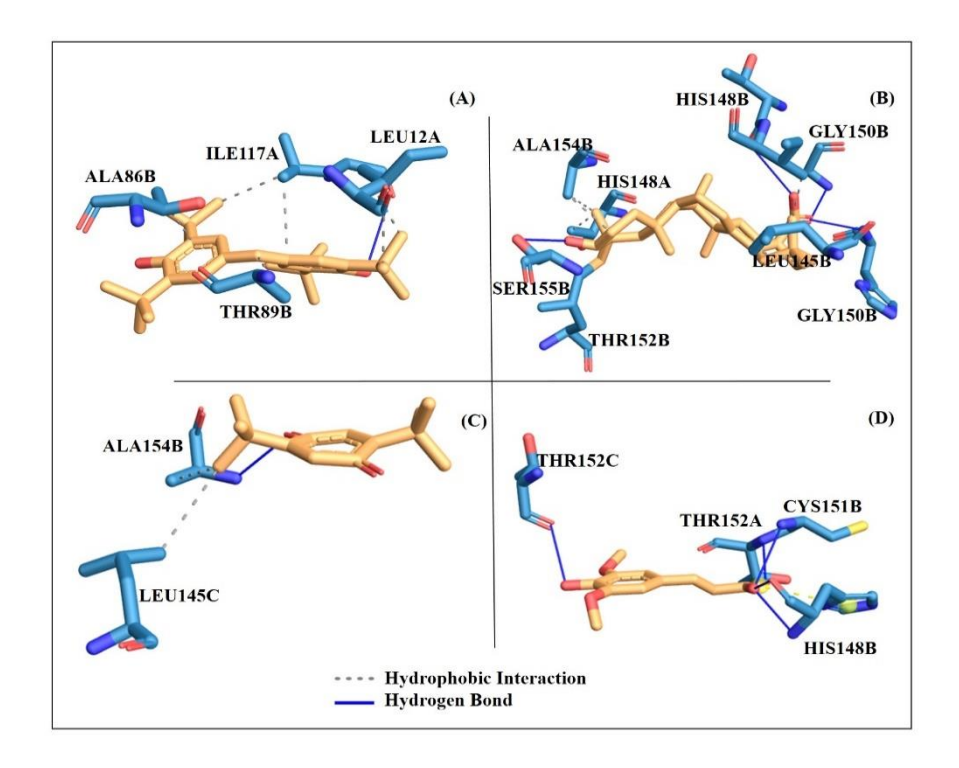


Figure 4.21: 3D Docking pose interactions of CD27 with bioactive compounds viz; (A) CID8372, (B) CID10494, (C) CID17161, and (D) CID637771.

4.10 ADME/T properties prediction

ADMETlab 3.0 and ProTox-3.0 online tools were used to get the ADMET (Absorption, Distribution, Metabolism, Excretion, and Toxicity) properties. The ADMET parameters evaluated for the 4,4'-M(2,6-DTBP), 2,5-DTBQ, sinapinic acid, and oleanolic acid were acute oral toxicity, blood-brain barrier, carcinogenicity, nutritional toxicity, hepatotoxicity, nephrotoxicity, neurotoxicity, cytochrome P450 inhibitors isoforms (CYP inhibitors), hepatotoxicity, human ethera-go-go-related gene inhibition (hERG), human intestinal absorption, human oral bioavailability, and P-glycoprotein inhibitor (P-gpi) (Tables 4.16 and 4.17). The results indicate that the compounds have strong oral bioavailability in humans, high gastrointestinal absorption, and good blood-brain barrier permeation. Lipinski's rule of five and Veber's filter were used to study the bioavailability of 4,4'-M(2,6-DTBP), 2,5-DTBQ, sinapinic acid, and oleanolic acid. According to Lipinski's rule of five, compounds with an octanol/water partition coefficient (LogPo/w) of less than five, a molecular weight (MW) of less than 500, H-bond acceptors (n-HBA) less than ten, and less than five H-bond donors (n-HBD) were predicted to exhibit favorable bioavailability (Lipinski et al., 1997). Additional parameters were expanded by the Veber rule to include topological polar surface area with values of 79.89-109.35 (preferably TPSA ≤140 Å2) and rotatable bonds (preferably n-ROTB < 10) (Veber et al., 2002). The Egan rule considered good bioavailability for compounds with (TPSA ≤ 132 Å² and -1 < LogP < 6) (Srivastava et al., 2022). The studied compound obeyed Lipinski's rule of five as well as Veber's filter and exhibited favorable bioavailability.

According to the toxicity prediction study (**Table 4.17**), the 4,4'-M(2,6-DTBP), 2,5-DTBQ, sinapinic acid, and oleanolic acid compounds were classified as class VI, V, IV and IV respectively, and showed no acute oral toxicity. This suggests that these compounds have reduced the oral toxicity and is not broken down in the gastrointestinal tract before reaching their target (Finch & Pillans, 2014). Furthermore, these compounds are non-hepatotoxic, non-nutritional toxic, non-nephrotoxic, non-neurotoxic, and an inhibitor of the hERG. In the case of metabolism, the compounds are an inhibitor of most of the CYP450 isoforms, with the exception of CYP3A4, CYP2D6, and CYP2E1. If a compound is a non-inhibitor of cytochrome P450, it will not hinder the biotransformation and will remain longer in systemic circulation, which can lead to increased drug potency and prolonged therapeutic effects (Cheng *et al.*, 2012). ProTox-3.0 prediction tool generated a toxicity radar chart that presents a visual summary of the 4,4'-M(2,6-DTBP)'s possible

toxicity targets, including toxicity class, Ames toxicity, hepatotoxicity, neurotoxicity, nephrotoxicity, oral rat acute toxicity (LD₅₀), mutagenicity, carcinogenicity, and others in comparison to the average for similar classes of chemicals.

Table 4.16: Drug-likeness, lipophilicity and physicochemical properties

Compound ID	MW	TPSA	n-HBD	n-HBA	n-ROTB	M Ref	Log P	L.V	V.V	Pre. LD ₅₀
	(g/mol)									(mg/kg)
CID8372	424.66	40.46	2	2	6	137.02	7.306	0	0	24,000
CID17161	220.31	34.14	0	2	2	66.23	4.131	0	0	2400
CID637775	224.21	75.99	2	5	4	58.12	1.68	0	0	1772
CID10494	456.7	57.53	2	3	1	136.65	7.23	0	0	2000

Note. [a] MW: molecular weight (<500, expressed as Dalton); [b] TPSA: Topological polar surface area (Å2); [c] n-HBD: number of hydrogen bond donors (≤5); [d] n-HBA: number of hydrogen bond acceptors (≤10); [e] n-ROTB: number of rotatable bonds; [f] M Ref: molar refractivity (40–230); [f] LogP: logarithm of partition coefficient (<5) of compound between n-octanol and water; [g] LV: Lipinski's violation; [h] V.V= Veber's violation; [i] Pre. LD50: Predicted LD50.

Table 4.17: Toxicity prediction of CID8372, CID17161, CID637771 and CID10494 using ProTox-3.0 online tool

Compound ID	Acute oral toxicity	Blood-Brain Barrier	Nutritional toxicity	Carcinogenicity	Hepatotoxicity	Nephrotoxicity	Neurotoxicity	GI- Absorption	Human Oral Bioavailability	p-glycoprotein inhibitor	hERG inhibitor	CYP1A2-inhibitor	CYP2C19 inhibitor	CYP2C9 inhibitor	CYP2D6 inhibitor	CYP3A4 inhibitor	CYP2E1 inhibitor
CID8372	Class VI	+	-	+	-	-	-	+	-	-	-	+	+	+	+	+	-
CID17161	Class V	+	-	-	-	-	+	+	-	-	-	-	-	+	-	-	-
CID637775	Class IV	+	-	-	-	+	-	+	-	+	+	-	-	-	-	-	-
CID10494	Class IV	+	+	+	+	-	-	+	-	+	-	-	-	-	-	-	-

Note. [a] + = active; [b] - = inactive

4.11 UV-VIS quantification

4.11.1 Determination of λ max values and linearity

Table 4.18 presents the wavelength corresponding to maximum absorbance (λ _max) of 4,4'-M(2,6-DTBP) and 2,5-DTBQ in solvents of different polarity. The λ _max values for 4,4'-M(2,6-DTBP) in different solvents were as follows: 210 nm in hexane, 275 nm in ethyl acetate, 210 nm in butanol, and 240 nm in water. For 2,5-DTBQ, the λ _max values were 235 nm in hexane, 265 nm in ethyl acetate, 275 nm in butanol, and 310 nm in water. The different λ _max values across various solvents indicated the possible solvent effects on the electronic structure of bioactive compounds. The current findings of λ _max agreed with that of Fihtengolts (1969), which shows that 4,4'-M(2,6-DTBP) absorbed best at a wavelength of 270 nm. **Table 4.19** presents the UV-Visible spectroscopy linearity of standard bioactive compounds (4,4'-M(2,6-DTBP) and 2,5-DTBQ) in different solvents. In order to calculate the correlation coefficient and regression equation for the standard values of studied compounds, the UV calibration curves were plotted as absorbance versus concentration, as illustrated in **Figure 4.22**.

Table 4.18: λ Max for 4,4'-M(2,6-DTBP) and 2,5-DTBQ in different solvents.

Standard compounds (5 μg/ml)	λ_max for 4,4'-M(2,6-DTBP) (nm)	λ_max for 2,5-DTBQ (nm)
Hexane	210	235
Ethyl acetate	275	265
Butanol	210	275
Distilled H ₂ O	240	310

Table 4.19: UV-Visible spectroscopy linearity of 4,4'-M(2,6-DTBP) and 2,5-DTBQ in different solvents

Absorbance in Hexane		Absorbance in Ethyl acetate		Absorbance	in Butanol	Absorbance in water		
4,4'-M(2,6-	2,5-DTBQ	4,4'-M(2,6-	2,5-DTBQ	4,4'-M(2,6- 2,5-DTBQ		4,4'-M(2,6- 2,5-DTBC		
DTBP)		DTBP)		DTBP)		DTBP)		
0.0802	0.0408	0.1276	0.0338	0.3188	0.0418	0.6188	0.0058	
0.1024	0.0528	0.1585	0.0647	0.3979	0.0493	0.8979	0.0102	
0.1175	0.0857	0.1874	0.0946	0.5574	0.0752	1.1574	0.0124	
0.1351	0.1141	0.2134	0.1325	0.7102	0.1192	1.5102	0.0129	
0.1572	0.1463	0.2518	0.1824	0.8533	0.1724	1.8533	0.0162	
0.1858	0.1751	0.2757	0.1845	1.0351	0.1787	2.2351	0.0178	
0.2104	0.2013	0.3033	0.2402	1.213	0.2202	2.513	0.021	
	4,4'-M(2,6- DTBP) 0.0802 0.1024 0.1175 0.1351 0.1572 0.1858	4,4'-M(2,6- 2,5-DTBQ DTBP) 0.0408 0.1024 0.0528 0.1175 0.0857 0.1351 0.1141 0.1572 0.1463 0.1858 0.1751	4,4'-M(2,6-DTBP) 2,5-DTBQ 4,4'-M(2,6-DTBP) 0.0802 0.0408 0.1276 0.1024 0.0528 0.1585 0.1175 0.0857 0.1874 0.1351 0.1141 0.2134 0.1572 0.1463 0.2518 0.1858 0.1751 0.2757	4,4'-M(2,6- 2,5-DTBQ 4,4'-M(2,6- 2,5-DTBQ DTBP) DTBP) 0.0338 0.1024 0.0528 0.1585 0.0647 0.1175 0.0857 0.1874 0.0946 0.1351 0.1141 0.2134 0.1325 0.1572 0.1463 0.2518 0.1824 0.1858 0.1751 0.2757 0.1845	4,4'-M(2,6-DTBP) 2,5-DTBQ 4,4'-M(2,6-DTBP) 2,5-DTBQ 4,4'-M(2,6-DTBP) 0.0802 0.0408 0.1276 0.0338 0.3188 0.1024 0.0528 0.1585 0.0647 0.3979 0.1175 0.0857 0.1874 0.0946 0.5574 0.1351 0.1141 0.2134 0.1325 0.7102 0.1572 0.1463 0.2518 0.1824 0.8533 0.1858 0.1751 0.2757 0.1845 1.0351	4,4'-M(2,6- 2,5-DTBQ 4,4'-M(2,6- 2,5-DTBQ 4,4'-M(2,6- 2,5-DTBQ DTBP) DTBP) DTBP) DTBP) DTBP) 0.0418 0.0802 0.0408 0.1276 0.0338 0.3188 0.0418 0.1024 0.0528 0.1585 0.0647 0.3979 0.0493 0.1175 0.0857 0.1874 0.0946 0.5574 0.0752 0.1351 0.1141 0.2134 0.1325 0.7102 0.1192 0.1572 0.1463 0.2518 0.1824 0.8533 0.1724 0.1858 0.1751 0.2757 0.1845 1.0351 0.1787	4,4'-M(2,6-DTBP) 2,5-DTBQ 4,4'-M(2,6-DTBP) 2,5-DTBQ 4,4'-M(2,6-DTBP) 2,5-DTBQ 4,4'-M(2,6-DTBP) 2,5-DTBQ 4,4'-M(2,6-DTBP) 2,5-DTBQ 4,4'-M(2,6-DTBP) 4,4'-M(2,6-DTBP) 2,5-DTBQ 4,4'-M(2,6-DTBP) 2,5-DTBQ 4,4'-M(2,6-DTBP) 4,4'-M(2,6-DTBP) 2,5-DTBQ 4,4'-M(2,6-DTBP) 4,4'-M(2,6-DTBP) 2,5-DTBQ 4,4'-M(2,6-DTBP) 4,4'-M(2,6-DTBP) 2,5-DTBQ 4,4'-M(2,6-DTBP) 2,5-DTBQ 4,4'-M(2,6-DTBP) 4,4'-M(2,6-DTBP) 2,5-DTBQ 0.6188 0.0418 0.0418 0.0418 0.0418 0.0418 0.0418 0.0418 0.0418 0.0418 0.0418 0.0418 0.0752 0.1574 0.0752	

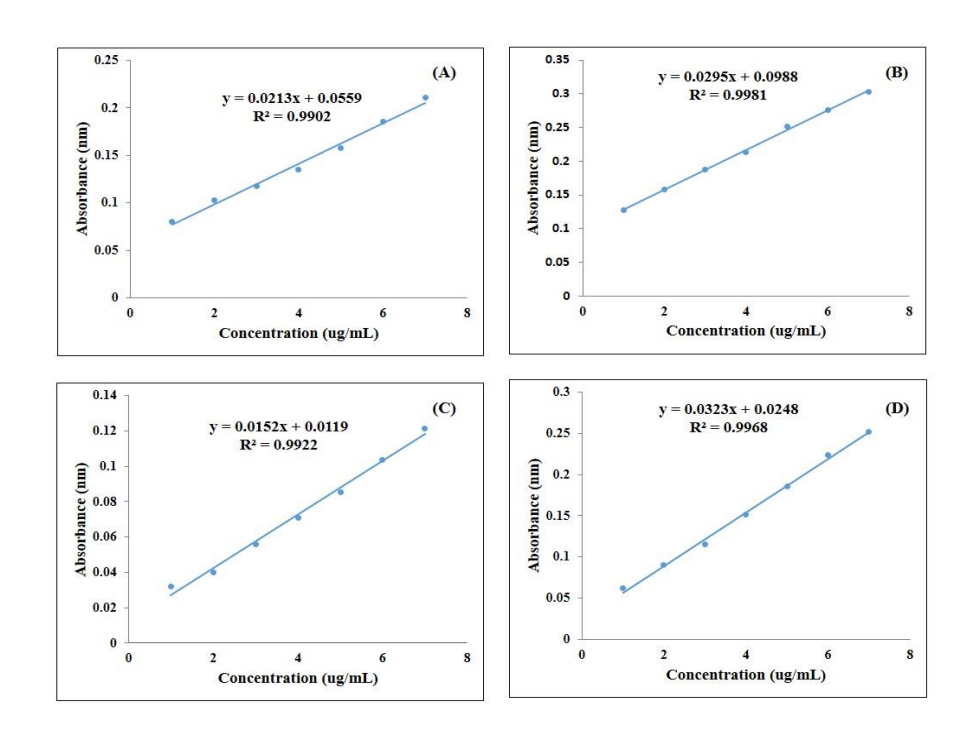


Figure 4.22: UV-VIS linearity graph for 4,4'-M(2,6-DTBP) in (A) Hexane, (B) Ethyl acetate, (C) Butanol, and (D) Water

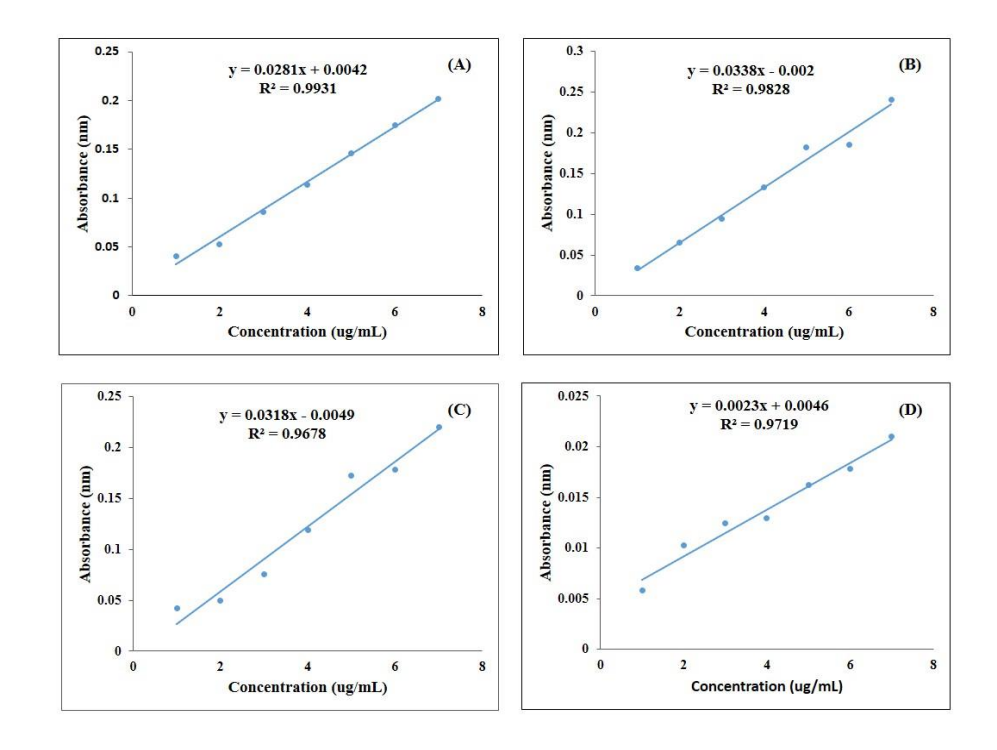


Figure 4.23: UV-VIS linearity graph for 2,5-DTBQ in (A) Hexane, (B) Ethyl acetate, (C) Butanol, and (D) Water

4.11.2 Analysis of extract fractions

The MEFM was subjected to liquid-liquid partition using solvents of different polarities, viz., hexane, ethyl acetate, butanol, and water. This further extraction was done in order to determine in which solvent the studied bioactive compounds "4,4'-M(2,6-DTBP) and 2,5-DTBQ" will be in higher concentration. The absorbance of the test solutions, namely n-hexane, ethyl acetate, nbutanol, and aqueous fractions, was measured at 210, 275, 210, and 240 nm for 4,4'-M(2,6-DTBP) and at 235, 265, 275, and 310 nm for 2,5-DTBQ, respectively. The concentration of bioactive compounds in these extract fractions was determined using the calibration curve method. As shown in the **Table 4.20**, the concentrations of the phytocompounds. For 4,4'-M(2,6-DTBP) were found to be 104.45±6.42, 49.25±2.90, 12.53±0.79, and 8.56±0.38 µg/ml in n-hexane, ethyl acetate, nbutanol, and aqueous fractions, respectively. Similarly, the concentrations of 2,5-DTBQ in different solvent fractions were found to be 156.36±2.47 µg/ml in-hexane, 130.63±1.65 µg/ml in ethyl acetate, 9.04±1.21 µg/ml in n-butanol, and 6.34±0.61 µg/ml in aqueous. These findings indicate that both compounds are hydrophobic in nature, as they exhibit higher concentrations in nonpolar solvents and lower concentrations in polar solvents. This information is crucial for selecting appropriate solvents for extraction and purification of those compounds from plant sources. The UV-VIS absorption spectra of 4,4'-M(2,6-DTBP) and 2,5-DTBQ in different solvents are presented in Figures 4.24 and 4.25, respectively.

Table 4.20: UV-Vis quantification of 4,4'-M(2,6-DTBP) and 2,5-DTBQ from MEFM in different sub fraction

Methanolic Extract sub-fractions	4,4'-M(2,6-DTBP)		2,5-D	ГВО
	λ_max (nm) Conc. (μg/ml)		λ_max (nm)	Conc. (µg/ml)
Hexane fraction	210	104.45±6.42***	235	156.36±2.47***
Ethyl acetate fraction	275	49.25±2.90**	265	130.63±1.65**
Butanol fraction	210	12.53±0.79*	275	9.04±1.21*
Aqueous fraction	240	8.56±0.38*	310	6.34±0.61*

Note: Values are expressed as **Mean \pm SD**, n = 3. *p < 0.05, **p < 0.01, ***p < 0.001

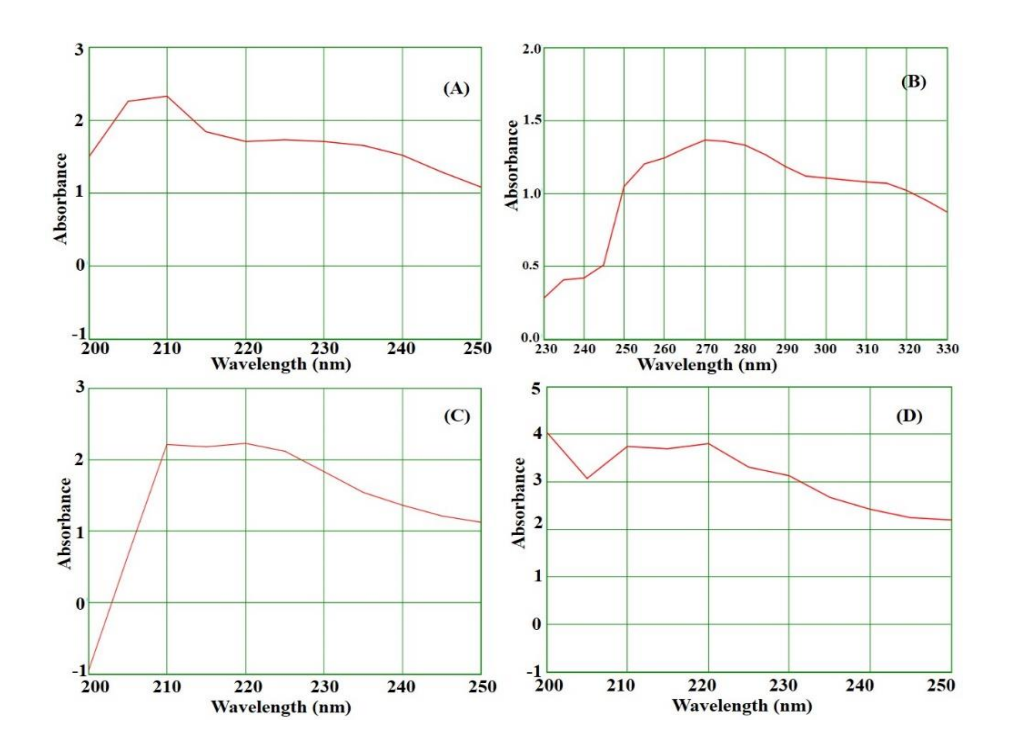


Figure 4.24: (A) UV-Vis absorption spectra of 2,5-DTBQ at the same concentration in different solvent fractions—(A) Hexane, (B) Ethyl acetate, (C) Butanol, and (D) Water

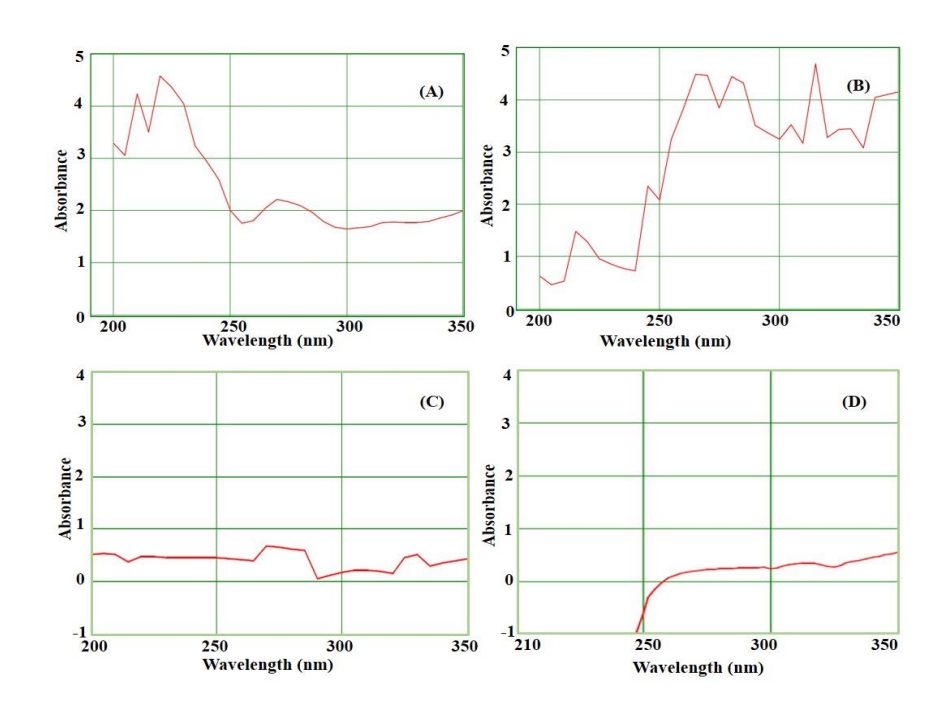


Figure 4.25: (A) UV-Vis absorption spectra of 2,5-DTBQ at the same concentration in different solvent fractions—(A) Hexane, (B) Ethyl acetate, (C) Butanol, and (D) Water

4.12 HPTLC analysis

The optimum mobile phase development for the bioactive compounds separation were achieved by using the solvent system of ethyl acetate: methanol: formic acid: water [20:2.5:0.5:2 (v/v)] as shown in the HPTLC fingerprint (**Figure 4.26**). The HPTLC analysis of MEFM revealed the presence of 4,4'-M(2,6-DTBP) and 2,5-DTBQ in a higher concentration. The chromatograms and peak tables were generated by scanning at 515 nm for 4,4'-M(2,6-DTBP) and 254 nm for 2,5-DTBQ. **Figures (4.27 and 4.29)** present the densitometry graphs, illustrating the isolation of 4,4'-M(2,6-DTBP) and 2,5-DTBQ from MEFM, respectively. The HPTLC fingerprint revealed that 4,4'-M(2,6-DTBP) and 2,5-DTBQ were abundantly present in MEFM, with an area percentage of 100% (**Table 21**) and 73.90% (**Table 22**), respectively. **Figures (4.28 and 4.30)** display the 3D and overlay of the chromatograms of all tracks, showing the detected bioactive compounds. The Rf (retention factor) values, peak area, peak height, and percentage area of the compound are depicted in (**Tables 21 and 22**). The specificity of the 4,4'-M(2,6-DTBP) and 2,5-DTBQ compounds in the extract was confirmed by comparison between the extract's Rf values and those of the standards, and the values were found to be similar. The clear separation of phytocompounds from MEFM are shown by these results, which proved the specificity of the technique used.

Table 4.21: HPTLC peak table of 4,4'-M(2,6-DTBP) and MEFM

Tract	Peak	Start Rf	Start Height	Max Rf	Max height	Max %	End Rf	End height	Area	area%	Assigned substance
1	1	0.72	11.0	0.76	446.3	100.00	0.80	0.40	14617.2	100.00	4,4'- M(2,6-DTBP)
2	1	0.72	2.3	0.78	196.5	100.00	0.80	12.3	7919.9	100.00	4,4'- M(2,6-DTBP)

Table 4.22: HPTLC peak table of 2,5-DTBQ and MEFM

Tract	Peak	Start Rf	Start Height	MaxRf	Max height	Max %	End Rf	End height	Area	area%	Assigned substance
1	1	0.71	8.7	0.82	419.2	83.81	0.92	0.5	26719.2	95.15	2,5-DTBQ
2	1	0.72	28.3	0.82	251.3	35.33	0.93	1.1	22391.5	73.90	2,5-DTBQ

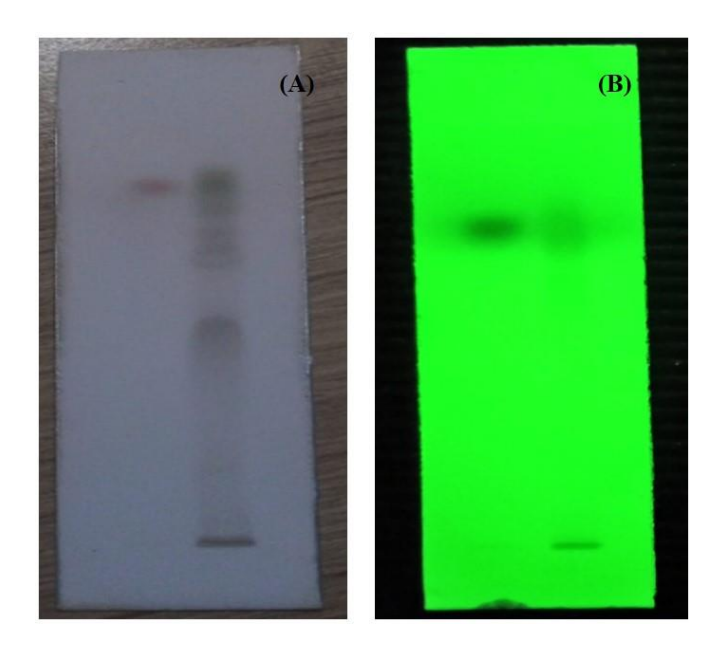


Figure 4.26: HPTLC fingerprinting of (A) 4,4'-M(2,6-DTBP) and (B) 2,5-DTBQ from MEFM

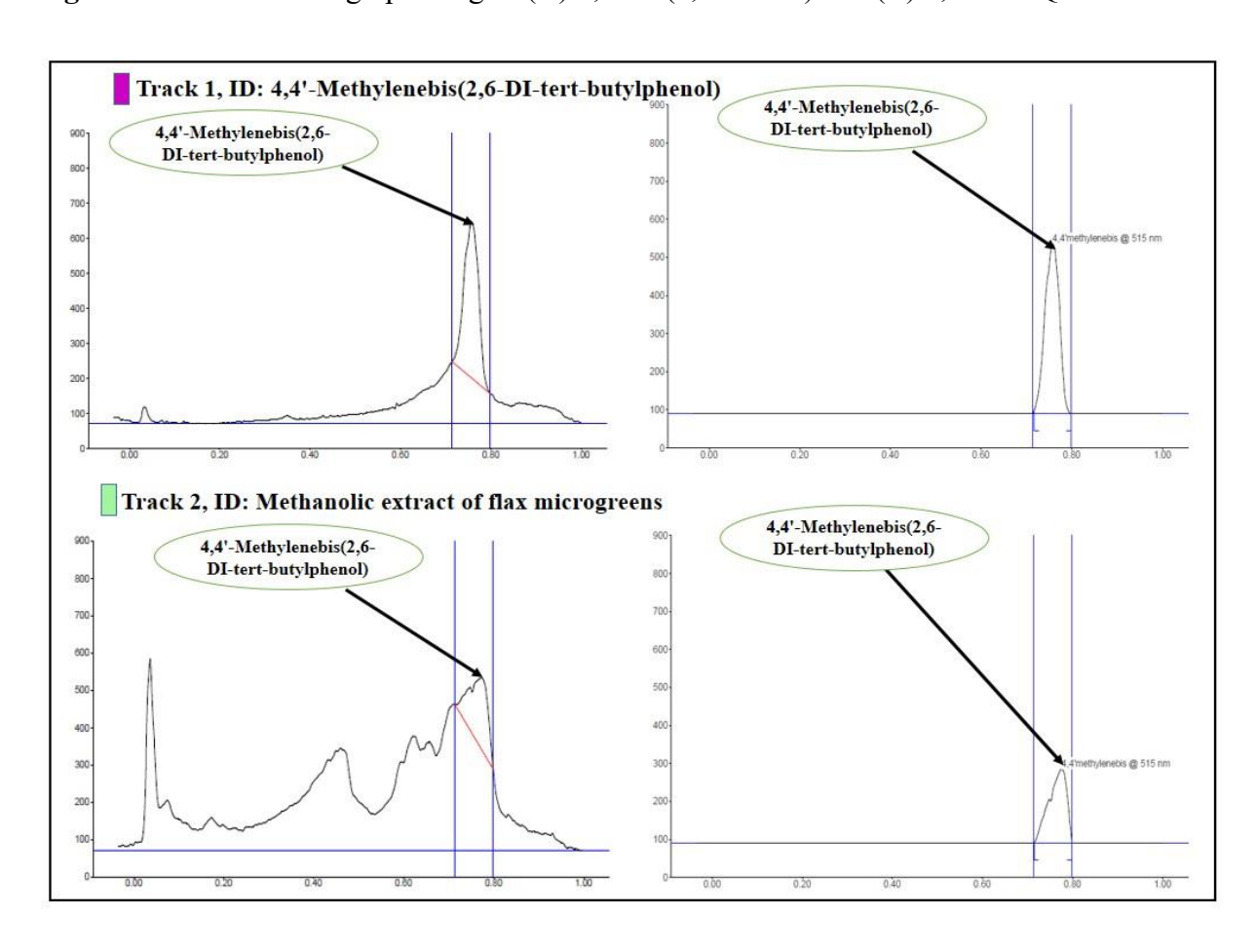


Figure 4.27: Densitometry graph showing isolation of 4,4'-M(2,6-DTBP) from MEFM

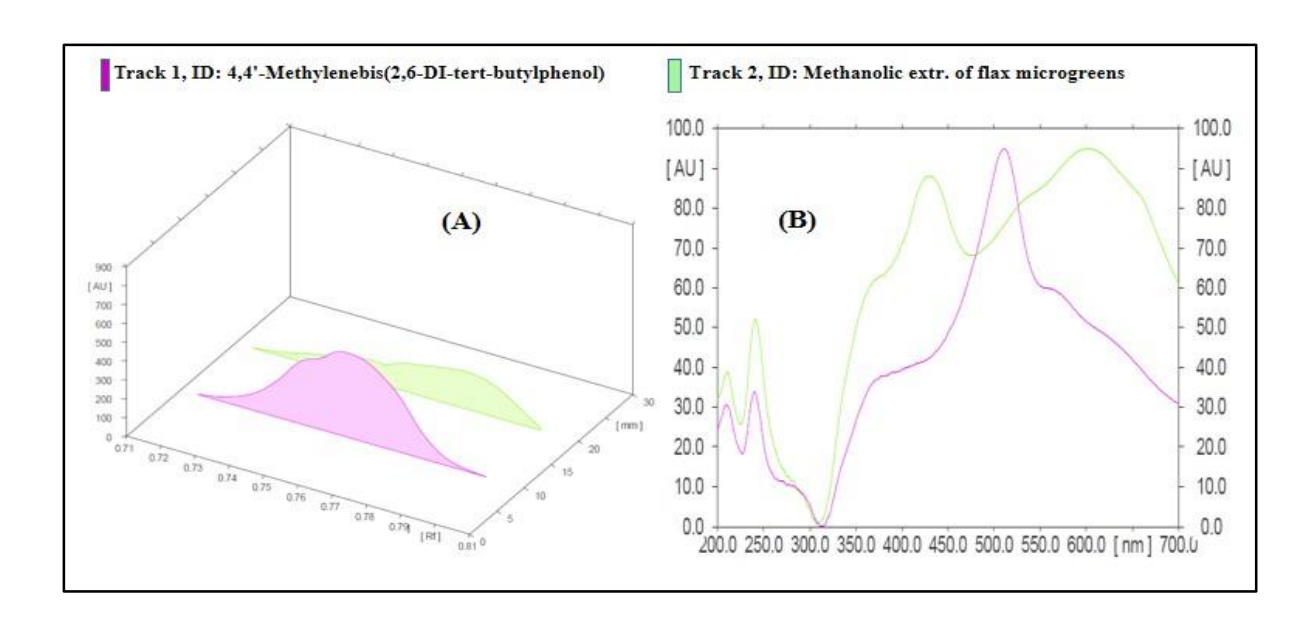


Figure 4.28: (A) 3D Chromatogram of 4,4'-M(2,6-DTBP) from extract and standard. (B) Overlay of HPTLC chromatogram of all tracks.

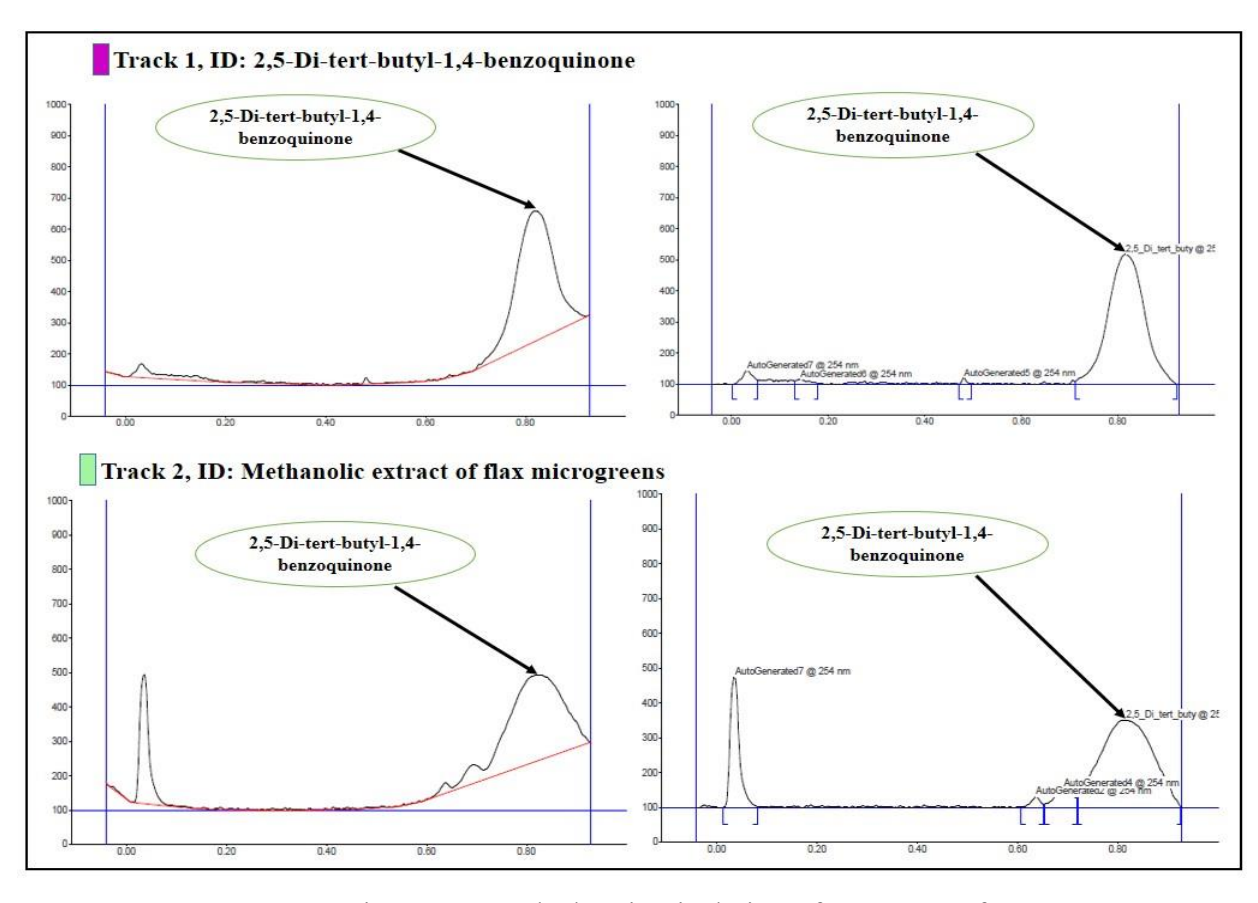


Figure 4.29: Densitometry graph showing isolation of 2,5-DTBQ from MEFM

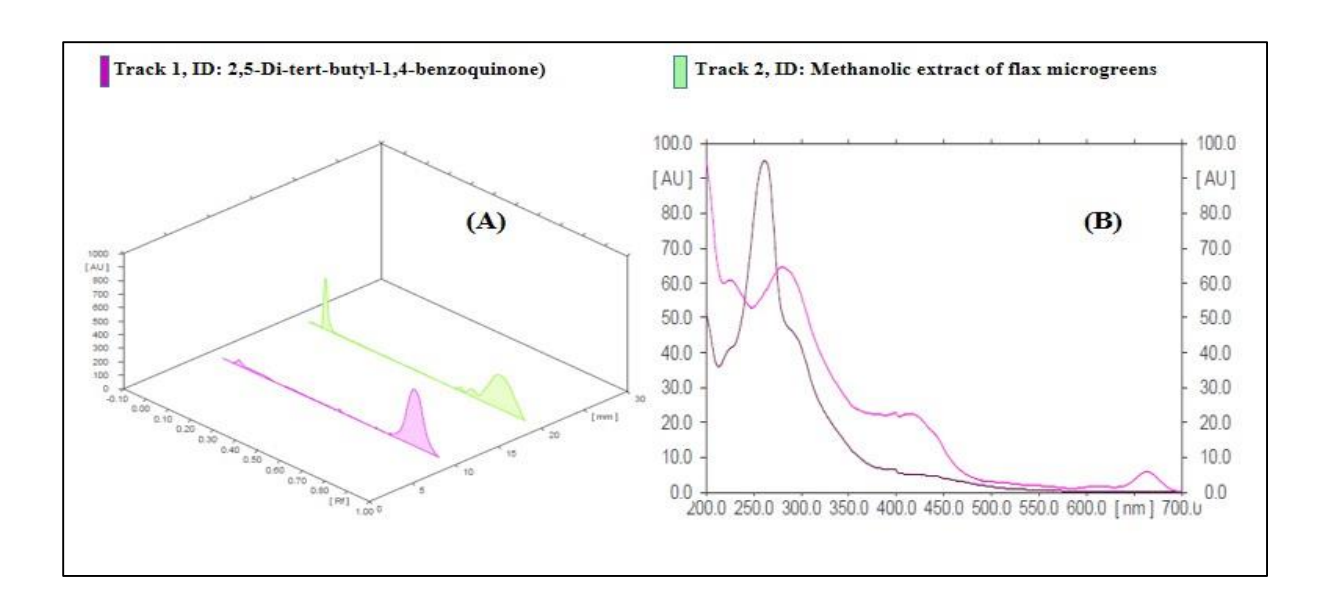


Figure 4.30: (A) 3D Chromatogram of 2,5-DTBQ from extract and standard. (B) Overlay of HPTLC chromatogram of all tracks.

4.13 In vitro Studies

4.13.1 Cell viability assay

A popular colorimetric method for determining cell viability and cytotoxicity is the MTT assay. It works by assessing the metabolic activity of living cells, where mitochondrial dehydrogenases reduce MTT (3-(4,5-dimethylthiazol-2-yl)-2,5-diphenyltetrazolium bromide) into purple formazan crystals. This reduction is primarily facilitated by mitochondrial dehydrogenase enzymes, with succinate dehydrogenase playing a significant role. The intensity of the purple color, measured spectrophotometrically at 570 nm, correlates with the number of viable cells (Karatop *et al.*, 2022; Kumar *et al.*, 2023). The cytotoxicity effects of the MEFM, 2,5-DTBQ, 4,4'-M(2,6-DTBP), and cisplatin (standard drug) against PC-3 were evaluated using the MTT assay (Figure 4.31), and the IC₅₀ values were generated from dose-response curve studies. The MEFM exhibits strong cytotoxic effect against cell lines, greater than the efficacy of the standard drug. Among the identified bioactive compounds, 2,5-DTBQ and 4,4'-M(2,6-DTBP) both demonstrate inhibitory effects on PC-3 cell lines. Notably, 2,5-DTBQ exhibits higher cytotoxicity compared to 4,4'-M(2,6-DTBP). However, the inhibitory activity of both compounds remains moderate when compared to the standard drug cisplatin, which is commonly used in prostate cancer treatment. The IC₅₀ values for the MEFM, 2,5-DTBQ, 4,4'-M(2,6-DTBP) and cisplatin were determined

using nonlinear regression analysis in Microsoft Excel. The IC₅₀ values of MEFM, 2,5-DTBQ, 4,4'-M(2,6-DTBP), and cisplatin were recorded as 377.5 µg/mL (95% CI: 377.48–377.52 µg/mL; $R^2 = 0.918$), 875.4 µg/mL (95% CI: 831–919.23 µg/mL; $R^2 = 0.9415$), 2324.78 µg/mL (95% CI: $2324.74-2324.82 \mu g/mL$; $R^2 = 0.9742$), and $273.97 \mu g/mL$ (95% CI: $273.94-274.00 \mu g/mL$; $R^2 = 0.9742$) 0.9908), respectively, as presented in **Table 4.23**. 4,4'-M(2,6-DTBP) and 2,5-DTBQ indicated lower potency compared to MEFM and cisplatin. These results suggest that MEFM and cisplatin exhibit a more potent anticancer effect due to their nonlinear sigmoidal response, while 2,5-DTBQ and 4,4'-M(2,6-DTBP) follow a linear response, requiring higher concentrations to achieve significant cytotoxicity. Even though 2,5-DTBQ and 4,4'-M(2,6-DTBP) show the high binding energies of -11.3 and -17.1 kcal/mol, respectively, they exhibit weak cytotoxicity, which is probably due to quick metabolism, low bioavailability, and poor cellular uptake. The reduced effectiveness may result from efflux via drug transporters, poor apoptosis activation, and the differences between in silico and in vitro conditions. The combination of the standard drug along with those bioactive compounds will enhance cytotoxicity in PC-3 cell lines. Figure 4.32 illusterates that MEFM, 2,5-DTBQ, 4,4'-M(2,6-DTBP), and cisplatin induced cellular shrinkage and caused morphological damages in PC-3 cell lines. According to Zhou et al. (2020), Linum usitatissimum (flaxseed) significantly inhibits the proliferation and invasion of human prostate cancer cells in vitro. This highlights its potential as a therapeutic or preventive agent against prostate cancer. Mueed et al. (2023) reported that flaxseed lignans induced cell death and G0/G1 cell cycle arrest in human prostate PC-3 cancer cells by suppressing a key oncogenic signaling pathway.

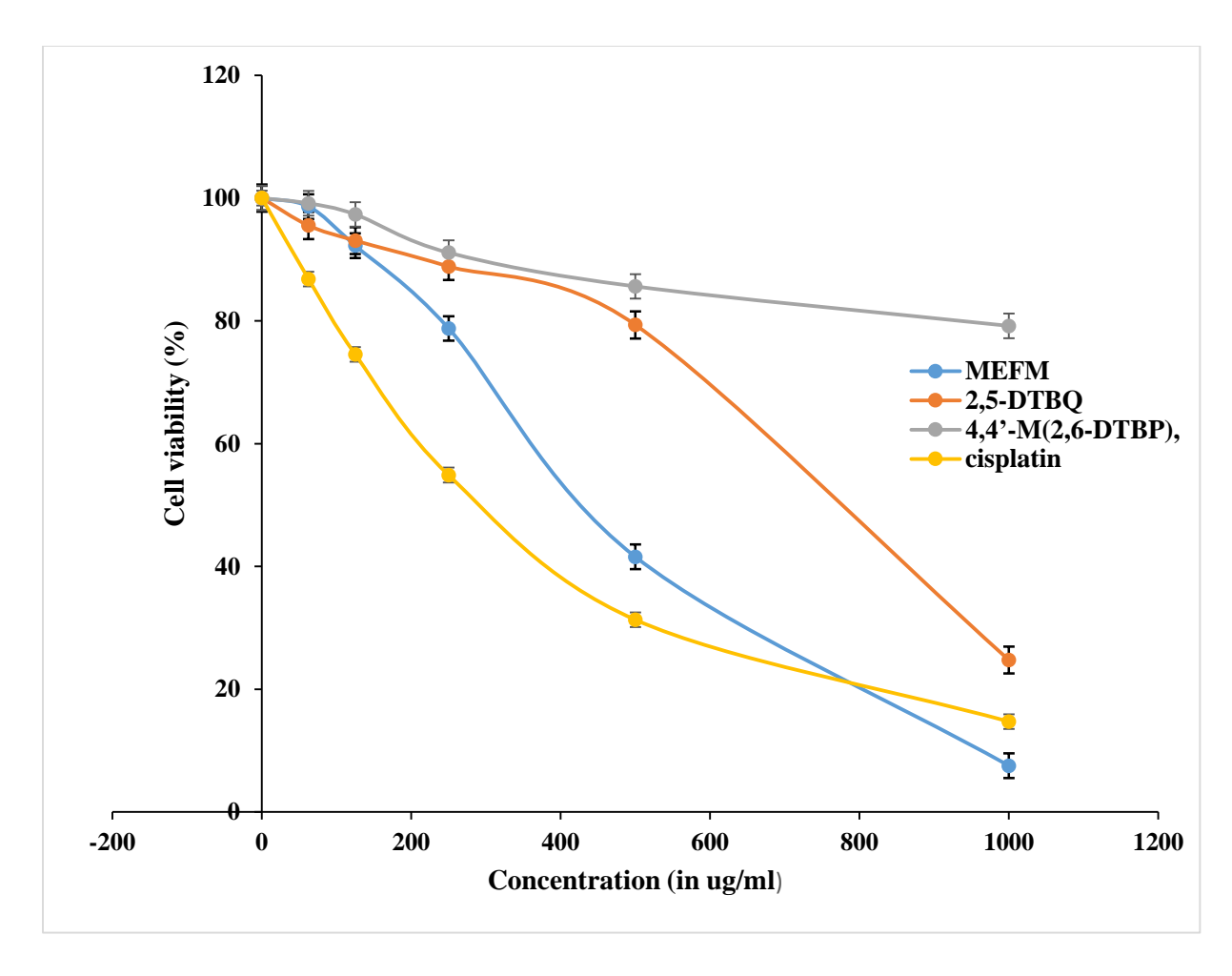


Figure 4.31: MTT assay showing dose–response curves of PC-3 prostate cancer cells (3 \times 10⁴) incubated and exposed to varying concentrations of MEFM, 2,5-DTBQ, 4,4'-M(2,6-DTBP), and Cisplatin (standard). Data are presented as mean \pm SD from three independent experiments.

Table 4.23: IC₅₀ and 95% CI values of cell proliferation inhibition of MEFM, 2,5-DTBQ, 4,4'-M(2,6-DTBP), and cisplatin

	PC-3 Cell lines	
	IC ₅₀ (μg/mL)	95% Confidence Interval (μg/mL
MEFM	377.5	377.48 – 377.52
2,5-DTBQ	875.4	831.61 – 919.23
4,4'-M(2,6-DTBP)	2324.78	2324.74 – 2324.82
Cisplatin	273.97	273.94 – 274.00

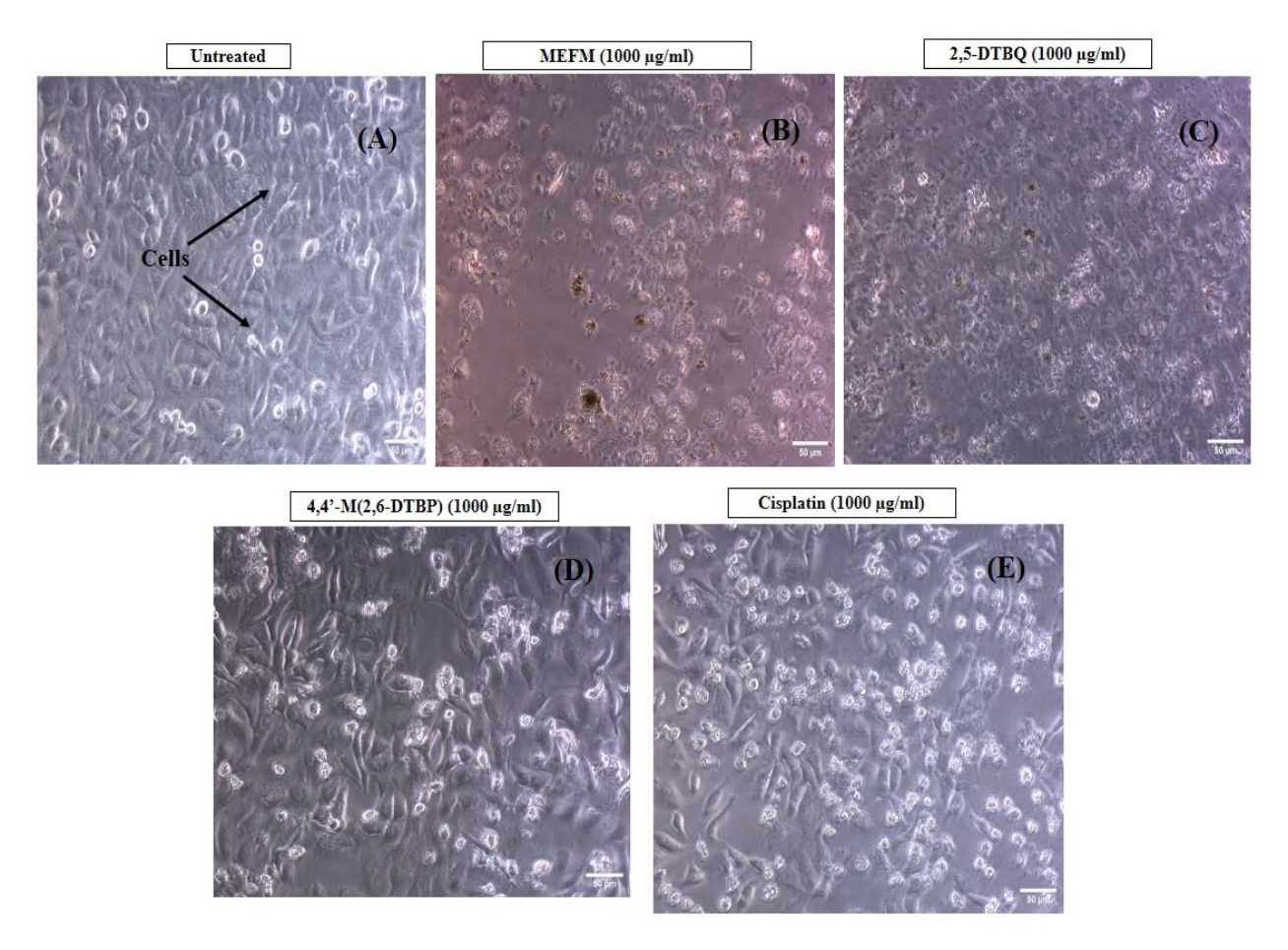


Fig. 4.32: Morphological changes in PC-3 cell lines after 24 h of treatment. (A) Untreated control, (B) MEFM, (C) 2,5-DTBQ, (D) 4,4'-M(2,6-DTBP), and (E) Cisplatin. Treated groups show reduced cell density and altered morphology compared to the control. Scale bar = $50 \mu m$; average cell size ranges between $12-20 \mu m$.

4.13.2 Annexin apoptotic assay

The annexin V apoptosis assay can identify and count apoptotic cells by recognizing phosphatidylserine (PS) proteins that are exposed at the cell membrane surface through its fluorescent labeling and flow cytometry measurements to differentiate live, early apoptotic, and late apoptotic cells (Khalef *et al.*, 2024). To understand the mode of action of the MEFM and its bioactive compound, the annexin V apoptosis assay was performed. The apoptotic assay of the untreated, MEFM, 2,5-DTBQ, and 4,4'-M(2,6-DTBP) bioactive compounds is presented in **Table 4.24**. MEFM, 2,5-DTBQ, and 4,4'-M(2,6-DTBP) exhibited a significantly increased total apoptosis of 41.03, 26.83, and 22.86%, respectively, compared to untreated cell lines (3.92%). In early apoptotic cells, the MEFM, 2,5-DTBQ, and 4,4'-M(2,6-DTBP) demonstrated significantly

higher cell death (40.9, 25.7, and 19.5%, respectively), whereas in late apoptotic cells, the cell death was found to be 0.13, 1.13, and 3.36%, respectively (**Table 4.24**). Although these test samples effectively induced cell death, their potency is lower compared to cisplatin, a standard PC-3 cell line's apoptotic inducer (Huang *et al.*, 2021). These results indicate that these phytocompounds were effective in inducing cell death during the early apoptosis stage, but their efficiency in destroying cells decreased during the late apoptosis stage. Analysis of cell apoptosis in MEFM, 2,5-DTBQ, and 4,4'-M(2,6-DTBP) after 24 h incubation in PC-3 cell lines is depicted in **Figure 4.33**. The results clearly demonstrate that MEFM exhibited a significantly higher apoptotic effect compared to the bioactive compounds. This enhanced effect may be attributed to the diverse array of bioactive compounds present in MEFM derived from flax microgreens.

Table 4.24: Percentage of cells after MEFM, 2,5-DTBQ, and 4,4'-M(2,6-DTBP) treatment (Annexin V Apoptosis Assay)

Sample Name		%	Geometric mean fluorescence intensity (MFI) of AbFlour 488 Annexin V (FL1-A parameter)			
	Live	Early	Late	Debris	Total	
		Apoptotic	Apoptotic		apoptosis	
Control (Untreated)	95.8	3.86	0.063	0.28	3.92	2002
MEFM	58.9	40.9	0.13	0.1	41.03	7934
2,5-DTBQ	71.2	25.7	1.13	1.99	26.83	5186
4,4'-M(2,6-DTBP)	72.4	19.5	3.36	4.73	22.86	5620

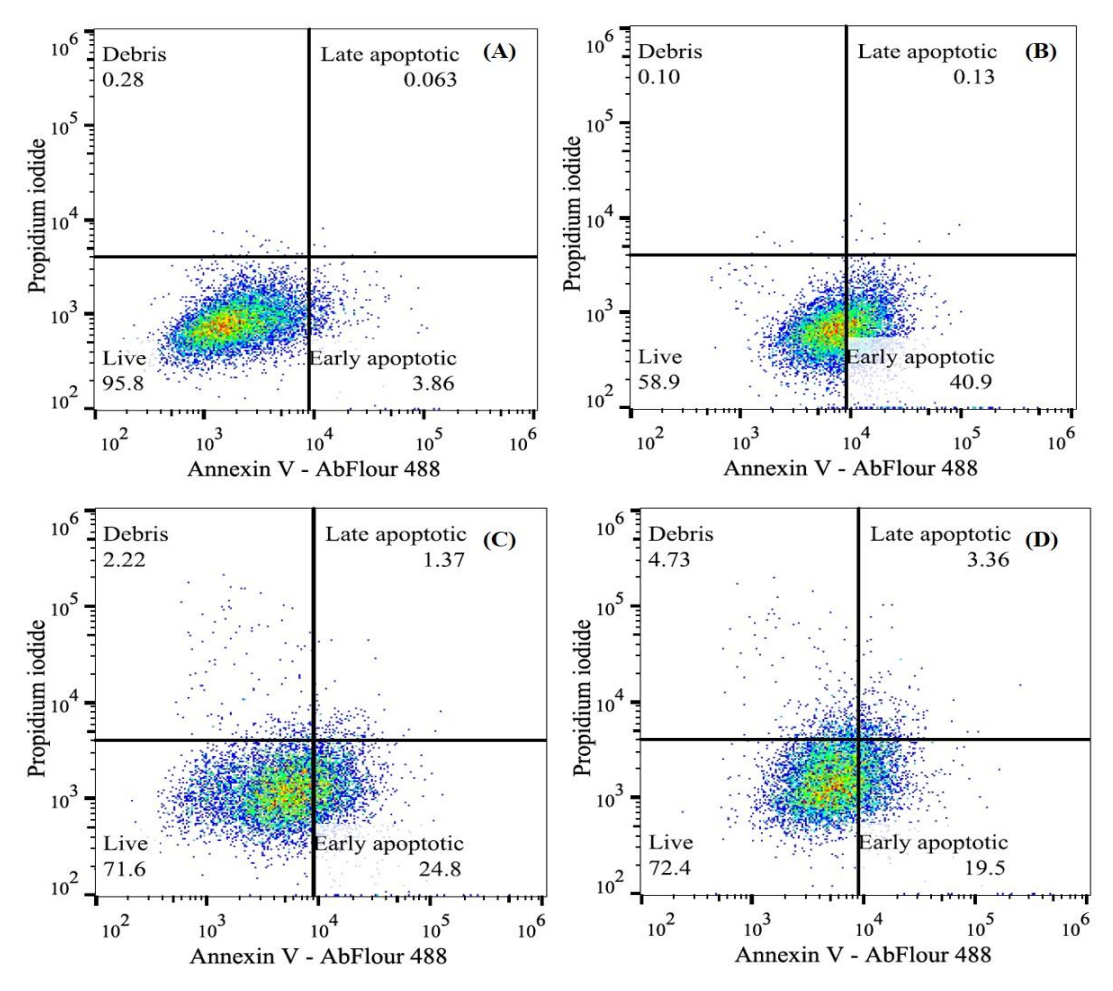


Figure 4.33: Annexin V Apoptosis Assay conducted on PC-3 cells under different treatment conditions: (A) Untreated control, (B) MEFM-treated, (C) 2,5-DTBQ-treated, and (D) 4,4'-M(2,6-DTBP)-treated cells

4.14 In vivo study

4.14.1 Acute toxicity

The acute toxicity test results of the methanolic extract of flax microgreens (MEFM) on wistar rats showed no death or any toxicity sign in the rats at the highest dose of 5000 mg/kg. Thus, the lethal dose of MEFM was found to be greater than 5000 mg/kg.

4.14.2 Effects of MEFM and its bioactive compounds on wistar rats body weight

The results from Table 4.25 indicate that prostate cancer (PC) induction significantly reduced the body weight gain (BWG) in male wistar rats, as clearly seen in the disease control group (BWG:16.37±1.64 g) compared to the normal control group (BWG: 46.19±2.78 g). The group

treated with the standard drug (finasteride: 10 mg/kg) showed improvement in recovery from the disease by increasing in body weight gain (BWG: 27.19±2.67 g). Among the tested bioactive compounds, 2,5-DTBQ (20 mg/kg) showed a significant higher effect (BWG: 19.72±1.73 g) than 4,4'-M(2,6-DTBP) (BWG: 23.68±8.25 g). The MEFM (200 mg/kg) exhibited significant recovery with a BWG: 25.52±5.57 g; however, it had significantly lower BWG when compared with the finasteride. This suggests that MEFM and its bioactive compounds may have therapeutic potential in alleviating PC-induced weight loss, with MEFM showing the most promising results as compared to its bioactive compounds. This is in agreement with the reports of Uroko *et al.* (2022) and Joshi *et al.* (2023), who reported a reduction in body weight could be attributed to loss of appetite because of discomfort caused by induction of PC.

Table 4.25: Effects of MEFM and its selected bioactive compounds on wistar rats body weight

Treatment	IBW (g)	FBW (g)	BWG (g)
Normal control	185.90 ± 2.72	233.15±2.57	46.19±2.78***
Disease control	188.80 ± 2.61	204.54±2.82	16.37±1.64
Finasteride (10 mg/kg)	200.95 ± 3.09	228.14±4.91	27.19±2.67**
4,4'-M(2,6-DTBP) (20 mg/kg)	204.58 ± 2.96	223.21±3.45	19.72±1.73*
2,5-DTBQ (20 mg/kg)	198.32 ± 5.28	221.04±3.70	23.68±8.25*
MEFM (200 mg/kg)	216.56 ± 3.12	242.08±5.34	25.52±5.57**

Note: Values are expressed as Mean \pm SD, n = 5 per group. *p < 0.05, **p < 0.01, ***p < 0.001 vs. Negative control group

4.14.3 Effects of MEFM and its bioactive compounds on the prostate weight (PW)

The weight of the prostate glands in each group was compared with that of the normal group (vehicle group). Rats' prostate weight was considerably higher after testosterone (5 mg/kg) treatment than in the control group. The results presented in **Table 4.26** illustrate the effects of MEFM and its bioactive compounds on prostate weight (PW), Prostate Index (PI), percentage of prostate growth inhibition, and), percentage of prostate index inhibition in PC-induced wistar rats. The results indicate that there is significantly increased prostate weight in the negative control (1.76 g) compared to the normal control (0.79 g), confirming the prostate enlargement due to cancer. The standard drug (finasteride: 10 mg/kg) reversed this enlargement effectively by

reducing the prostate weight to 0.78 g with nearly complete inhibition (100.81%), which is almost similar to normal control. It also significantly decreased the prostate index to 0.34%, with inhibition percentages of 100.81% for prostate weight and 99.34% for the prostate index.

Among the test samples, MEFM (200 mg/kg) showed the highest effectiveness, closer to finasteride, reducing prostate weight to 0.89 g and prostate index to 0.37%. The inhibition percentages are 89.46% for prostate weight and 94.09% for the prostate index. 2,5-DTBQ (20 mg/kg) demonstrated stronger effects, reducing prostate weight to 0.96 g and prostate index to 0.44%, with inhibition rates of 81.86% and 81.2%, respectively. On the other hand, 4,4'-M(2,6-DTBP) (20 mg/kg) showed moderate efficacy, reducing prostate weight to 1.17 g and the prostate index to 0.52%, with inhibition rates of 60.73% and 64.62%, respectively. The observed increase in prostate weight may be due to uncontrolled proliferation of cellular components within the prostate tissue (Akbari *et al.*, 2021). This observation aligns with Joshi *et al.* (2023), who identified prostate weight increase as a significant biomarker of prostate cancer. Consequently, numerous studies have evaluated the inhibitory effects of various substances on prostate cancer development by measuring changes in prostate weight.

Table 4.26: Effects of MEFM and its selected bioactive compounds on prostate weight and relative prostate weight

Treatment			% of Prostate	% of Prostate
	Prostate weight	Prostate Index	growth inhibition	Index Inhibition
	(g)	(%)	(%)	(%)
Normal control	0.79±006***			
Negative control	1.76±0.3			
Finasteride (10 mg/kg)	$0.78\pm0.09^{***}$	$0.34\pm0.03^{***}$	100.81	99.34
4,4'-M(2,6-DTBP) (20 mg/kg)	1.17±0.15**	0.52±0.06**	60.73	64.62
2,5-DTBQ (20 mg/kg)	0.96±0.10**	0.44±0.05**	81.86	81.2
MEFM (200 mg/kg)	0.89±0.13**	0.37±0.06**	89.46	94.09

Note: Values are expressed as Mean \pm SD, n = 5 per group. *p < 0.05, **p < 0.01, ***p < 0.001 vs. Negative control group

4.14.4 Effects on serum level of testosterone and prostate specific antigen (PSA).

Testosterone and prostate-specific antigen (PSA) levels are commonly evaluated in the context of prostate disorders and are considered important markers for prostate cancer. **Figure 4.34** shows that the disease control group has significantly higher testosterone levels (28.9975 pg/mL) compared to the normal control group (16.375 pg/mL). The group treated with the standard drug (finasteride) effectively reduces the testosterone levels close to normal (16 pg/mL). Among the tested compounds, 2,5-DTBQ and 4,4'-M(2,6-DTBP) demonstrated testosterone-lowering effects, with mean concentrations of 16.223 pg/mL and 17.555 pg/mL, respectively, compared to finasteride. MEFM showed a strong reduction to 14.504 pg/mL, which is significantly lower than the normal control group. These findings suggested that MEFM and its bioactive compounds have the potential to counteract disease-induced testosterone elevation, particularly MEFM which has greater efficacy than the standard treatment.

The results presented in **Figure 4.35** indicate a significant increase (P<0.05) in prostate-specific antigen (PSA) levels in the disease control group (8.596 pg/mL) compared to the normal control group (1.7 pg/mL). Finasteride treatment reduces PSA levels effectively to 1.6526 pg/mL, near-normal levels. Similarly, the test compounds 4,4'-M(2,6-DTBP), 2,5-DTBQ, and MEFM lower PSA levels to 1.5678, 1.65, and 1.5348 pg/mL, respectively. The results indicate all the tested compounds exhibit PSA-lowering effects compared to finasteride, with the extract showing the highest reduction. According to the findings of Abd-Alhussen *et al.* (2024), the oral administration of flaxseeds ethanolic extract effectively decreased prostate gland weight, prostate index and serum PSA levels in testosterone-induced benign prostatic hyperplasia. The lignan-rich flaxseed hull extract dose-dependently prevented TP-induced prostate enlargement in rats, with higher enterolactone levels correlating with extract dose, suggesting its potential in BPH prevention (Bisson *et al.*, 2019).

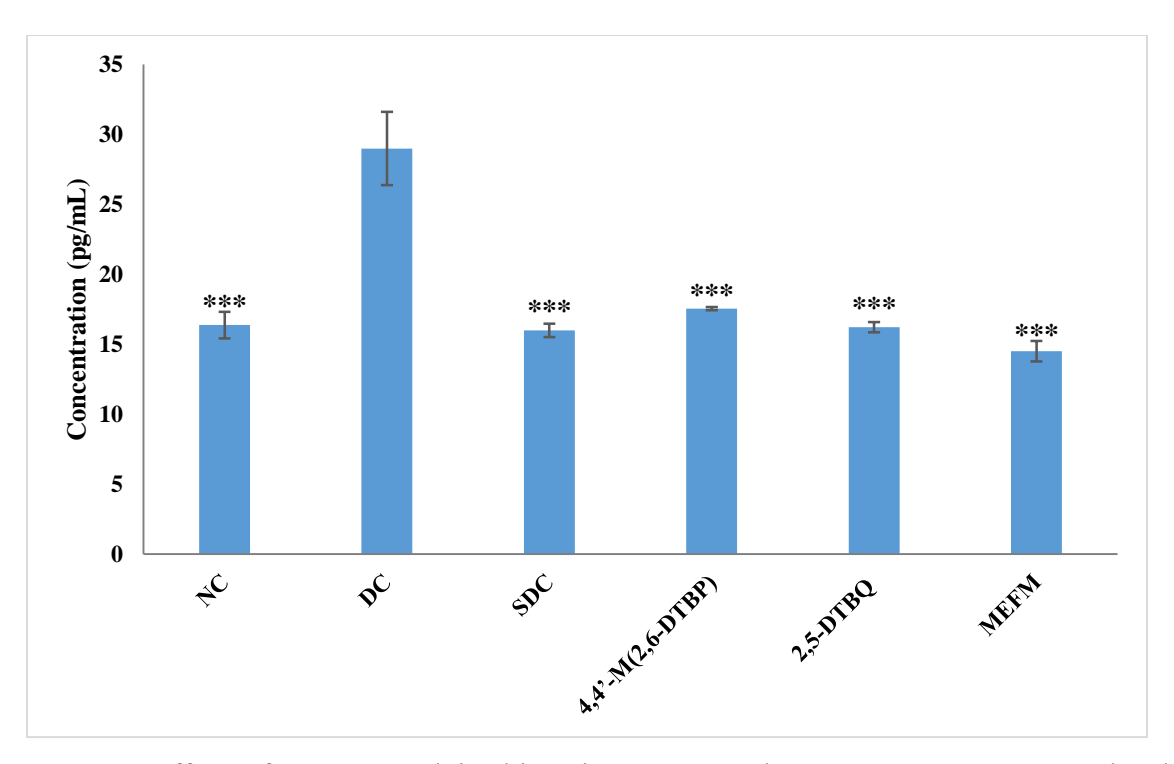


Figure 4.34: Effect of MEFM and its bioactive compounds on serum testosterone level in Testosterone-induced PC wistar rats. NC: Normal control, DC: Disease control, SDC: standard drug control (Finasteride). n=5, Data are shown in triplicate as mean \pm SD. Mean values (bar graphs), Standard deviation (vertical lines). Mean values (bar graphs), Standard deviation (vertical lines). Asterisk (***) above the bars is statistically significance ($P \le 0.001$) compared to the **Disease Control (DC)** group.

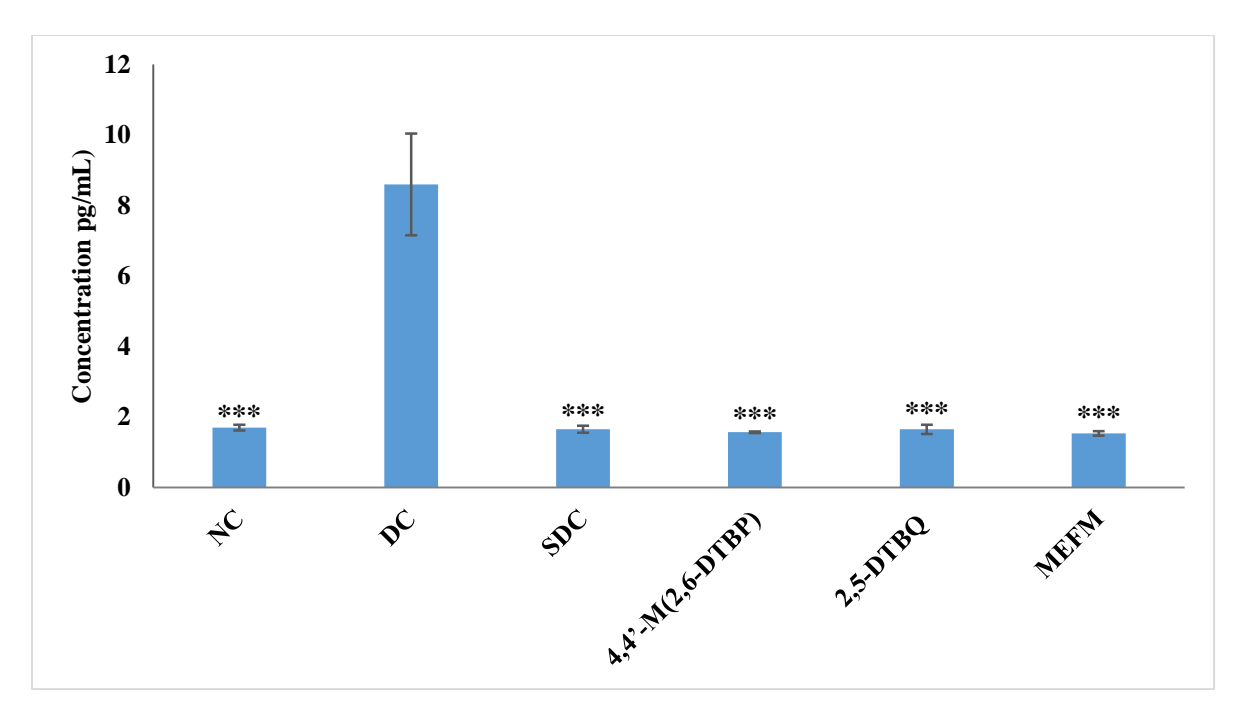


Figure 4.35: Effect of MEFM and its bioactive compounds on Prostate Specific Antigen (PSA) level in Testosterone-induced PC wistar rats. NC: Normal control, DC: Disease control, SDC: standard drug control (Finasteride). n=5, Data are shown in triplicate as mean \pm SD. Mean values (bar graphs), Standard deviation (vertical lines). Mean values (bar graphs), Standard deviation (vertical lines). Asterisk (***) above the bars is statistically significance ($P \le 0.001$) compared to the **Disease Control (DC)** group.

4.14.2 Histopathology results of prostate

The **Figure 4.36** presents the histopathological evaluation of prostate tissues (magnification $40\times$, scale bar = 100 μ m; $60\times$, scale bar = 50 μ m), revealed significant differences across the experimental groups. Normal control rats showed healthy and well-organized glandular structures of the prostate, while the disease control group showed distinct abnormalities such as prostatic intraepithelial neoplasia (PIN) architectural patterns characterized by the loss of basal epithelial cells and disrupted tissue architecture, indicating prostate enlargement. Treatment with finasteride substantially restored normal histology, showing closely resembling that of the normal group. A reduced intraepithelial development, slightly elevated chromatin content, and better-retained cytoplasmic content were all notable signs of the MEFM-treated group's partial recovery. The groups treated with 2,5-DTBQ and 4,4'-M(2,6-DTBP) also showed improvement, though to a lesser extent, with 2,5-DTBQ performing better than 4,4'-M(2,6-DTBP).

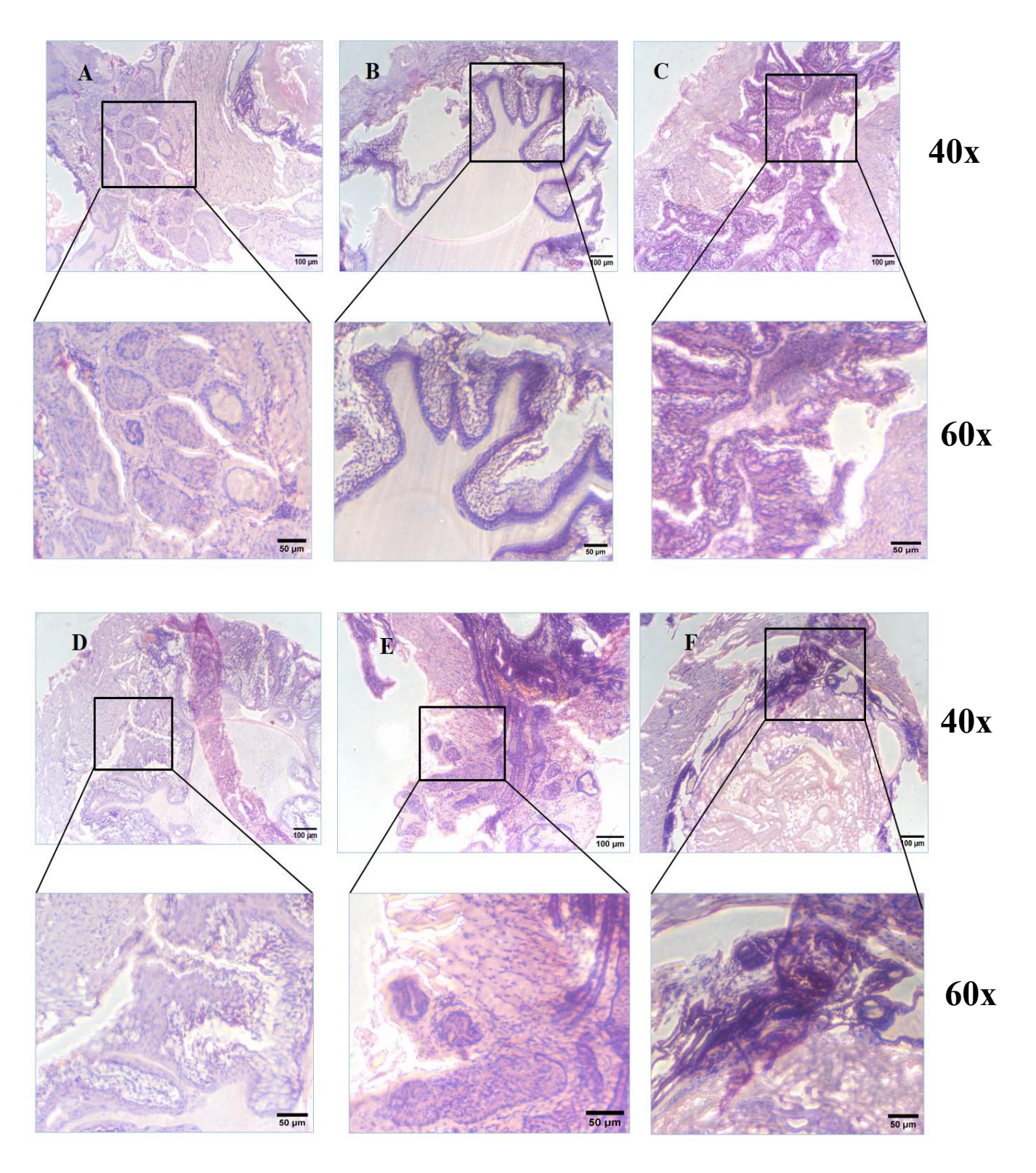


Figure 4.36: Prostate tissue histopathological analysis: (A) Normal control group, (B) Disease control group, and treatment groups: (C) Standard drug control (Finasteride: 10 mg/kg), (D) 4,4'-M(2,6-DTBP) (20 mg/kg), (E) 2,5-DTBQ (20 mg/kg), and (F) MEFM (200 mg/kg) for 21 days.

CHAPTER FIVE

5.0 Summary, conclusion and recommendations

5.1 Summary

Prostate cancer's significant impact on men's health, ranking as the deadliest cancer after skin cancer, underscores the importance of exploring potential treatments and preventive measures. Almost two-thirds of the cancers diagnosed among men are prostate cancer. As of the 2018 SEER Cancer Statistics Review, the prevalence rate is nearly 60% in men over 65 years. While the lignans and polyphenols in flaxseeds have shown promising potential in preventing and treating various types of cancers, there appears to be a lack of studies investigating the potential effects of flax microgreens specifically on prostate cancer. Previous literature proved that the flax microgreens have a high concentration of phenolic compounds, superior proteins and free amino acids, and a good fatty acid composition, making them an important plant source of components that are beneficial to health, but no research has been shown the anti-cancerous effects of flax microgreens and its bioactive compounds against prostate cancer. Therefore, this study addresses that gap by evaluating the therapeutic potential of flax microgreens and their bioactive compounds using a multi-faceted approach including Gas Chromatography-Mass Spectrometry (GC-MS), UV-visible spectroscopy, High Performance Thin Layer Chromatography (HPTLC), and both *in silico*, *in vitro*, and *in vivo* models.

Qualitative phytochemical screening of the methanolic extract of flax microgreens (MEFM) revealed a broad spectrum of bioactive compounds, including alkaloids, saponins, flavonoids, steroids, phenolics, and others, although tannins, terpenoids, and emodins were absent. The extract demonstrated robust antioxidant activity in a dose-dependent manner, with DPPH radical scavenging reaching 84.2% at 1000 µg/mL. It also showed considerable metal-chelating and reducing power capabilities.

GC-MS analysis identified 60 distinct phytochemicals in the extract. These compounds were subsequently evaluated through molecular docking against eight prostate cancer-related protein targets (AURKA, DLL3, N-Myc, CTLA-4, 5AR, AR, LSD1, and CD27). Among bioactive compounds, 4,4'-M(2,6-DTBP) demonstrated the highest binding affinity across all protein targets, followed closely by 2,5-DTBQ and they were selected for further studies. These two best

active compounds were further identified and characterized using UV-Vis and HPTLC methods. Both were most concentrated in non-polar fractions, with hexane extracts showing the highest levels. HPTLC analysis confirmed their presence, with 4,4'-M(2,6-DTBP) and 2,5-DTBQ accounting for 100% and 73.9% of the compound areas, respectively.

In vitro cytotoxicity testing against PC-3 prostate cancer cell lines showed that MEFM had greater anticancer activity than the standard drug, cisplatin. Among the identified compounds, 2,5-DTBQ exhibited stronger activity than 4,4'-M(2,6-DTBP), although both were less potent than cisplatin overall. The IC₅₀ values further reflected this trend: MEFM (377.5 μg/mL), 2,5-DTBQ (875.4 μg/mL), 4,4'-M(2,6-DTBP) (2324.78 μg/mL), and cisplatin (273.97 μg/mL). The discrepancy between docking and *in vitro* results may be attributed to differences in bioavailability, metabolic stability, and cellular uptake. Apoptosis assays confirmed that MEFM and the identified compounds induced significant cell death compared to controls, though their potency was still lower than cisplatin. MEFM induced 41.03% apoptosis, while 2,5-DTBQ and 4,4'-M(2,6-DTBP) induced 26.83% and 22.86%, respectively. The early apoptosis phase accounted for the majority of cell death in all treated groups.

In vivo study, acute toxicity testing showed no toxicity for MEFM at a dose of 5000 mg/kg. Therapeutically, MEFM and its major compounds significantly mitigated prostate cancer signs symptoms in rat models. MEFM showed the most distinct protective effects by reducing the prostate weight and prostate index by over 89% and 94%, respectively, results comparable to those achieved by finasteride, the standard treatment. 2,5-DTBQ also performed well, while 4,4'-M(2,6-DTBP) had a moderate effect. Histopathological analysis supported these findings. MEFM-treated wistar rats showed considerable tissue recovery, with more normalized glandular structures and reduced signs of neoplasia. While both selected compounds improved histological profiles, 2,5-DTBQ again showed greater efficacy than 4,4'-M(2,6-DTBP). The assessment of the anticancer efficacy of the methanolic extract of flax microgreens and its selected bioactive compounds may serve as one of the potential solutions to the current issue of prostate cancer, aligning with the United Nations Sustainable Development Goals (UNSDGs) 3, 9, 12, and 15 which focus on plant-based cancer therapy, development and scientific innovation, promoting sustainable production of nutraceuticals and ecological significance of medicinal plants. Figure 5.1 illustrates the summary of the thesis workflow and findings.

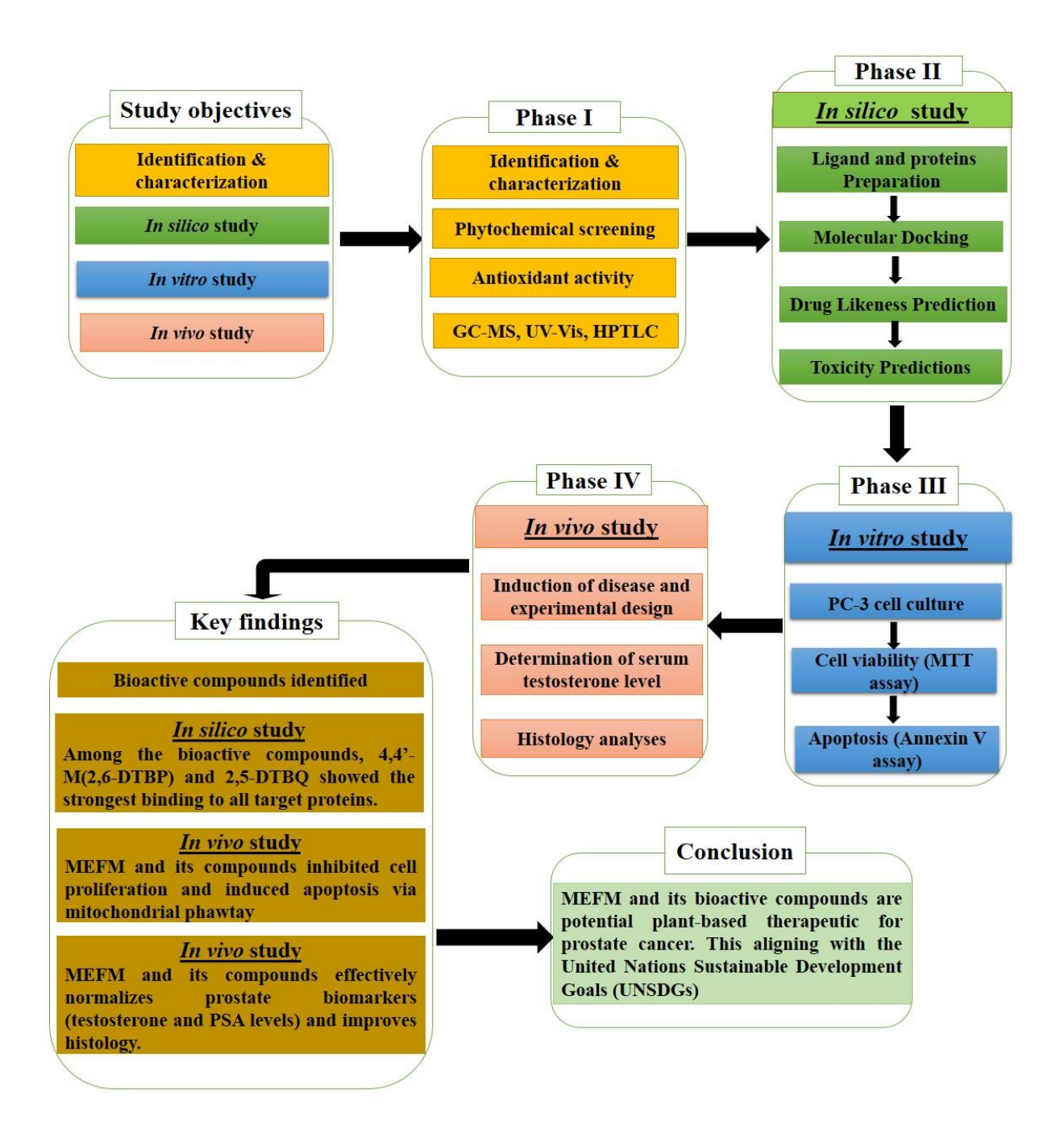


Figure 5.1: Summary of the thesis workflow and findings, outlining the research objectives, identification of bioactive compounds, *in silico* molecular analyses, *in vitro* and *in vivo* experimental evaluations, and the key findings leading to the study's overall conclusion

5.2 Conclusion

This study provides compelling evidence supporting the therapeutic potential of flax microgreens, specifically their methanolic extract (MEFM), as a novel, plant-based candidate for prostate cancer (PC) prevention and treatment. Given the global burden of prostate cancer as one of the most prevalent and deadliest malignancies among men, especially in aging populations, the urgent demand for alternative and complementary therapies remains unfulfilled. This work explores a comprehensive approach by integrating phytochemical analysis, *in silico* modeling, and both *in vitro* and *in vivo* validations to investigate the efficacy of MEFM and its key bioactive constituents as shown in **figure 5.2**.

Phytochemical screening revealed that MEFM is rich in diverse classes of bioactive compounds, including flavonoids, phenolics, saponins, and alkaloids, many of which are known for their antioxidant and anticancer properties. Antioxidant assays confirmed that MEFM possesses robust free radical scavenging, metal-chelating, and reducing capabilities, highlighting its potential to reduce oxidative stress, a known contributor to carcinogenesis.

Through Gas Chromatography-Mass Spectrometry (GC-MS), 60 distinct phytochemicals were identified, among which 4,4'-M(2,6-DTBP) and 2,5-DTBQ emerged as prominent candidates based on their abundance and strong binding affinities to key prostate cancer targets. Molecular docking studies against eight prostate cancer-related proteins revealed strong interactions, particularly for 4,4'-M(2,6-DTBP), highlighting its multi-targeted potential. *In silico* ADME/T analysis also predicted favorable pharmacokinetic and safety profiles for these compounds.

UV-Vis and HPTLC analyses confirmed the presence and abundance of these two bioactive compounds in MEFM, particularly in non-polar solvent fractions. Despite their strong *in silico* binding affinities, *in vitro* cytotoxicity studies using PC-3 prostate cancer cell lines demonstrated that the whole MEFM exhibited greater cytotoxic potential (IC₅₀ = 377.5 μ g/mL) than the isolated compounds 2,5-DTBQ (IC₅₀ = 875.4 μ g/mL) and 4,4'-M(2,6-DTBP) (IC₅₀ = 2324.78 μ g/mL). Apoptotic assays validated these findings, showing significantly higher early apoptosis induction by MEFM compared to its individual components. These outcomes recommend that the higher

efficacy of MEFM may be attributed to synergistic interactions among its multiple phytochemicals, enhancing its biological activity.

In vivo studies further confirmed MEFM's therapeutic promise. Acute toxicity testing revealed that MEFM is well-tolerated at doses up to 5000 mg/kg, confirming its safety profile. In the context of prostate cancer mode, MEFM effectively prevented weight loss and significantly reduced prostate weight and index to levels nearly equivalent to finasteride, the standard clinical drug. Also, histopathological evaluations showed that MEFM treatment helped restore prostate glandular architecture and cellular integrity, indicating real biological recovery. While 2,5-DTBQ and 4,4'-M(2,6-DTBP) also demonstrated therapeutic effects, they were consistently less effective than the full extract.

From the result obtained, it can be concluded that, MEFM shows strong potential as a safe, multi-targeted, plant-derived candidate for prostate cancer prevention and treatment. Its higher effectiveness compared to isolated bioactive compounds supports the hypothesis of synergism among the various phytochemicals present in the whole extract, enhancing its overall therapeutic impact.

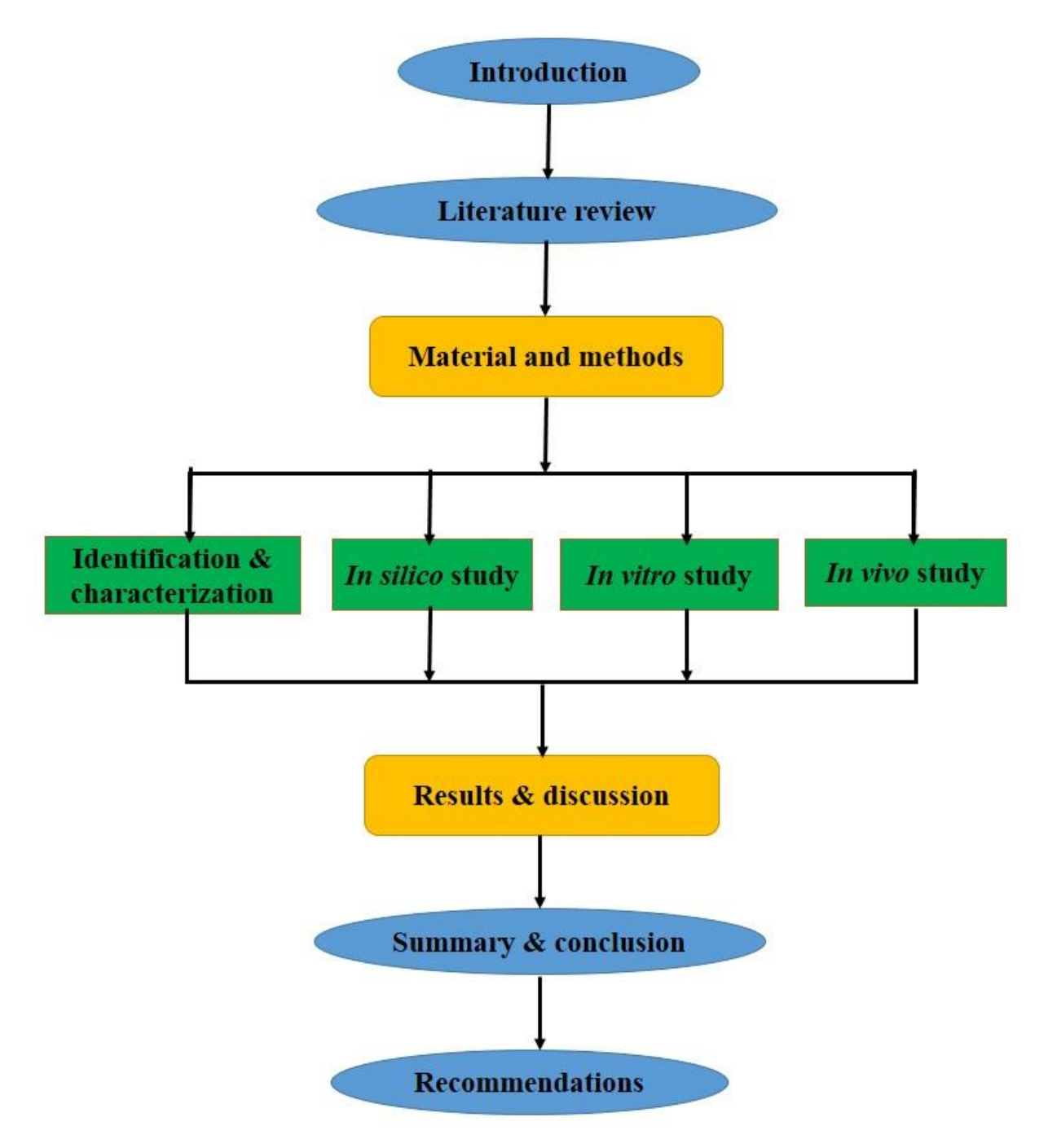


Figure 5.2: Flowchart showing the thesis structure, including introduction, literature review, materials and methods, results and discussion, summary and conclusion, and recommendations.

5.3 Recommendations

Based on the findings presented in this study, the following recommendations were raised:

1. Pharmacokinetics and bioavailability studies:

Despite promising *in silico* and *in vitro* results, the relatively moderate cytotoxicity of 2,5-DTBQ and 4,4'-M(2,6-DTBP) *in vitro* suggests a need for deeper investigation into their pharmacokinetics. Future studies should focus on evaluating their absorption, distribution, metabolism, and excretion (ADME) profiles in vivo to understand their bioavailability and systemic behavior.

2. Formulation and delivery optimization:

To overcome limitations such as poor cellular uptake or rapid metabolism, advanced drug delivery systems (e.g., nano-formulations, liposomes, or polymer-based carriers) should be explored to enhance the bioavailability and therapeutic efficacy of MEFM and its bioactive compounds.

3. Mechanistic pathway analysis:

While apoptosis assays confirmed the cytotoxic nature of MEFM and its compounds, further molecular studies are needed to elucidate the exact pathways involved in inducing apoptosis (e.g., caspase activation, mitochondrial membrane potential disruption, or ROS-mediated pathways).

4. Long-term in vivo efficacy and safety trials:

Conduct extended *in vivo* studies to assess long-term safety, organ-specific toxicity, and sustained efficacy of MEFM in different prostate cancer models, including hormone-independent or metastatic PC models.

5. Clinical translation and human trials:

Given the extract's favorable safety profile, future research should move toward preclinical and clinical trial phases. Pilot human studies would help assess tolerability, optimal dosing, and therapeutic potential in patients at different stages of prostate cancer.

6. Target validation and CRISPR-based studies:

Molecular docking indicated strong interactions with key prostate cancer targets. CRISPR or siRNA gene-silencing techniques can be employed to validate these targets in cellular systems, confirming the biological relevance of MEFM–protein interactions.

7. Metabolomics and proteomics approaches:

Incorporating omics technologies will allow comprehensive profiling of metabolic and proteomic changes induced by MEFM treatment, providing a systems-level understanding of its mode of action and identifying potential biomarkers for therapeutic response.

8. Future studies should employ complementary assays such as scratch wound, LDH membrane-leak, ROS measurement, and marker expression to provide deeper mechanistic insights and strengthen the translational relevance of MEFM and its bioactive compounds in prostate cancer therapy.

References

- A. Ivanenkov, Y., V. Chufarova, N., S. Veselov, M., & G. Majouga, A. (2014). Dietary polyphenols for prostate cancer therapy. *Current Bioactive Compounds*, 10(2), 76-111.
- Abd-Alhussen, J. K., Al-Kurdy, M. J., & Hussein, S. A. (2024). In vivo assessment of the antibenign prostatic hyperplasia effect of hot ethanolic extract of flax seeds in male rats. *Open Veterinary Journal*, 14(8), 1928.
- Abdulal, Z. A., Altahhan, M. Y., Qindil, A. F., Al-Juhani, A. M., Alatawi, M. A., Hassan, H. M., & Al-Gayyar, M. M. (2024). Ferulic acid inhibits tumor proliferation and attenuates inflammation of hepatic tissues in experimentally induced HCC in rats. *Journal of Investigative Medicine*, 72(8), 900-910.
- Abolghasemi, R., Ebrahimi-Barough, S., Bahrami, N., & Aid, J. (2022). Atorvastatin inhibits viability and migration of MCF7 breast cancer cells. *Asian Pacific journal of cancer prevention: APJCP*, 23(3), 867.
- Abusnina, W., Auyoung, E. Y., Megri, M., & Pacioles, T. (2018). Small cell carcinoma of prostate: a case report of a patient with concomitant transitional cell cancer of the bladder. *Journal of Investigative Medicine High Impact Case Reports*, 6, 2324709618760644.
- Adamiecki, R., Hryniewicz-Jankowska, A., Ortiz, M. A., Li, X., Porter-Hansen, B. A., Nsouli, I., ... & Kotula, L. (2022). In vivo models for prostate cancer research. *Cancers*, *14*(21), 5321.
- Adhikari, T., & Saha, P. (2022). Quantitative estimation of immunomodulatory flavonoid quercetin by HPTLC in different leafy vegetables available in West Bengal. *Pharmacognosy Research*, 14(4).
- Adhikari, T., Ray, P. B., & Saha, P. (2025). Comparative study of quercetin content in marketed seeds of linum usitatissimum 1.(flax), salvia hispanica 1.(chia), and helianthus annuus 1.(sunflower) and their microgreens using hptlc from west bengal. *Indian Journal of Pharmaceutical Education and Research*, 59(1s), s221-s228.
- Agamah, F. E., Mazandu, G. K., Hassan, R., Bope, C. D., Thomford, N. E., Ghansah, A., & Chimusa, E. R. (2020). Computational/in silico methods in drug target and lead prediction. *Briefings in bioinformatics*, 21(5), 1663-1675.

- Aggarwal, S., Thareja, S., Verma, A., Bhardwaj, T. R., & Kumar, M. (2010). An overview on 5α-reductase inhibitors. *Steroids*, 75(2), 109-153.
- Agu, P. C., Afiukwa, C. A., Orji, O. U., Ezeh, E. M., Ofoke, I. H., Ogbu, C. O., ... & Aja, P. M. (2023). Molecular docking as a tool for the discovery of molecular targets of nutraceuticals in diseases management. *Scientific reports*, *13*(1), 13398.
- Ahmad, S., Singh, S., Srivastava, M. R., Shukla, S., Rai, S., & Shamsi, A. S. (2021). Molecular docking simplified: literature review. *Adv. Med. Dent. Health Sci*, *4*, 37-44.
- Ahmed, M. E., Mahmoud, A. M., Reitano, G., Zeina, W., Lehner, K., Day, C. A., ... & Andrews, J. R. (2024). Survival patterns based on First-site-specific visceral metastatic prostate Cancer: are outcomes of visceral metastases the same?. *European Urology Open Science*, 66, 38-45.
- Akbari, F., Azadbakht, M., Megha, K., Dashti, A., Vahedi, L., Barzegar Nejad, A., ... & Sadati, M. (2021). Evaluation of Juniperus communis L. seed extract on benign prostatic hyperplasia induced in male Wistar rats. *African Journal of Urology*, 27, 1-11.
- Akter, Y., Junaid, M., Afrose, S. S., Nahrin, A., Alam, M. S., Sharmin, T., ... & Hosen, S. Z. (2021). A comprehensive review on Linum usitatissimum medicinal plant: its phytochemistry, pharmacology, and ethnomedicinal uses. *Mini reviews in medicinal chemistry*, 21(18), 2801-2834.
- Alachaher, F. Z., Dali, S., Dida, N., & Krouf, D. (2018). Comparison of phytochemical and antioxidant properties of extracts from flaxseed (Linum usitatissimum) using different solvents. *International Food Research Journal*, 25(1).
- Alam, M., Ashraf, G. M., Sheikh, K., Khan, A., Ali, S., Ansari, M. M., ... & Hassan, M. I. (2022). Potential therapeutic implications of caffeic acid in cancer signaling: past, present, and future. *Frontiers in pharmacology*, *13*, 845871.
- Al-Ankoshy, A. A. M., & Al-Shamahy, H. A. (2021). Assessment of HOXB13 mutation in prostate cancer (Prca). *Nveo-natural volatiles & essential oils Journal* | *NVEO*, 5152-5159. Fu, Y. B. (2023). Pale flax (Linum bienne): An underexplored flax wild relative. In *The flax genome* (pp. 37-53). Cham: Springer International Publishing.

- Albuquerque, U. P., Medeiros, P. M. D., Ramos, M. A., Ferreira, W. S., Nascimento, A. L. B., Avilez, W. M. T., & Melo, J. G. D. (2014). Are ethnopharmacological surveys useful for the discovery and development of drugs from medicinal plants?. *Revista Brasileira de Farmacognosia*, 24(02), 110-115.
- American Cancer Society. (2022). *Prostate Cancer Stages*. Retrieved from <u>American Cancer Society</u>.
- Anuranjana, P. V., Beegum, F., Divya, K. P., George, K. T., Viswanatha, G. L., Nayak, P. G., ... & Nandakumar, K. (2023). Mechanisms behind the pharmacological application of Biochanin-A: a review. *F1000Research*, *12*, 107.
- Aravinth, A., Perumal, P., Rajaram, R., Dhanasundaram, S., Narayanan, M., Maharaja, S., & Manikumar, A. (2023). Isolation and characterization of 2, 4-di-tert-butyl phenol from the brown seaweed, Dictyota ciliolata and assessment of its anti-oxidant and anticancer characteristics. *Biocatalysis and Agricultural Biotechnology*, *54*, 102933.
- Aronson, W. J., Barnard, R. J., Freedland, S. J., Henning, S., Elashoff, D., Jardack, P. M., ... & Kobayashi, N. (2010). Growth inhibitory effect of low fat diet on prostate cancer cells: results of a prospective, randomized dietary intervention trial in men with prostate cancer. *The Journal of urology*, 183(1), 345-350
- Ashong, A. (2024). Examining the role of phytochemicals in cancer prevention and treatment. *Clinical Nutrition and Hospital Dietetics*, 44(3), 1-2.
- Asma, S. T., Acaroz, U., Imre, K., Morar, A., Shah, S. R. A., Hussain, S. Z., ... & Ince, S. (2022). Natural products/bioactive compounds as a source of anticancer drugs. *Cancers*, *14*(24), 6203.
- Atmaca, H., Oguz, F., & Ilhan, S. (2022). Drug delivery systems for cancer treatment: A Review of marine-derived polysaccharides. *Current Pharmaceutical Design*, 28(13), 1031-1045.
- Azzam, K. A. (2023). SwissADME and pkCSM webservers predictors: An integrated online platform for accurate and comprehensive predictions for in silico ADME/T properties of artemisinin and its derivatives. *Kompleksnoe Ispolzovanie Mineralnogo Syra= Complex use of mineral resources*, 325(2), 14-21.

- Banerjee, P., Kemmler, E., Dunkel, M., & Preissner, R. (2024). ProTox 3.0: A Webserver for the prediction of toxicity of chemicals. *Nucleic Acids Research*, *52*(W1), W513-W520.
- Banfalvi, G. (2017). Methods to detect apoptotic cell death. Apoptosis, 22(2), 306-323.
- Behera, S., Ghanty, S., Ahmad, F., Santra, S., & Banerjee, S. (2012). UV-Visible spectrophotometric method development and validation of assay of paracetamol tablet formulation. *J Anal Bioanal Techniques*, *3*(6), 151-7.
- Beltran, H., Oromendia, C., Danila, D. C., Montgomery, B., Hoimes, C., Szmulewitz, R. Z., ... & Tagawa, S. T. (2019). A phase II trial of the aurora kinase a inhibitor alisertib for patients with castration-resistant and neuroendocrine prostate cancer: Efficacy and biomarkers. *Clinical Cancer Research*, 25(1), 43-51.
- Bertram-Ralph, E., & Amare, M. (2023). Factors affecting drug absorption and distribution. *Anaesthesia & Intensive Care Medicine*, 24(4), 221-227.
- Bisoyi, P. (2022). Malignant tumors—as cancer. In *Understanding Cancer* (pp. 21-36). Academic Press.
- Bisson, J. F., Hidalgo, S., Simons, R., & Verbruggen, M. (2014). Preventive effects of lignan extract from flax hulls on experimentally induced benign prostate hyperplasia. *Journal of medicinal food*, 17(6), 650-656.
- Boesen, L. (2019). Magnetic resonance imaging—transrectal ultrasound image fusion guidance of prostate biopsies: current status, challenges and future perspectives. *Scandinavian journal of urology*, *53*(2-3), 89-96.
- Boyle, T. J., Steele, L. A. M., & Yonemoto, D. T. (2012). Synthesis and characterization of 4, 4'-methylenebis (2, 6-di-tert-butylphenol) derivatives of a series of metal alkoxides and alkyls. *Journal of Coordination Chemistry*, 65(3), 487-505.
- Boyraz, M. Ü., Shekhany, B., & Süzergöz, F. (2021). Cellular imaging analysis of MTT assay based on tetrazolium reduction. *Harran Üniversitesi Tıp Fakültesi Dergisi*, 18(1), 95-99.
- Briguglio, G., Costa, C., Pollicino, M., Giambò, F., Catania, S., & Fenga, C. (2020). Polyphenols in cancer prevention: New insights. *International Journal of Functional Nutrition*, 1(2), 9.

- Brito, V. S. F. D. (2016). *Development of novel 4-azasteroid derivatives as potential 5a-reductase inhibitors Synthesis, biological and computational evaluation* (Doctoral dissertation).
- Buchbinder, E., & Hodi, F. S. (2015). Cytotoxic T lymphocyte antigen-4 and immune checkpoint blockade. *The Journal of clinical investigation*, *125*(9), 3377-3383.
- Butt SR, Saheb Khan M, Gonzalez-Exposito MR, Gonzalez-Exposito MR, Murias C, Arkenau HT, Patrikidou A. (2019). Immunotherapy landscape in prostate cancer: successes, failures and promises. *Ann Urol Oncol*, 2(2): 71-88.
- Cai HongCai, C. H., Zhang GuoWei, Z. G., Yan ZeChen, Y. Z., & Shang XueJun, S. X. (2018). The effect of Xialiqi capsule on testosterone-induced benign prostatic hyperplasia in rats.
- Camp, N. J., & Tavtigian, S. V. (2002). Meta-analysis of associations of the Ser217Leu and Ala541Thr variants in ELAC2 (HPC2) and prostate cancer. *The American Journal of Human Genetics*, 71(6), 1475-1478.
- Casati, L., Ciceri, S., Maggi, R., & Bottai, D. (2023). Physiological and pharmacological overview of the gonadotropin releasing hormone. *Biochemical pharmacology*, *212*, 115553.
- Cháirez-Ramírez, M. H., de la Cruz-López, K. G., & García-Carrancá, A. (2021). Polyphenols as antitumor agents targeting key players in cancer-driving signaling pathways. *Frontiers in pharmacology*, 12, 710304.
- Chang, C. P., Yeh, T. K., Chen, C. T., Wang, W. P., Chen, Y. T., Tsai, C. H., ... & Chi, Y. H. (2024). Discovery of a long half-life AURKA inhibitor to treat MYC-amplified solid tumors as a monotherapy and in combination with everolimus. *Molecular Cancer Therapeutics*, 23(6), 766-779.
- Charalambous, A., & Kouta, C. (2016). Cancer related fatigue and quality of life in patients with advanced prostate cancer undergoing chemotherapy. *BioMed research international*, 2016(1), 3989286.
- Chaudhry, G. E. S., Akim, A. M., Sung, Y. Y., & Muhammad, T. S. T. (2022). Cancer and apoptosis. In *Apoptosis and cancer: methods and protocols* (pp. 191-210). New York, NY: Springer US.

- Chen, H., Griffin, A. R., Wu, Y. Q., Tomsho, L. P., Zuhlke, K. A., Lange, E. M., ... & Cooney, K. A. (2003). RNASEL mutations in hereditary prostate cancer. *Journal of medical genetics*, 40(3), e21-e21.
- Cheng, F., Li, W., Zhou, Y., Shen, J., Wu, Z., Liu, G., Lee, P.W. and Tang, Y. (2012). admetSAR: a comprehensive source and free tool for assessment of chemical ADMET properties. *J. Chem. Inf. Model*, *52(11)* 3099–3105
- Cheng, J., Hao, Y., Shi, Q., Hou, G., Wang, Y., Wang, Y., Xiao, W., Othman, J., Qi, J., Wang, Y. and Chen, Y. (2023). Discovery of novel Chinese medicine compounds targeting 3CL protease by virtual screening and molecular dynamics simulation. *Molecules*, 28(3), 937.
- Cheng, W., Kang, K., Zhao, A., & Wu, Y. (2024). Dual blockade immunotherapy targeting PD-1/PD-L1 and CTLA-4 in lung cancer. *Journal of Hematology & Oncology*, 17(1), 54.
- Chera, E. I., Pop, R. M., Pârvu, M., Sorițău, O., Uifălean, A., Cătoi, F. A., ... & Pârvu, A. E. (2022). Flaxseed ethanol extracts' antitumor, antioxidant, and anti-inflammatory potential. *Antioxidants*, 11(5), 892.
- Chew, Y. L., Goh, J. K., & Lim, Y. Y. (2009). Assessment of in vitro antioxidant capacity and polyphenolic composition of selected medicinal herbs from Leguminosae family in Peninsular Malaysia. *Food chemistry*, 116(1), 13-18.
- Chhillar, H., Chopra, P., & Ashfaq, M. A. (2021). Lignans from linseed (*Linum usitatissimum L.*) and its allied species: Retrospect, introspect and prospect. *Critical Reviews in Food Science and Nutrition*, 61(16), 2719-2741.
- Chiang, E. P. I., Tsai, S. Y., Kuo, Y. H., Pai, M. H., Chiu, H. L., Rodriguez, R. L., & Tang, F. Y. (2014). Caffeic acid derivatives inhibit the growth of colon cancer: involvement of the PI3-K/Akt and AMPK signaling pathways. *PloS one*, *9*(6), e99631.
- Chopra, B., & Dhingra, A. K. (2021). Natural products: A lead for drug discovery and development. *Phytotherapy Research*, *35*(9), 4660-4702.
- Chou, J., Egusa, E. A., Wang, S., Badura, M. L., Lee, F., Bidkar, A. P., ... & Aggarwal, R. (2023). Immunotherapeutic targeting and PET imaging of DLL3 in small-cell neuroendocrine prostate cancer. *Cancer research*, 83(2), 301-315.

- Chu, L. W., Ritchey, J., Devesa, S. S., Quraishi, S. M., Zhang, H., & Hsing, A. W. (2011). Prostate cancer incidence rates in Africa. *Prostate cancer*, 2011(1), 947870.
- Chulpanova, D. S., Kitaeva, K. V., Rutland, C. S., Rizvanov, A. A., & Solovyeva, V. V. (2020).
 Mouse tumor models for advanced cancer immunotherapy. *International journal of molecular sciences*, 21(11), 4118.
- Cucchiara, V., Yang, J. C., Mirone, V., Gao, A. C., Rosenfeld, M. G., & Evans, C. P. (2017). Epigenomic regulation of androgen receptor signaling: potential role in prostate cancer therapy. *Cancers*, *9*(1), 9.
- Cullis, C. A. (Ed.). (2019). *Genetics and genomics of Linum*. Cham, Switzerland: Springer International Publishing.
- Dalawai, D., Murthy, H. N., Dewir, Y. H., Sebastian, J. K., & Nag, A. (2023). Phytochemical composition, bioactive compounds, and antioxidant properties of different parts of Andrographis macrobotrys Nees. *Life*, *13*(5), 1166.
- Dallakyan, S., & Olson, A. J. (2015). Small-molecule library screening by docking with PyRx. *Chemical biology: methods and protocols*, 243-250.
- Daoud, N. E. H., Borah, P., Deb, P. K., Venugopala, K. N., Hourani, W., Alzweiri, M., ... & Tiwari, V. (2021). ADMET profiling in drug discovery and development: perspectives of in silico, in vitro and integrated approaches. *Current Drug Metabolism*, 22(7), 503-522.
- Dardenne, E., Beltran, H., Benelli, M., Gayvert, K., Berger, A., Puca, L., ... & Rickman, D. S. (2016). N-Myc induces an EZH2-mediated transcriptional program driving neuroendocrine prostate cancer. *Cancer cell*, 30(4), 563-577
- Daryanani, A., & Turkbey, B. (2022, May). Recent advancements in CT and MR imaging of prostate cancer. In *Seminars in nuclear medicine* (Vol. 52, No. 3, pp. 365-373). WB Saunders.
- De Amorim Ribeiro, I. C., da Costa, C. A. S., da Silva, V. A. P., Côrrea, L. B. N. S., Boaventura, G. T., & Chagas, M. A. (2017). Flaxseed reduces epithelial proliferation but does not affect basal cells in induced benign prostatic hyperplasia in rats. *European journal of nutrition*, 56, 1201-1210.

- de Morais, E. F., de Oliveira, L. Q. R., Farias Morais, H. G. D., Souto Medeiros, M. R. D., Freitas, R. D. A., Rodini, C. O., & Coletta, R. D. (2024). The anticancer potential of kaempferol: a systematic review based on in vitro studies. *Cancers*, 16(3), 585.
- De Silva, S. F., & Alcorn, J. (2019). Flaxseed lignans as important dietary polyphenols for cancer prevention and treatment: Chemistry, pharmacokinetics, and molecular targets. *Pharmaceuticals*, 12(2), 68.
- Desai, K., McManus, J. M., & Sharifi, N. (2021). Hormonal therapy for prostate cancer. *Endocrine reviews*, 42(3), 354-373.
- Dhiani, B. A., Nurulita, N. A., & Fitriyani, F. (2022). Protein-protein Docking Studies of Estrogen Receptor Alpha and TRIM56 Interaction for Breast Cancer Drug Screening. *Indonesian Journal of Cancer Chemoprevention*, 13(1), 46-54.
- Dmitriev, A. A., Pushkova, E. N., Novakovskiy, R. O., Beniaminov, A. D., Rozhmina, T. A., Zhuchenko, A. A., ... & Melnikova, N. V. (2021). Genome sequencing of fiber flax cultivar atlant using oxford nanopore and illumina platforms. *Frontiers in genetics*, 11, 590282.
- Dong, F., Jones, J. S., Stephenson, A. J., Magi-Galluzzi, C., Reuther, A. M., & Klein, E. A. (2008). Prostate cancer volume at biopsy predicts clinically significant upgrading. *The Journal of urology*, 179(3), 896-900
- Draisma, G., Postma, R., Schröder, F. H., van der Kwast, T. H., & de Koning, H. J. (2006). Gleason score, age and screening: modeling dedifferentiation in prostate cancer. *International journal of cancer*, 119(10), 2366-2371.
- Du, R., Huang, C., Liu, K., Li, X., & Dong, Z. (2021). Targeting AURKA in Cancer: molecular mechanisms and opportunities for Cancer therapy. *Molecular cancer*, 20, 1-27.
- Duan, Y., Yang, X., Zeng, X., Wang, W., Deng, Y., & Cao, D. (2024). Enhancing molecular property prediction through task-oriented transfer learning: integrating universal structural insights and domain-specific knowledge. *Journal of Medicinal Chemistry*, 67(11), 9575-9586.
- Duarte, S., Shah, M. A., & Sanches Silva, A. (2025). Flaxseed in Diet: A Comprehensive Look at Pros and Cons. *Molecules*, 30(6), 1335.

- Dumanović, J., Nepovimova, E., Natić, M., Kuča, K., & Jaćević, V. (2021). The significance of reactive oxygen species and antioxidant defense system in plants: A concise overview. *Frontiers in plant science*, 11, 552969.
- Durlacher, C. T., Li, Z. L., Chen, X. W., He, Z. X., & Zhou, S. F. (2016). An update on the pharmacokinetics and pharmacodynamics of alisertib, a selective Aurora kinase A inhibitor. *Clinical and Experimental Pharmacology and Physiology*, 43(6), 585-601.
- Džidić-Krivić, A., Kusturica, J., Sher, E. K., Selak, N., Osmančević, N., Karahmet Farhat, E., & Sher, F. (2023). Effects of intestinal flora on pharmacokinetics and pharmacodynamics of drugs. *Drug metabolism reviews*, 55(1-2), 126-139.
- Eeles, R. A., Kote-Jarai, Z., Giles, G. G., Olama, A. A. A., Guy, M., Jugurnauth, S. K., ... & Easton, D. F. (2008). Multiple newly identified loci associated with prostate cancer susceptibility. *Nature genetics*, 40(3), 316-321.
- Elasbali, A. M., Al-Soud, W. A., Al-Oanzi, Z. H., Qanash, H., Alharbi, B., Binsaleh, N. K., ... & Adnan, M. (2022). Cytotoxic activity, cell cycle inhibition, and apoptosis-inducing potential of athyrium hohenackerianum (lady fern) with its phytochemical profiling. *Evidence-Based Complementary and Alternative Medicine*, 2022(1), 2055773.
- Erul, E., Gülpınar, Ö., Kuru Öz, D., Berber, H., Kiremitci, S., & Ürün, Y. (2024). Primary prostatic stromal sarcoma: A case report and review of the literature. *Medicina*, 60(12), 1918.
- Esguerra, J. D., Bernardo, J. M., Gimao, K. M., Peralta, M. E., Tiu, C. J., Hernandez, G. G., & Alejandro, G. J. (2024). Mechanism-based antioxidant activity of Rubiaceae species collected from Ilocos Norte, Philippines. *Notulae Scientia Biologicae*, *16*(2), 11888-11888.
- Farag, S. M., Essa, E. E., Alharbi, S. A., Alfarraj, S., & El-Hassan, G. A. (2021). Agro-waste derived compounds (flax and black seed peels): Toxicological effect against the West Nile virus vector, Culex pipiens L. with special reference to GC–MS analysis. *Saudi Journal of Biological Sciences*, 28(9), 5261-5267.
- Fazekas, T., Shim, S. R., Basile, G., Baboudjian, M., Kói, T., Przydacz, M., ... & Rajwa, P. (2024). Magnetic resonance imaging in prostate cancer screening: A systematic review and meta-analysis. *JAMA oncology*, 10(6), 745-754.

- Feng, Z., Chen, M., Xue, Y., Liang, T., Chen, H., Zhou, Y., ... & Xie, X. Q. (2021). MCCS: A novel recognition pattern-based method for fast track discovery of anti-SARS-CoV-2 drugs. *Briefings in bioinformatics*, 22(2), 946-962.
- Ferlay, J., Colombet, M., Soerjomataram, I., Mathers, C., Parkin, D. M., Piñeros, M., ... & Bray, F. (2019). Estimating the global cancer incidence and mortality in 2018: GLOBOCAN sources and methods. *International journal of cancer*, 144(8), 1941-1953.
- Ferraldeschi, R., Welti, J., Luo, J., Attard, G., & De Bono, J. S. (2015). Targeting the androgen receptor pathway in castration-resistant prostate cancer: progresses and prospects. *Oncogene*, *34*(14), 1745-1757.
- Ferreira, L. L., & Andricopulo, A. D. (2019). ADMET modeling approaches in drug discovery. *Drug discovery today*, 24(5), 1157-1165.
- Fihtengolts, V. (1969). Atlas of UV absorption spectra of substances used in synthetic rubber manufacture. *NIST Chemistry WebBook, NIST Standard Reference Database*, 69.
- Fu, C., & Chen, Q. (2025). The future of pharmaceuticals: Artificial intelligence in drug discovery and development. *Journal of Pharmaceutical Analysis*, 101248.
- Fucassi, F., Heikal, A., Mikhalovska, L. I., Standen, G., Allan, I. U., Mikhalovsky, S. V., & Cragg,
 P. J. (2014). Metal chelation by a plant lignan, secoisolariciresinol diglucoside. *Journal of Inclusion Phenomena and Macrocyclic Chemistry*, 80, 345-351.
- Furtado, P., Lima, M. V. A., Nogueira, C., Franco, M., & Tavora, F. (2011). Review of small cell carcinomas of the prostate. *Prostate Cancer*, 2011(1), 543272.
- Gadelmawla, M. H., Alazzouni, A. S., Farag, A. H., Gabri, M. S., & Hassan, B. N. (2022). Enhanced effects of ferulic acid against the harmful side effects of chemotherapy in colon cancer: docking and in vivo study. *The Journal of Basic and Applied Zoology*, 83(1), 28.
- Gai, F., Janiak, M. A., Sulewska, K., Peiretti, P. G., & Karamać, M. (2023). Phenolic compound profile and antioxidant capacity of flax (Linum usitatissimum L.) harvested at different growth stages. *Molecules*, 28(4), 1807.

- Gallagher, D. J., Gaudet, M. M., Pal, P., Kirchhoff, T., Balistreri, L., Vora, K., ... & Offit, K. (2010). Germline BRCA mutations denote a clinicopathologic subset of prostate cancer. *Clinical cancer research*, *16*(7), 2115-2121.
- Gasmi, A., Mujawdiya, P. K., Noor, S., Lysiuk, R., Darmohray, R., Piscopo, S., ... & Bjørklund, G. (2022). Polyphenols in metabolic diseases. *Molecules*, *27*(19), 6280.
- George, B. P., Chandran, R., & Abrahamse, H. (2021). Role of phytochemicals in cancer chemoprevention: Insights. *Antioxidants*, 10(9), 1455.
- Girish, Y. R., Sharath Kumar, K. S., Prashantha, K., Rangappa, S., & Sudhanva, M. S. (2023). Significance of antioxidants and methods to evaluate their potency. *Materials Chemistry Horizons*, 2(2), 93-112.
- Gomez, L., Kovac, J. R., & Lamb, D. J. (2015). CYP17A1 inhibitors in castration-resistant prostate cancer. *Steroids*, *95*, 80-87.
- Gopal, J. V., Subashini, E., & Kannabiran, K. (2013). Extraction of quinone derivative from Streptomyces sp. VITVSK1 isolated from Cheyyur saltpan, Tamilnadu, India. *Journal of the Korean Society for Applied Biological Chemistry*, 56, 361-367
- Graham, N. J., Souter, L. H., & Salami, S. S. (2024). A systematic review of family history, race/ethnicity, and genetic risk on prostate cancer detection and outcomes: considerations in PSA-based screening. In *Urologic Oncology: Seminars and Original Investigations*. Elsevier.
- Grudzińska, M., Galanty, A., & Paśko, P. (2023). Can edible sprouts be the element of effective chemopreventive strategy?-A systematic review of in vitro and in vivo study. *Trends in Food Science & Technology*, 104130.
- Gulati, P., kumar Verma, A., Kumar, A., & Solanki, P. (2023). Para-cresyl sulfate and BSA conjugation for developing aptasensor: Spectroscopic methods and molecular simulation. *ECS Journal of Solid State Science and Technology*, *12*(7), 073004.
- Gulcin, İ., & Alwasel, S. H. (2022). Metal ions, metal chelators and metal chelating assay as antioxidant method. *Processes*, 10(1), 132. https://doi.org/10.3390/pr10010132

- Gustafson, W. C., Meyerowitz, J. G., Nekritz, E. A., Chen, J., Benes, C., Charron, E., ... & Weiss, W. A. (2014). Drugging MYCN through an allosteric transition in Aurora kinase A. *Cancer cell*, 26(3), 414-427.
- Haake, S. M., Rios, B. L., Pozzi, A., & Zent, R. (2024). Integrating integrins with the hallmarks of cancer. *Matrix Biology*.
- Hadzi-Djokic, J. (2024). Hormone therapy for advanced prostate cancer. In *prostate cancer:* advancements in the pathogenesis, diagnosis and personalized therapy (pp. 295-324). Cham: Springer Nature Switzerland.
- Hanaa, M. H., Ismail, H. A., Mahmoud, M. E., & Ibrahim, H. M. (2017). Antioxidant activity and phytochemical analysis of flaxseeds (Linum usitatisimum L.). *Minia J Agric Res Develop*, *37*(1), 129.
- Haque, M., Khan, F. N., Yadav, S., Kaur, V., Kaushik, N., Kumar, A., & Langyan, S. (2024). Chemistry, bioactivity, and health effects of linseed food products as nutraceutical and dietary supplements. In *Linseed* (pp. 79-90). Academic Press.
- Harris, A. E., Metzler, V. M., Lothion-Roy, J., Varun, D., Woodcock, C. L., Haigh, D. B., ... & Jeyapalan, J. N. (2022). Exploring anti-androgen therapies in hormone dependent prostate cancer and new therapeutic routes for castration resistant prostate cancer. Frontiers in endocrinology, 13, 1006101.
- Hartwell, J. L. (1982). *Plants used against cancer: a survey* (Vol. 2). Quarterman Publications.
- Hazafa, A., Iqbal, M. O., Javaid, U., Tareen, M. B. K., Amna, D., Ramzan, A., ... & Naeem, M. (2022). Inhibitory effect of polyphenols (phenolic acids, lignans, and stilbenes) on cancer by regulating signal transduction pathways: A review. *Clinical and Translational Oncology*, 1-14.
- Helal, M. M. U. (2023). Emerging biomarkers and potential therapeutics of the BCL-2 protein family: the apoptotic and anti-apoptotic context
- Helmy, S. A., El-Mofty, S., El Gayar, A. M., El-Sherbiny, I. M., & El-Far, Y. M. (2022). Novel doxorubicin/folate-targeted trans-ferulic acid-loaded PLGA nanoparticles combination: In-

- vivo superiority over standard chemotherapeutic regimen for breast cancer treatment. *Biomedicine & Pharmacotherapy*, 145, 112376.
- Helsen, C., Van den Broeck, T., Voet, A., Prekovic, S., Van Poppel, H., Joniau, S., & Claessens, F. (2014). Androgen receptor antagonists for prostate cancer therapy. *Endocrine-related cancer*, 21(4), T105-T118.
- Ho, S. T., Lin, C. C., Tung, Y. T., & Wu, J. H. (2019). Molecular mechanisms underlying yatein-induced cell-cycle arrest and microtubule destabilization in human lung adenocarcinoma cells. *Cancers*, 11(9), 1384.
- Hsu, F. N., Chen, M. C., Chiang, M. C., Lin, E., Lee, Y. T., Huang, P. H., ... & Lin, H. (2011). Regulation of androgen receptor and prostate cancer growth by cyclin-dependent kinase 5. *Journal of Biological Chemistry*, 286(38), 33141-33149.
- https://www.cancer.org/cancer/types/prostate-cancer/treating/surgery.html
- https://www.cancerresearchuk.org/about-cancer/prostate-cancer/treatment
- Huang, H., Li, P., Ye, X., Zhang, F., Lin, Q., Wu, K., & Chen, W. (2021). Isoalantolactone increases the sensitivity of prostate cancer cells to cisplatin treatment by inducing oxidative stress. *Frontiers in Cell and Developmental Biology*, *9*, 632779.
- Huang, X., Wang, N., Ma, Y., Liu, X., Guo, H., Song, L., ... & Guo, Q. (2024). Flaxseed polyphenols: Effects of varieties on its composition and antioxidant capacity. *Food Chemistry: X*, 23, 101597.
- Hugosson, J., Månsson, M., Wallström, J., Axcrona, U., Carlsson, S. V., Egevad, L., ... & Hellström, M. (2022). Prostate cancer screening with PSA and MRI followed by targeted biopsy only. *New England Journal of Medicine*, *387*(23), 2126-2137.
- Ifeanyi, O. E. (2018). A Review on Bladder Tumor Antigens. *Cancer Therapy & Oncology International Journal*, 9(3), 72-83.
- Ishola, I. O., Yemitan, K. O., Afolayan, O. O., Anunobi, C. C., & Durojaiye, T. E. (2018). Potential of Moringa oleifera in the treatment of benign prostate hyperplasia: Role of antioxidant defence systems. *Medical Principles and Practice*, *27*(1), 15-22.

- Islam, M. M., Sreeharsha, N., Alshabrmi, F. M., Asif, A. H., Aldhubiab, B., Anwer, M. K., ... & Rehman, A. (2023). From seeds to survival rates: investigating Linum usitatissimum's potential against ovarian cancer through network pharmacology. *Frontiers in Pharmacology*, 14, 1285258.
- Islami, F., Ward, E. M., Sung, H., Cronin, K. A., Tangka, F. K., Sherman, R. L., ... & Benard, V. B. (2021). Annual report to the nation on the status of cancer, part 1: national cancer statistics. *JNCI: Journal of the National Cancer Institute*, 113(12), 1648-1669.
- Ito, Y., & Sadar, M. D. (2018). Enzalutamide and blocking androgen receptor in advanced prostate cancer: lessons learnt from the history of drug development of antiandrogens. *Research and Reports in Urology*, 23-32.
- Jacob, A., Raj, R., Allison, D. B., & Myint, Z. W. (2021). Androgen receptor signaling in prostate cancer and therapeutic strategies. *Cancers*, *13*(21), 5417.
- Jafari, S., Molavi, O., Kahroba, H., Hejazi, M. S., Maleki-Dizaji, N., Barghi, S., ... & Jadidi-Niaragh, F. (2020). Clinical application of immune checkpoints in targeted immunotherapy of prostate cancer. *Cellular and Molecular Life Sciences*, 77, 3693-3710.
- Jambor, I., Kuisma, A., Ramadan, S., Huovinen, R., Sandell, M., Kajander, S., ... & Seppänen, M. (2016). Prospective evaluation of planar bone scintigraphy, SPECT, SPECT/CT, 18F-NaF PET/CT and whole body 1.5 T MRI, including DWI, for the detection of bone metastases in high risk breast and prostate cancer patients: SKELETA clinical trial. *Acta oncològica*, 55(1), 59-67.
- Jang, W. Y., Kim, M. Y., & Cho, J. Y. (2022). Antioxidant, anti-inflammatory, anti-menopausal, and anti-cancer effects of lignans and their metabolites. *International journal of molecular sciences*, 23(24), 15482.
- Johnsson, P. (2009). Bioactive phytochemicals in flaxseed. *Acta Universitatis Agriculturae Sueciae*, (2009: 57).
- Joshi, B. P., Bhandare, V. V., Patel, P., Sharma, A., Patel, R., & Krishnamurthy, R. (2023).
 Molecular modelling studies and identification of novel phytochemical inhibitor of DLL3. *Journal of Biomolecular Structure and Dynamics*, 41(7), 3089-3109.

- Joshi, B. P., Bhandare, V. V., Vankawala, M., Patel, P., Patel, R., Vyas, B., & Krishnamurty, R. (2023). Friedelin, a novel inhibitor of CYP17A1 in prostate cancer from Cassia tora. *Journal of Biomolecular Structure and Dynamics*, 41(19), 9695-9720.
- Kadam, P. V., Yadav, K. N., Bhingare, C. L., & Patil, M. J. (2018). Standardization and quantification of curcumin from Curcuma longa extract using UV visible spectroscopy and HPLC. *Journal of Pharmacognosy and Phytochemistry*, 7(5), 1913-1918.
- Kajla, P., Sharma, A., & Sood, D. R. (2015). Flaxseed—a potential functional food source. *Journal of food science and technology*, *52*, 1857-1871.
- Karatop, E. U., Cimenci, C. E., & Aksu, A. M. (2022). Colorimetric cytotoxicity assays. In *Cytotoxicity-Understanding Cellular Damage and Response*. IntechOpen.
- Kari, S., Subramanian, K., Altomonte, I. A., Murugesan, A., Yli-Harja, O., & Kandhavelu, M. (2022). Programmed cell death detection methods: a systematic review and a categorical comparison. *Apoptosis*, 27(7), 482-508.
- Kari, S., Subramanian, K., Altomonte, I. A., Murugesan, A., Yli-Harja, O., & Kandhavelu, M. (2022). Programmed cell death detection methods: a systematic review and a categorical comparison. *Apoptosis*, 27(7), 482-508.
- Kaur, B., Rolta, R., Salaria, D., Kumar, B., Fadare, O.A., da Costa, R.A., Ahmad, A., Al-Rawi, M.B.A., Raish, M., & Rather, I. A. (2022). An in silico investigation to explore anti-cancer potential of Foeniculum vulgare Mill. Phytoconstituents for the management of human breast cancer. *Molecules*, 27(13), 4077.
- Kauser, S., Hussain, A., Ashraf, S., Fatima, G., Javaria, S., Abideen, Z. U., ... & Korma, S. A. (2024). Flaxseed (Linum usitatissimum); phytochemistry, pharmacological characteristics and functional food applications. *Food Chemistry Advances*, 4, 100573.
- Kaushal, J. B., Takkar, S., Batra, S. K., & Siddiqui, J. A. (2024). Diverse landscape of genetically engineered mouse models: Genomic and molecular insights into prostate cancer. *Cancer Letters*, 216954.

- Kazemi, M., Dadkhah Tehrani, M. H., Khaleghi, A. A., & Mohammadi, M. (2023). A systematic review on the effect of brachytherapy in the treatment of prostate cancer. *Tehran University of Medical Sciences Journal*, 81(9), 623-631.
- Khalef, L., Lydia, R., Filicia, K., & Moussa, B. (2024). Cell viability and cytotoxicity assays: Biochemical elements and cellular compartments. *Cell biochemistry and function*, 42(3), e4007.
- Khurana, M., Kaur, P., Mujwar, S., Singh, M., & Sahu, S. K. (2024). Mutations within apoptosis gene and caspases. In *Caspases as Molecular Targets for Cancer Therapy* (pp. 15-32). Academic Press.
- Khushbu, S. S. (2024). A current insight into Aurora kinase inhibitors and their potential as anticancer agents (Doctoral dissertation, Brac University).
- Kim, D., Kim, K. I., & Baek, S. H. (2021). Roles of lysine-specific demethylase 1 (LSD1) in homeostasis and diseases. *Journal of Biomedical Science*, 28(1), 41.
- Kim, T. J., Lee, Y. H., & Koo, K. C. (2021). Current status and future perspectives of androgen receptor inhibition therapy for prostate cancer: a comprehensive review. *Biomolecules*, 11(4), 492.
- Ko, L. C., Gravina, N., Berghausen, J., & Abdo, J. (2025). Rising trends in prostate cancer among asian men: global concerns and diagnostic solutions. *Cancers*, 17(6), 1013.
- Koh, K. A., Sesso, H. D., Paffenbarger, R. S., & Lee, I. M. (2006). Dairy products, calcium and prostate cancer risk. *British Journal of Cancer*, *95*(11), 1582-1585.
- Koklesova, L., Liskova, A., Samec, M., Qaradakhi, T., Zulli, A., Smejkal, K., ... & Kubatka, P. (2020). Genoprotective activities of plant natural substances in cancer and chemopreventive strategies in the context of 3P medicine. *EPMA Journal*, *11*, 261-287.
- Koksal E, Bursal E, Dikici E, Tozoğlu F, Gulcin I (2011). Antioxidant activity of *Melissa officinalis* leaves. *Journal of Medicinal Plants Research* 5(2):217-222.
- Kouroukli, O., Bravou, V., Giannitsas, K., & Tzelepi, V. (2024). Tissue-based diagnostic biomarkers of aggressive variant prostate cancer: A narrative review. *Cancers*, 16(4), 805.

- Kumar, A., Rai, Y., & Bhatt, A. N. (2023). Anti-cancer drug-induced mitochondrial alteration becomes a limitation of metabolic viability-based MTT assay in analyzing growth inhibition.
- Kumar, R., Sena, L. A., Denmeade, S. R., & Kachhap, S. (2023). The testosterone paradox of advanced prostate cancer: mechanistic insights and clinical implications. *Nature Reviews Urology*, 20(5), 265-278.
- Kumar, S., Mohan, A., Sharma, N. R., Kumar, A., Girdhar, M., Malik, T., & Verma, A. K. (2024). Computational frontiers in aptamer-based nanomedicine for precision therapeutics: a comprehensive review. *ACS omega*, *9*(25), 26838-26862.
- Laskowski, R. A., & Swindells, M. B. (2011). LigPlot+: multiple ligand-protein interaction diagrams for drug discovery. |*Journal of Chemical Information and Modeling*, 51, 2778–2786. https://doi.org/10.1021/ci200227u
- Lawal, M., Verma, A. K., Umar, I. A., Gadanya, A. M., Umar, B., Yahaya, N., & Auwal, B. (2020). Analysis of new potent anti-diabetic molecules from phytochemicals of Pistia strateotes with Sglt1 and G6pc proteins of Homo Sapiens for treatment of diabetes mellitus. An in silico approach. Silico Approach IOSR JPBS, 15, 59-73.
- Lee, J. K., Phillips, J. W., Smith, B. A., Park, J. W., Stoyanova, T., McCaffrey, E. F., ... & Witte, O. N. (2016). N-Myc drives neuroendocrine prostate cancer initiated from human prostate epithelial cells. *Cancer cell*, 29(4), 536-547.
- Leissner, K. H., & Tisell, L. E. (1979). The weight of the human prostate. *Scandinavian journal of urology and nephrology*, *13*(2), 137-142.
- Lewandowska, H., Kalinowska, M., Lewandowski, W., Stępkowski, T. M., & Brzoska, K. (2016). The role of natural polyphenols in cell signaling and cytoprotection against cancer development. *The Journal of nutritional biochemistry*, *32*, 1-19.
- Li, X., Li, J., Dong, S., Li, Y., Wei, L., Zhao, C., ... & Wang, Y. (2019). Effects of germination on tocopherol, secoisolarlciresinol diglucoside, cyanogenic glycosides and antioxidant activities in flaxseed (Linum usitatissimum L.). *International Journal of Food Science and Technology*, 54(7), 2346-2354

- Liadi, Y. M. (2024). *HMGA2: A Biomarker Associated with Resistance to Enzalutamide in Prostate Cancer Cells* (Doctoral dissertation, Morgan State University).
- Linstrom, P.J.; Mallard, W.G. (Eds.) NIST Chemistry WebBook; NIST Standard Reference Database Number 69; National Institute of Standards and Technology: Gaithersburg, MD, USA. Available online: https://webbook.nist.gov/chemistry/ (ccessed on 1 August 2024).
- Lipinski, C. A., Lombardo, F., Dominy, B. W., & Feeney, P. J. (1997). Experimental and computational approaches to estimate solubility and permeability in drug discovery and development settings. *Advanced drug delivery reviews*, 23(1-3), 3-25
- Liss, M. A., & Thompson, I. M. (2018). Prostate cancer prevention with 5-alpha reductase inhibitors: Concepts and controversies. *Current opinion in urology*, 28(1), 42-45.
- Liu, W., Maben, Z., Wang, C., Lindquist, K. C., Li, M., Rayannavar, V., ... & Chaparro-Riggers, J. (2021). Structural delineation and phase-dependent activation of the costimulatory CD27: CD70 complex. *Journal of Biological Chemistry*, 297(4).
- Liu, X., Allen, J. D., Arnold, J. T., & Blackman, M. R. (2008). Lycopene inhibits IGF-I signal transduction and growth in normal prostate epithelial cells by decreasing DHT-modulated IGF-I production in co-cultured reactive stromal cells. *Carcinogenesis*, 29(4), 816-823
- Li-Zhen, H., Wasiuk, A., Testa, J., Weidlick, J., Sisson, C., Crocker, A., ... & Keler, T. (2015). The mechanism of anti-tumor immunity induced by varlilumab, a CD27 agonist mAb, is model dependent. *Journal for ImmunoTherapy of Cancer*, 3(Suppl 2).
- Lorke, D. (1983). A new approach to practical acute toxicity testing. *Archives of toxicology*, *54*, 275-287.
- Lu, S., Wang, J., Chitsaz, F., Derbyshire, M. K., Geer, R. C., Gonzales, N. R., ... & Marchler-Bauer, A. (2020). CDD/SPARCLE: The conserved domain database in 2020. *Nucleic acids research*, 48(D1), D265-D268.
- Luo, H., Rankin, G. O., Liu, L., Daddysman, M. K., Jiang, B. H., & Chen, Y. C. (2009). Kaempferol inhibits angiogenesis and VEGF expression through both HIF dependent and independent pathways in human ovarian cancer cells. *Nutrition and cancer*, 61(4), 554-563.

- Luo, X., Gao, J., Liu, M., Cao, D., Zong, Y., Liu, B., & Wei, L. (2023). Bioinformatics analysis of cysteine transmembrane gene cys in transgenic tobacco. *Plant Gene and Trait*, 14.
- Madan, R. A (2017). Phase II trial of enzalutamide in combination with PSA-TRICOM in patients with non-metastatic castration sensitive prostate cancer.
- Mandal, S., & Mandal, S. K. (2009). Rational drug design. *European journal of pharmacology*, 625(1-3), 90-100.
- Manini, C., & López, J. I. (2020). Unusual faces of bladder cancer. Cancers, 12(12), 3706.
- Mariko, M., Takako, I., Tomoe, I., Shiori, T., Kaoru, I., & Akihiko, H. "Summary information of human health hazard assessment of existing chemical substances (V)." *Bulletin of National Institute of Health Sciences* (2019): 66.
- Matowa, P. R., Gundidza, M., Gwanzura, L., & Nhachi, C. F. (2020). A survey of ethnomedicinal plants used to treat cancer by traditional medicine practitioners in Zimbabwe. *BMC Complementary Medicine and Therapies*, 20, 1-13.
- Matsuo, M., Mihara, K., Okuno, M., Ohkawa, H., & Miyamoto, J. (1984). Comparative metabolism of 3, 5-di-tert-butyl-4-hydroxytoluene (BHT) in mice and rats. *Food and chemical toxicology*, 22(5), 345-354.
- Maylin, Z. R., Smith, C., Classen, A., Asim, M., Pandha, H., & Wang, Y. (2024). Therapeutic exploitation of neuroendocrine transdifferentiation drivers in prostate cancer. *Cells*, *13*(23), 1999.
- Mazurakova, A., Samec, M., Koklesova, L., Biringer, K., Kudela, E., Al-Ishaq, R. K., ... & Golubnitschaja, O. (2022). Anti-prostate cancer protection and therapy in the framework of predictive, preventive and personalised medicine—comprehensive effects of phytochemicals in primary, secondary and tertiary care. *EPMA Journal*, *13*(3), 461-486.
- Mbah-Omeje, K. N., Iyke, C. A., & Amughe, S. C. (2022). Prostate cancer screening in Nigerian men: Perceived barriers and recommendations. *Prostate*, 8(10).
- Mensah, J. E., Akpakli, E., Kyei, M., Klufio, K., Asiedu, I., Asante, K., ... & Quist, E. A. (2025). Prostate-specific antigen, digital rectal examination, and prostate cancer detection: A study

- based on more than 7000 transrectal ultrasound-guided prostate biopsies in Ghana. *Translational Oncology*, 51, 102163.
- Mohler, J. L., Armstrong, A. J., Bahnson, R. R., D'Amico, A. V., Davis, B. J., Eastham, J. A., ... & Freedman-Cass, D. A. (2016). Prostate cancer, version 1.2016. *Journal of the National Comprehensive Cancer Network*, 14(1), 19-30.
- Mohsen, N. (2022). Role of MRI, ultrasound, and computed tomography in the management of prostate cancer. *Pet Clin*, 17(4), 565-83.
- Monica, S. J., & Joseph, M. (2016). Phytochemical screening of flaxseed (Linum usitatissimum L.). *Int. J. Sci. Res*, *5*(3), 218-220.
- Morris, D. H. (2007). *Flax: A health and nutrition primer*. Flax Council of Canada. Available via www. flaxcouncil.ca
- Mosmann, T. (1983). Rapid colorimetric assay for cellular growth and survival: application to proliferation and cytotoxicity assays. *Journal of immunological methods*, 65(1-2), 55-63.
- Mottet, N., et al. (2020). *EAU-ESTRO-ESUR-SIOG Guidelines on Prostate Cancer*. European Association of Urology. Retrieved from <u>EAU Guidelines</u>.
- Mueed, A., Deng, Z., Korma, S. A., Shibli, S., & Jahangir, M. (2023). Anticancer potential of flaxseed lignans, their metabolites and synthetic counterparts in relation with molecular targets: current challenges and future perspectives. *Food & Function*, 14(5), 2286-2303.
- Mueed, A., Ibrahim, M., Shibli, S., Madjirebaye, P., Deng, Z., & Jahangir, M. (2024). The fate of flaxseed-lignans after oral administration: A comprehensive review on its bioavailability, pharmacokinetics, and food design strategies for optimal application. *Critical Reviews in Food Science and Nutrition*, 64(13), 4312-4330.
- Muhammad, I. I., & Pandey, D. K. (2024). A validated HPTLC quantification of artemisinin from different extracts of Artemisia annua L. and its inhibitory activity against serine hydroxyl methyltransferase (SHMT). *Journal of Applied Biology & Biotechnology*. 2024; 12(6):1-10.

- Muhammad, I. I., & Pandey, D. K. (2024). HPTLC quantification of quercetin from leaf extracts of C. occidentalis L. and its inhibitory activity against protease enzyme of P. falciparum. *Vegetos*, 37(5): 1804-1816.
- Muhammed, M. T., & Aki-Yalcin, E. (2024). Molecular docking: Principles, advances, and its applications in drug discovery. *Letters in Drug Design & Discovery*, 21(3), 480-495.
- Mukherjee, A. G., & Gopalakrishnan, A. V. (2024). Sex hormone-binding globulin and its critical role in prostate cancer: A comprehensive review. *The Journal of Steroid Biochemistry and Molecular Biology*, 106606.
- Muller, R. L., Faria, E. F., Carvalhal, G. F., Reis, R. B., Mauad, E. C., Carvalho, A. L., & Freedland, S. J. (2013). Association between family history of prostate cancer and positive biopsies in a Brazilian screening program. *World journal of urology*, *31*, 1273-1278.
- Mumtaz, S. M., Shahrukh, M., Bhardwaj, G., & Altamish, M. (2025). Quinones as potential therapeutic agents for metabolic disorders. In *Quinone-Based Compounds in Drug Discovery* (pp. 169-190). Academic Press.
- Munteanu, I. G., & Apetrei, C. (2021). Analytical methods used in determining antioxidant activity: A review. *International journal of molecular sciences*, 22(7), 3380.
- Muralikrishna, A., Padmavathi, V., & Padmaja, A. (2013). Synthesis and antioxidant activity of styrylsulfonylmethyl 1, 3, 4-oxadiazoles, pyrazolyl/isoxazolyl-1, 3, 4-oxadiazoles. *Chemical & Pharmaceutical Bulletin*, 61(12), 1291-1297.
- Mustafa, M., Ahmad, R., Tantry, I. Q., Ahmad, W., Siddiqui, S., Alam, M., ... & Islam, S. (2024). Apoptosis: a comprehensive overview of signaling pathways, morphological changes, and physiological significance and therapeutic implications. *Cells*, *13*(22), 1838.
- Mvondo, J. G. M., Matondo, A., Mawete, D. T., Bambi, S. M. N., Mbala, B. M., & Lohohola, P. O. (2021). In silico ADME/T properties of quinine derivatives using SwissADME and pkCSM webservers. *Int. J. Trop. Dis. Health*, *42*(11), 1-12.
- Nadal, R., Schweizer, M., Kryvenko, O. N., Epstein, J. I., & Eisenberger, M. A. (2014). Small cell carcinoma of the prostate. *Nature Reviews Urology*, *11*(4), 213-219.

- Nader, R., El Amm, J., & Aragon-Ching, J. B. (2018). Role of chemotherapy in prostate cancer. *Asian journal of andrology*, 20(3), 221-229.
- Narita, S., Nara, T., Sato, H., Koizumi, A., Huang, M., Inoue, T., & Habuchi, T. (2019). Research evidence on high-fat diet-induced prostate cancer development and progression. *Journal of clinical medicine*, 8(5), 597.
- Nasser, N. J. (2022). Androgen flare after LHRH initiation is the side effect that makes most of the beneficial effect when it coincides with radiation therapy for prostate cancer. *Cancers*, *14*(8), 1959.
- National Cancer Institute. (2023). *Prostate Cancer Treatment (PDQ®)–Patient Version*. Retrieved from National Cancer Institute.
- Nelson, M., Dornbier, R., Kirshenbaum, E., Eguia, E., Sweigert, P., Baker, M., ... & Bresler, L. (2020). Use of surgery for post-prostatectomy incontinence. *The Journal of Urology*, 203(4), 786-791.
- Ng, K. L. (2021). The etiology of prostate cancer. Exon Publications, 17-27.
- Nikonova, A. S., Astsaturov, I., Serebriiskii, I. G., Dunbrack, R. L., & Golemis, E. A. (2013). Aurora A kinase (AURKA) in normal and pathological cell division. *Cellular and Molecular Life Sciences*, 70, 661-687.
- Niwa, H., Sato, S., Handa, N., Sengoku, T., Umehara, T., & Yokoyama, S. (2020). Development and Structural Evaluation of N-alkylated Trans-2-phenylcyclopropylamine-based LSD1 Inhibitors. *ChemMedChem*, 15(9), 787-793.
- Nkwocha, B. I., & Singh, M. (2023). Abiraterone-Induced Hypokalemia: A Case Report. *Cureus*, 15(7).
- Nnadi, C. O., Okorie, N. H., & Nwodo, N. J. (2021). Evaluation of in vitro antiprotozoal and cytotoxic activities of selected medicinal plants used in Nigerian folk medicine. 609-612.
- Nouri-Majd, S., Salari-Moghaddam, A., Aminianfar, A., Larijani, B., & Esmaillzadeh, A. (2022). Association between red and processed meat consumption and risk of prostate cancer: a systematic review and meta-analysis. *Frontiers in Nutrition*, *9*, 801722.

- Obinata, D., Takayama, K., Inoue, S., & Takahashi, S. (2024). Exploring androgen receptor signaling pathway in prostate cancer: A path to new discoveries. *International Journal of Urology*, *31*(6), 590-597.
- Obukohwo, O. M., Kingsley, N. E., Rume, R. A., & Victor, E. (2021). The concept of male reproductive anatomy.
- Okwundu, N., Grossman, D., Hu-Lieskovan, S., Grossmann, K. F., & Swami, U. (2021). The dark side of immunotherapy. *Annals of Translational Medicine*, *9*(12), 1041.
- Ortiz, C. L. D., Completo, G. C., Nacario, R. C., & Nellas, R. B. (2019). Potential inhibitors of galactofuranosyltransferase 2 (GlfT2): molecular docking, 3D-QSAR, and in silico ADMETox studies. *Scientific reports*, *9*(1), 17096.
- Otto, T., & Sicinski, P. (2017). Cell cycle proteins as promising targets in cancer therapy. *Nature Reviews Cancer*, 17(2), 93-115.
- Otto, T., Horn, S., Brockmann, M., Eilers, U., Schüttrumpf, L., Popov, N., ... & Eilers, M. (2009). Stabilization of N-Myc is a critical function of Aurora A in human neuroblastoma. *Cancer cell*, 15(1), 67-78.
- Ouis, N., & Hariri, A. (2023). Antioxidant Properties of the Aerial Part of Celery and Flaxseeds. *Agriculturae Conspectus Scientificus*, 88(3), 207-213.
- Paliwal, A., Jain, S., Kumar, S., Wal, P., Khandai, M., Khandige, P. S., ... & Srivastava, S. (2024). Predictive Modelling in pharmacokinetics: from in-silico simulations to personalized medicine. *Expert Opinion on Drug Metabolism & Toxicology*, 20(4), 181-195.
- Palmieri, C., Fonseca-Alves, C. E., & Laufer-Amorim, R. (2022). A review on canine and feline prostate pathology. *Frontiers in veterinary science*, *9*, 881232.
- Pansare, T. A., Panchaware, P., Makadi, A., Jankar, S., & Verma, D. (2020). Ayurvedic nutritional, phytochemical, therapeutic and pharmacological overview on atasi (*Linum usitatissimum linn*.).

- Park, S. W., Lee, B. H., Song, S. H., & Kim, M. K. (2023). Revisiting the Ramachandran plot based on statistical analysis of static and dynamic characteristics of protein structures. *Journal of Structural Biology*, *215*(1), 107939.
- Patel, G. K., Chugh, N., & Tripathi, M. (2019). Neuroendocrine differentiation of prostate cancer—An intriguing example of tumor evolution at play. *Cancers*, 11(10), 1405.
- Patel, S. R., & Das, M. (2023). Small cell lung cancer: emerging targets and strategies for precision therapy. *Cancers*, 15(16), 4016. Otto, T., Horn, S., Brockmann, M., Eilers, U., Schüttrumpf, L., Popov, N., ... & Eilers, M. (2009). Stabilization of N-Myc is a critical function of Aurora A in human neuroblastoma. *Cancer cell*, 15(1), 67-78.
- Paul Gravestock, B. M. B. S., Matthew, S., Veeratterapillay, R., & Rakesh Heer, B. M. B. S. (2022). Prostate cancer diagnosis: Biopsy approaches. *Exon Publications*, 141-168.
- Pavagada Sudarshan, G. (2013). Genetic analysis of seed and flower colour in flax (Linum usitatissimum L.) and identification of a candidate gene in the D locus (Doctoral dissertation, University of Saskatchewan).
- Perillo, B., Tramontano, A., Pezone, A., & Migliaccio, A. (2020). LSD1: More than demethylation of histone lysine residues. *Experimental & molecular medicine*, *52*(12), 1936-1947.
- Perumal, P. K., Huang, C. Y., Singhania, R. R., Patel, A. K., Haldar, D., Chen, C. W., & Dong, C. D. (2024). In vitro evaluation of antioxidant potential of polysaccharides and oligosaccharides extracted from three different seaweeds. *Journal of Food Science and Technology*, 61(8), 1481-1491.
- Pettersen, E. F., Goddard, T. D., Huang, C. C., Couch, G. S., Greenblatt, D. M., Meng, E. C., & Ferrin, T. E. (2004). UCSF Chimera—a visualization system for exploratory research and analysis. *Journal of computational chemistry*, 25(13), 1605-1612.
- Pinzi, L., & Rastelli, G. (2019). Molecular docking: Shifting paradigms in drug discovery. *International journal of molecular sciences*, 20(18), 4331.
- Pippione, A. C., Boschi, D., Pors, K., Oliaro-Bosso, S., & Lolli, M. L. (2017). Androgen-AR axis in primary and metastatic prostate cancer: chasing steroidogenic enzymes for therapeutic intervention. *Journal of Cancer Metastasis and Treatment*, *3*(12), 328-361.

- Prasad, K. (2013). Secoisolariciresinol diglucoside (SDG) isolated from flaxseed, an alternative to ACE inhibitors in the treatment of hypertension. *International Journal of Angiology*, 22(04), 235-238.
- Prutianu, I., Căruntu, I. D., Manole, M. B., Giușcă, S. E., Profire, B., Timofte, A. D., ... & Gafton, B. (2021). Developments in prostate cancer therapy: From the androgen receptor to antiandrogens and beyond. *Farmacia*, 69(3).
- Puccinelli, M., Maggini, R., Angelini, L. G., Santin, M., Landi, M., Tavarini, S., ... & Incrocci, L. (2022). Can light Spectrum composition increase growth and nutritional quality of Linum usitatissimum L. sprouts and microgreens?. *Horticulturae*, 8(2), 98.
- Quinn, T. P., Sanda, M. G., Howard, D. H., Patil, D., & Filson, C. P. (2021). Disparities in magnetic resonance imaging of the prostate for traditionally underserved patients with prostate cancer. *Cancer*, 127(16), 2974-2979.
- Qureshi, O. S., Zheng, Y., Nakamura, K., Attridge, K., Manzotti, C., Schmidt, E. M., ... & Sansom, D. M. (2011). Trans-endocytosis of CD80 and CD86: A molecular basis for the cell-extrinsic function of CTLA-4. *Science*, *332*(6029), 600-603.
- Ragupathy, R., Rathinavelu, R., & Cloutier, S. (2011). Physical mapping and BAC-end sequence analysis provide initial insights into the flax (Linum usitatissimum L.) genome. *BMC genomics*, 12, 1-17.
- Rahimlou, M., & Hejazi, J. (2022). Perspective chapter: Flaxseed (*Linumusitatissimum L*)—chemical structure and health-related functions. In *Lignin-Chemistry, Structure, and Application*. IntechOpen.
- Raith, F., O'Donovan, D. H., Lemos, C., Politz, O., & Haendler, B. (2023). Addressing the reciprocal crosstalk between the AR and the PI3K/AKT/mTOR signaling pathways for prostate cancer treatment. *International Journal of Molecular Sciences*, 24(3), 2289.
- Rajasree, R. S., Ittiyavirah, S. P., Naseef, P. P., Kuruniyan, M. S., Anisree, G. S., & Elayadeth-Meethal, M. (2021). An evaluation of the antioxidant activity of a methanolic extract of Cucumis melo L. fruit (F1 hybrid). *Separations*, 8(8), 123.

- Rana, A., Samtiya, M., Dhewa, T., Mishra, V., & Aluko, R. E. (2022). Health benefits of polyphenols: A concise review. *Journal of Food Biochemistry*, 46(10), e14264.
- Rao, C. M. M. P., Yejella, R. P., Rehman, R. S. A., & Basha, S. H. (2015). Molecular docking based screening of novel designed chalcone series of compounds for their anti-cancer activity targeting EGFR kinase domain. *Bioinformation*, 11(7), 322.
- Rawla, P. (2019). Epidemiology of prostate cancer. World journal of oncology, 10(2), 63.
- Rebbeck, T. R. (2017, January). Prostate cancer genetics: variation by race, ethnicity, and geography. In *Seminars in radiation oncology* (Vol. 27, No. 1, pp. 3-10). WB Saunders.

References

- Reid, A. H., Attard, G., Barrie, E., & De Bono, J. S. (2008). CYP17 inhibition as a hormonal strategy for prostate cancer. *Nature Clinical Practice Urology*, *5*(11), 610-620.
- Riaz, B., Zahoor, M. K., Zahoor, M. A., Majeed, H. N., Javed, I., Ahmad, A., ... & Sultana, K. (2018). Toxicity, phytochemical composition, and enzyme inhibitory activities of some indigenous weed plant extracts in fruit fly, Drosophila melanogaster. *Evidence-Based Complementary and Alternative Medicine*, 2018(1), 2325659.
- Riviere, J. E. (2009). Absorption, distribution, metabolism, and elimination. *Veterinary* pharmacology and therapeutics, 9.
- Robitaille, J., & Langlois, V. S. (2020). Consequences of steroid-5α-reductase deficiency and inhibition in vertebrates. *General and comparative endocrinology*, 290, 113400.
- Rohrmann, S., Platz, E. A., Kavanaugh, C. J., Thuita, L., Hoffman, S. C., & Helzlsouer, K. J. (2007). Meat and dairy consumption and subsequent risk of prostate cancer in a US cohort study. *Cancer Causes & Control*, 18, 41-50.
- Rojas-Armas, J. P., Arroyo-Acevedo, J. L., Ortiz-Sánchez, J. M., Palomino-Pacheco, M., Herrera-Calderón, O., Calva, J., ... & Hilario-Vargas, J. (2020). Cordia lutea L. Flowers: a promising medicinal plant as chemopreventive in induced prostate carcinogenesis in rats. *Evidence-Based Complementary and Alternative Medicine*, 2020(1), 5062942. doi: 10.1155/2020/5062942.

- Rosário-Ferreira, N., Baptista, S.J., Barreto, C.A., Rodrigues, F.E., Silva, T.F., Ferreira, S.G., Vitorino, J.N., Melo, R., Victor, B.L., Machuqueiro, M. and Moreira, I.S. (2021). In silico end-to-end protein–ligand interaction characterization pipeline: the case of SARS-CoV-2. *ACS Synthetic Biology*, *10*(11), 3209-3235.
- Rotte, A. (2019). Combination of CTLA-4 and PD-1 blockers for treatment of cancer. *Journal of experimental & clinical cancer research*, 38(1), 255.
- Rubio-Viqueira, B., & Hidalgo, M. (2009). Direct in vivo xenograft tumor model for predicting chemotherapeutic drug response in cancer patients. *Clinical pharmacology & therapeutics*, 85(2), 217-221.
- Rudin, C. M., Pietanza, M. C., Bauer, T. M., Ready, N., Morgensztern, D., Glisson, B. S., ... & Spigel, D. R. (2017). Rovalpituzumab tesirine, a DLL3-targeted antibody-drug conjugate, in recurrent small-cell lung cancer: A first-in-human, first-in-class, open-label, phase 1 study. *The Lancet Oncology*, *18*(1), 42-51.
- Rudrapal, M., Khairnar, S. J., Khan, J., Dukhyil, A. B., Ansari, M. A., Alomary, M. N., ... & Devi, R. (2022). Dietary polyphenols and their role in oxidative stress-induced human diseases: Insights into protective effects, antioxidant potentials and mechanism (s) of action. *Frontiers in pharmacology*, *13*, 806470.
- Saad, F., & Shore, N. D. (2021). Relugolix: A novel androgen deprivation therapy for management of patients with advanced prostate cancer. *Therapeutic Advances in Medical Oncology*, 13, 1758835921998586.
- Saah, S.A., Sakyi, P.O., Adu-Poku, D., Boadi, N.O., Djan, G., Amponsah, D., Devine, R.N. & Ayittey, K. (2023). Docking and molecular dynamics identify leads against 5 alpha reductase 2 for benign prostate hyperplasia treatment. *Journal of Chemistry*, 2023(1), 8880213.
- Saddam, M., Paul, S. K., Habib, M. A., Fahim, M. A., Mimi, A., Islam, S., ... & Helal, M. M. U. (2024). Emerging biomarkers and potential therapeutics of the BCL-2 protein family: the apoptotic and anti-apoptotic context. *Egyptian Journal of Medical Human Genetics*, 25(1), 12.

- Sahay, A., Piprodhe, A., & Pise, M. (2020). In silico analysis and homology modeling of strictosidine synthase involved in alkaloid biosynthesis in catharanthus roseus. *Journal of Genetic Engineering and Biotechnology*, 18(1), 44.
- Said, M. M., Hassan, N. S., Schlicht, M. J., & Bosland, M. C. (2015). Flaxseed suppressed prostatic epithelial proliferation in a rat model of benign prostatic hyperplasia. *Journal of Toxicology and Environmental Health, Part A*, 78(7), 453-465.
- Sajjad, H., Imtiaz, S., Noor, T., Siddiqui, Y. H., Sajjad, A., & Zia, M. (2021). Cancer models in preclinical research: A chronicle review of advancement in effective cancer research. *Animal models and experimental medicine*, 4(2), 87-103.
- Salciccia, S., Gentilucci, A., Cattarino, S., & Sciarra, A. (2016). GNRH-agonist or antagonist in the treatment of prostate cancer: A comparision based on oncological results. *Urologia Journal*, 83(4), 173-178.
- Salehi, B., Fokou, P. V. T., Yamthe, L. R. T., Tali, B. T., Adetunji, C. O., Rahavian, A., ... & Sharifi-Rad, J. (2019). Phytochemicals in prostate cancer: From bioactive molecules to upcoming therapeutic agents. *Nutrients*, *11*(7), 1483. doi: 10.3390/nu11071483
- Samaržija, I. (2021). Site-specific and common prostate cancer metastasis genes as suggested by meta-analysis of gene expression data. *Life*, 11(7), 636.
- Šamec, D., Karalija, E., Šola, I., Vujčić Bok, V., & Salopek-Sondi, B. (2021). The role of polyphenols in abiotic stress response: The influence of molecular structure. *Plants*, *10*(1), 118.
- Samuolienė, G., Brazaitytė, A., Viršilė, A., Miliauskienė, J., Vaštakaitė-Kairienė, V., & Duchovskis, P. (2019). Nutrient levels in Brassicaceae microgreens increase under tailored light-emitting diode spectra. *Frontiers in plant science*, 10, 1475.
- Sangeetha, S., Marimuthu, P., Doraisamy, P., & Sarada, D. V. L. (2010). Evaluation of antioxidant activity of the antimicrobial fraction from Sphaeranthus indicus. *International Journal of Applied Biology and Pharmaceutical Technology*, *1*(2), 431-436.

- Sankarapillai, J., Krishnan, S., Ramamoorthy, T., Sudarshan, K. L., & Mathur, P. (2024). Descriptive epidemiology of prostate cancer in India, 2012–2019: Insights from the National Cancer Registry Programme. *Indian Journal of Urology*, 40(3), 167-173.
- Santin, M., Sciampagna, M. C., Mannucci, A., Puccinelli, M., Angelini, L. G., Tavarini, S., ... & Castagna, A. (2022). Supplemental UV-B exposure influences the biomass and the content of bioactive compounds in Linum usitatissimum L. sprouts and microgreens. *Horticulturae*, 8(3), 213.
- Santos-Sánchez, N. F., Salas-Coronado, R., Villanueva-Cañongo, C., & Hernández-Carlos, B. (2019). *Antioxidant compounds and their antioxidant mechanism*. IntechOpen.
- Scalapino, K. J., & Daikh, D. I. (2008). CTLA-4: a key regulatory point in the control of autoimmune disease. *Immunological reviews*, 223(1), 143-155.
- Schmidt, L. J., & Tindall, D. J. (2011). Steroid 5 α-reductase inhibitors targeting BPH and prostate cancer. *The Journal of steroid biochemistry and molecular biology*, *125*(1-2), 32-38.
- Shalal, O. S., & Irayyif, S. M. (2023). Evaluation of cytotoxicity and apoptotic effects of Simarouba glauca on the prostate cancer cell lines PC3. *Journal of the Pakistan Medical Association*, 73(9), S113-S118.
- Shariat, S. F., & Roehrborn, C. G. (2008). Using biopsy to detect prostate cancer. *Reviews in urology*, 10(4), 262.
- Sharifi, M. (2023). Finding the Best Gene Candidate (s) as a Potential Therapeutic Target for N-MYC Overexpressing Neuroendocrine Prostate Cancer (NEPC) (Doctoral dissertation).
- Sharma, A., Shahzad, B., Rehman, A., Bhardwaj, R., Landi, M., & Zheng, B. (2019). Response of phenylpropanoid pathway and the role of polyphenols in plants under abiotic stress. *Molecules*, 24(13), 2452.
- Sharma, M., Gupta, S., Dhole, B., & Kumar, A. (2017). The prostate gland. In *Basics of Human Andrology: A Textbook* (pp. 17-35). Singapore: Springer Singapore.
- Shastry, R. A., Karur, N., Habbu, P., Madagundi, S. D., Patil, B. S., & Kulkarni, V. H. (2021). Pharmacognostical evaluation and in vitro cytotoxic activity of alcoholic and aqueous

- extracts of corm of amorphophallus paeoniifolius (Dennst). RGUHS Journal of Pharmaceutical Sciences, 11(4).
- Sicilia, T., Niemeyer, H. B., Honig, D. M., & Metzler, M. (2003). Identification and stereochemical characterization of lignans in flaxseed and pumpkin seeds. *Journal of agricultural and food chemistry*, *51*(5), 1181-1188.
- Siegel, R. L., Giaquinto, A. N., & Jemal, A. (2024). Cancer statistics, 2024. *CA: A cancer journal for clinicians*, 74(1), 12-49.
- Siegel, R. L., Miller, K. D., & Jemal, A. (2018). Cancer statistics, 2018. *CA: A cancer journal for clinicians*, 68(1), 7-30.
- Siegel, R. L., Miller, K. D., Fuchs, H. E., & Jemal, A. (2021). Cancer statistics, 2021. *CA: A cancer journal for clinicians*, 71(1), 7-33.
- Siemińska, I., & Baran, J. (2022). Myeloid-derived suppressor cells as key players and promising therapy targets in prostate cancer. *Frontiers in Oncology*, *12*, 862416.
- Sigrist, C. J., De Castro, E., Cerutti, L., Cuche, B. A., Hulo, N., Bridge, A., ... & Xenarios, I. (2012). New and continuing developments at PROSITE. *Nucleic acids research*, 41(D1), D344-D347.
- Silva, D., Abreu-Mendes, P., Mourato, C., Martins, D., Cruz, R., & Mendes, F. (2020). Prostate cancer, new treatment advances—Immunotherapy. *Actas Urológicas Españolas (English Edition)*, 44(7), 458-468.
- Silva, K. C., Tambwe, N., Mahfouz, D. H., Wium, M., Cacciatore, S., Paccez, J. D., & Zerbini, L.
 F. (2024). Transcription factors in prostate cancer: insights for disease development and diagnostic and therapeutic approaches. *Genes*, 15(4), 450.
- Silva, L. A., Andriolo, R. B., Atallah, Á. N., & da Silva, E. M. (2014). Surgery for stress urinary incontinence due to presumed sphincter deficiency after prostate surgery. *Cochrane Database of Systematic Reviews*, (9).
- Singh, S. V., Srivastava, S. K., Choi, S., Lew, K. L., Antosiewicz, J., Xiao, D., ... & Herman-Antosiewicz, A. (2005). Sulforaphane-induced cell death in human prostate cancer cells is

- initiated by reactive oxygen species. *Journal of Biological Chemistry*, 280(20), 19911-19924.
- Singh, S., Pandey, V. P., Yadav, K., Yadav, A., & Dwivedi, U. N. (2020). Natural products as anticancerous therapeutic molecules targeted towards topoisomerases. *Current Protein and Peptide Science*, 21(11), 1103-1142.
- Siripurapu, V., Pasli, M., Bhatt, A., Ashley, L. W., Gordon, J., & Peach, M. S. (2023). Treatment trends and prognostic factors related to histology of squamous cell carcinoma of the prostate: A SEER review.
- Song, P., Shu, M., Yang, L., Di, X., Liu, P., Liu, Z., ... & Dong, Q. (2022). The prognosis of radical prostatectomy, external beam radiotherapy plus brachytherapy, and external beam radiotherapy alone for patients above 70 years with very high-risk prostate cancer: A population-matched study. *Urologia Internationalis*, 106(1), 11-19.
- Spackman, P. R., Turner, M. J., McKinnon, J. J., Wolff, S. K., Grimwood, D. J., Jayatilaka, D., & Spackman, M. A. (2021). CrystalExplorer: A program for Hirshfeld surface analysis, visualization and quantitative analysis of molecular crystals. *Journal of Applied Crystallography*, 54(3), 1006-1011
- Srivastava, V., Yadav, A., & Sarkar, P. (2022). Molecular docking and ADMET study of bioactive compounds of Glycyrrhiza glabra against main protease of SARS-CoV2. *Materials Today: Proceedings*, 49, 2999-3007.
- Stanzione, F., Giangreco, I., & Cole, J. C. (2021). Use of molecular docking computational tools in drug discovery. *Progress in medicinal chemistry*, 60, 273-343.
- Starzer, A. M., & Berghoff, A. S. (2019). New emerging targets in cancer immunotherapy: CD27 (TNFRSF7). *ESMO open*, 4, e000629.
- Stavropoulos, P., Mavroeidis, A., Papadopoulos, G., Roussis, I., Bilalis, D., & Kakabouki, I. (2023). On the path towards a "greener" EU: A mini review on flax (Linum usitatissimum L.) as a case study. *Plants*, *12*(5), 1102.
- Stepień, A. E., Trojniak, J., & Tabarkiewicz, J. (2025). Anti-oxidant and anti-cancer properties of flaxseed. *International Journal of Molecular Sciences*, 26(3), 1226.

- Sucharitha, P., Reddy, K. R., Satyanarayana, S. V., & Garg, T. (2022). Absorption, distribution, metabolism, excretion, and toxicity assessment of drugs using computational tools. In *Computational approaches for novel therapeutic and diagnostic designing to mitigate SARS-CoV-2 infection* (pp. 335-355). Academic Press.
- Sun, M., Choueiri, T. K., Hamnvik, O. P. R., Preston, M. A., De Velasco, G., Jiang, W., ... & Trinh, Q. D. (2016). Comparison of gonadotropin-releasing hormone agonists and orchiectomy: effects of androgen-deprivation therapy. *JAMA oncology*, *2*(4), 500-507.
- Surh, Y. J., & from Turmeric, C. (2005). 10 Chemopreventive phenolic compounds in common spices. *Carcinogenic and Anticarcinogenic Food Components*, 197.
- Tehami, W., Nani, A., Khan, N. A., & Hichami, A. (2023). New insights into the anticancer effects of p-coumaric acid: focus on colorectal cancer. *Dose-Response*, 21(1), 15593258221150704.
- Thomas, E., Panjagari, N. R., Ganguly, S., Kapila, S., & Singh, A. K. (2024). Flaxseed lignan: Metabolism, extraction and isolation techniques, potential health benefits and food applications. *Indian Journal of Dairy Science*, 77(5).
- Thompson, K. L. (2022). *Human Postmortem Microbiome Signatures of the Prostate Gland* (Master's thesis, Alabama State University).
- Thomson, R. H. (1997). Naturally occurring quinones IV (4th ed.). Blackie Academic and Professional, London.
- Tian, X., Srinivasan, P. R., Tajiknia, V., Uruchurtu, A. F. S. S., Seyhan, A. A., Carneiro, B. A., ...
 & El-Deiry, W. S. (2024). Targeting apoptotic pathways for cancer therapy. *The Journal of clinical investigation*, 134(14).
- Udhane, S. S., Dick, B., Hu, Q., Hartmann, R. W., & Pandey, A. V. (2016). Specificity of anti-prostate cancer CYP17A1 inhibitors on androgen biosynthesis. *Biochemical and biophysical research communications*, 477(4), 1005-1010.
- UniProt Consortium. (2019). UniProt: a worldwide hub of protein knowledge. *Nucleic acids* research, 47(D1), D506-D515.

- Uroko, R. I., Ijioma, S. N., Ogwo, E. U., & Awah, F. M. (2022). Combined ethanol extract of Hypselodelphys poggeana and Spermacoce radiata leaves ameliorate benign prostatic hyperplasia in rats via modulation of serum sex hormonal levels. *J. Res. Pharm*, 26(4), 742-752.
- Usman, R. B., Adamu, M., Isyaku, I. M., & Bala, H. A. (2020). Quantitative and qualitative phytochemicals and proximate analysis of Aloe vera (Aloe barbadensis miller). *International Journal of Advanced Academic Research*, 6(1), 95-104.
- Van Norman, G. A. (2020). Limitations of animal studies for predicting toxicity in clinical trials:

 Part 2: Potential alternatives to the use of animals in preclinical trials. *Basic to Translational Science*, *5*(4), 387-397.
- Vargas-Madriz, Á. F., Kuri-García, A., Vargas-Madriz, H., Chávez-Servín, J. L., & Ayala-Tirado, R. A. (2021). Phenolic profile and antioxidant capacity of fruit Averrhoa carambola L.: a review. *Food Science and Technology*, 42, e69920.
- Vaselkiv, J. B., Ceraolo, C., Wilson, K. M., Pernar, C. H., Rencsok, E. M., Stopsack, K. H., ... & Mucci, L. A. (2022). 5-Alpha reductase inhibitors and prostate cancer mortality among men with regular access to screening and health care. *Cancer Epidemiology, Biomarkers & Prevention*, 31(7), 1460-1465.
- Vásquez, B. (2014). Morphological characteristics of prostate in mammals. *International Journal of Medical and Surgical Sciences*, *1*(1), 63-72.
- Veber, D. F., Johnson, S. R., Cheng, H. Y., Smith, B. R., Ward, K. W., & Kopple, K. D. (2002).
 Molecular properties that influence the oral bioavailability of drug candidates. *Journal of medicinal chemistry*, 45(12), 2615-2623.
- Velavan, S. (2015). Phytochemical techniques-a review. World Journal of Science and Research, 1(2), 80-91.
- Verma, A. K., Gulati, P., Lakshmi, G. B. V. S., Solanki, P. R., & Kumar, A. (2023). Interaction studies of gut metabolite; trimethylene amine oxide with bovine serum albumin through spectroscopic, dft and molecular docking approach. *bioRxiv*, 2023-04.

- Verma, A. K., Mishra, A., Dhiman, T. K., Sardar, M., & Solanki, P. R. (2022). Experimental and In Silico interaction studies of Alpha Amylase-Silver nanoparticle: a nano-bioconjugate. *BioRxiv*, 2022-06.
- Verma, A. K., Sharma, S., Jayaraj, A., & Deep, S. (2023). In silico study of interaction of (ZnO) 12 nanocluster to glucose oxidase-FAD in absence and presence of glucose. *Journal of Biomolecular Structure and Dynamics*, 41(24), 15234-15242.
- Verma, A. K., Sharma, S., Jayaraj, A., & Deep, S. (2023). In silico study of interaction of (ZnO) 12 nanocluster to glucose oxidase-FAD in absence and presence of glucose. *Journal of Biomolecular Structure and Dynamics*, 41(24), 15234-15242.
- Viveky, N., Thorpe, L., Alcorn, J., Hadjistavropoulos, T., & Whiting, S. (2015). Safety evaluation of flaxseed lignan supplementation in older adults residing in long-term care homes. *JNHR-J. Nurs. Home Res*, 1, 84-88.
- W Watson, G., M Beaver, L., E Williams, D., H Dashwood, R., & Ho, E. (2013). Phytochemicals from cruciferous vegetables, epigenetics, and prostate cancer prevention. *The AAPS journal*, 15, 951-961.
- Wang, J. J., Lei, K. F., & Han, F. J. E. R. M. P. S. (2018). Tumor microenvironment: Recent advances in various cancer treatments. *European Review for Medical & Pharmacological Sciences*, 22(12).
- Wang, L., Hou, Y., Wang, R., Pan, Q., Li, D., Yan, H., & Sun, Z. (2021). Inhibitory effect of astaxanthin on testosterone-induced benign prostatic hyperplasia in rats. Marine drugs, 19(12), 652.
- Waterhouse, A., Bertoni, M., Bienert, S., Studer, G., Tauriello, G., Gumienny, R., ... & Schwede, T. (2018). SWISS-MODEL: Homology modelling of protein structures and complexes. *Nucleic acids research*, 46(W1), W296-W303.
- Watson, P. A., Arora, V. K., & Sawyers, C. L. (2015). Emerging mechanisms of resistance to androgen receptor inhibitors in prostate cancer. *Nature Reviews Cancer*, 15(12), 701-711.
- Welén, K., & Damber, J. E. (2022). Androgens, aging, and prostate health. *Reviews in Endocrine* and *Metabolic Disorders*, 23(6), 1221-1231.

- Westaby, D., Jiménez-Vacas, J. M., Figueiredo, I., Rekowski, J., Pettinger, C., Gurel, B., ... & Sharp, A. (2024). BCL2 expression is enriched in advanced prostate cancer with features of lineage plasticity. *The Journal of Clinical Investigation*, 134(18).
- Wibmer, A. G., Burger, I. A., Sala, E., Hricak, H., Weber, W. A., & Vargas, H. A. (2016). Molecular imaging of prostate cancer. *Radiographics*, *36*(1), 142-159.
- Xia, B. W., Zhao, S. C., Chen, Z. P., Chen, C., Liu, T. S., Yang, F., & Yan, Y. (2021). Relationship between serum total testosterone and prostate volume in aging men. *Scientific reports*, 11(1), 14122.
- Yachdav, G., Kloppmann, E., Kajan, L., Hecht, M., Goldberg, T., Hamp, T., ... & Rost, B. (2014). PredictProtein—an open resource for online prediction of protein structural and functional features. *Nucleic acids research*, 42(W1), W337-W343.
- Yang, D. Y., Seo, W. W., Park, R. W., Rhee, S. Y., Cha, J. M., Hah, Y. S., ... & Ha, J. Y. (2024). Comparison of Finasteride and Dutasteride on Risk of Prostate Cancer in Patients with Benign Prostatic Hyperplasia: A Pooled Analysis of 15 Real-world Databases. *The World Journal of Men's Health*, 43(1), 188.
- Yang, Q. E. (2021). Human cancer xenografts in immunocompromised mice provide an advanced genuine tumor model for research and drug development-A revisit of murine models for human cancers. *Biochimica et Biophysica Acta (BBA)-General Subjects*, 1865(8), 129929.
- Yin, S., Liu, H., Wang, J., Feng, S., Chen, Y., Shang, Y., ... & Si, F. (2021). Osthole induces apoptosis and inhibits proliferation, invasion, and migration of human cervical carcinoma hela cells. *Evidence-Based Complementary and Alternative Medicine*, 2021(1), 8885093.
- You, Y., Lai, X., Pan, Y., Zheng, H., Vera, J., Liu, S., ... & Zhang, L. (2022). Artificial intelligence in cancer target identification and drug discovery. *Signal Transduction and Targeted Therapy*, 7(1), 156.
- Young, B., O'Dowd, G., & Woodford, P. (2013). Wheater's Functional Histology-Inkling Enhanced E-Book: Wheater's Functional Histology E-Book. Elsevier Health Sciences.

- Young, G. J., Harrison, S., Turner, E. L., Walsh, E. I., Oliver, S. E., Ben-Shlomo, Y., ... & Metcalfe,
 C. (2017). Prostate-specific antigen (PSA) testing of men in UK general practice: a 10-year longitudinal cohort study. *BMJ open*, 7(10), e017729.
- Yu, C., Sonnen, A. F. P., George, R., Dessailly, B. H., Stagg, L. J., Evans, E. J., ... & Davis, S. J. (2011). Rigid-body ligand recognition drives cytotoxic T-lymphocyte antigen 4 (CTLA-4) receptor triggering. *Journal of Biological Chemistry*, 286(8), 6685-6696.
- Zanwar, A. A., Hegde, M. V., & Bodhankar, S. L. (2014). Flax lignan in the prevention of atherosclerotic cardiovascular diseases. In *Polyphenols in human health and disease* (pp. 915-921). Academic Press.
- Zanwar, A., Hegde, M., & Bodhankar, S. (2011). Cardioprotective activity of flax lignan concentrate extracted from seeds of in isoprenalin induced myocardial necrosis in rats. *Interdisciplinary toxicology*, 4(2), 90-97.
- Zare, S., Sabzalian, M. R., & Mirlohi, A (2022). Flaxseed, its Lignans Content and their Effect on Hormonal Cancers in Humans. World Journal of Agriculture and Soil Science. 7(5): 2022, 000672.
- Zerdan, M. B., Bilen, M. A., & Yu, J. (2025). Therapeutic targeting of Aurora Kinase A in advanced prostate cancer. *Serican Journal of Medicine*, 2(2).
- Zhang, C., Hu, Y., & Shi, C. (2020). Targeting natural killer cells for tumor immunotherapy. *Frontiers in immunology*, 11, 60.
- Zhang, C., Liu, L., Pan, Y., Qin, R., Wang, W., Zhou, M., & Zhang, Y. (2024). Detection methodologies and mechanisms of reactive oxygen species generated in Fenton/Fenton-like processes. *Separation and Purification Technology*, 129578.
- Zhang, Z., Li, X., Sang, S., McClements, D. J., Chen, L., Long, J., ... & Qiu, C. (2022). Polyphenols as plant-based nutraceuticals: Health effects, encapsulation, nano-delivery, and application. *Foods*, 11(15), 2189.
- Zhao, J., Chen, J., Sun, G., Shen, P., & Zeng, H. (2024). Luteinizing hormone-releasing hormone receptor agonists and antagonists in prostate cancer: Effects on long-term survival and

- combined therapy with next-generation hormonal agents. *Cancer Biology & Medicine*, 21(11), 1012-1032.
- Zhao, Z., Wu, D., Gao, S., Zhou, D., Zeng, X., Yao, Y., ... & Zeng, G. (2023). The association between dairy products consumption and prostate cancer risk: A systematic review and meta-analysis. *British Journal of Nutrition*, 129(10), 1714-1731.
- Zhou, X., Huang, N., Chen, W., Xiaoling, T., Mahdavi, B., Raoofi, A., ... & Atabati, H. (2020). HPLC phenolic profile and induction of apoptosis by Linum usitatissimum extract in LNCaP cells by caspase3 and Bax pathways. *Amb Express*, 10, 1-11.

APPENDICES

Appendix-I

Molecular docking result of flax microgreens bioactive compounds against prostate cancer target proteins.

		Target proteins (PDB ID)							
SN	Compound	DLL3	CTLA-4	CD27	AURKA	N-Myc	5AR	AR	LSD1
	CID:	(4xmb.2)	(3osk.1)	(7kxo)	(4j8m)	(5ixo.1)	(7bw1)	(3l3x)	(6kgm)
1	534410	-5.0	-5.7	-7.3	-8.0	-6.5	-8.3	-8.3	-8.7
2	7976	-3.0	-3.0	-4.1	-4.3	-3.3	-4.0	-4.5	-4.5
3	111244	-3.0	-3.5	-4.5	-4.8	-3.6	-4.9	-5.6	-5.1
4	10413	-3.2	-3.0	-4.0	-4.2	-3.5	-4.2	-4.5	-4.5
5	7938	-3.2	-3.4	-4.8	-4.7	-3.7	-4.5	-4.9	-5.0
6	7974	-2.8	-3.1	-3.8	-5.4	-3.5	-4.4	-4.0	-4.7
7	137584	-2.9	-3.3	-4.1	-4.9	-3.5	-4.8	-5.6	-5.0
8	18372057	-3.1	-3.7	-4.7	-5.1	-4.1	-5.1	-5.7	-5.0
9	558410	-3.2	-3.5	-4.5	-4.6	-3.9	-5.0	-6.1	-5.4
10	5364729	-3.2	-3.5	-4.5	-4.9	-3.9	-5.0	-5.4	-5.3
11	119838	-3.9	-3.9	-5.5	-5.2	-4.0	-5.6	-8.1	-5.8
12	5367771	-3.3	-3.5	-4.8	-4.4	-4.0	-5.4	-6.1	-5.5
13	332	-3.8	-4.5	-5.2	-5.5	-4.6	-6.2	-6.2	-6.4
14	83742	-3.6	-3.5	-4.8	-4.3	-3.7	-4.9	-5.6	-5.4
15	5988	-5.4	-4.9	-7.9	-5.4	-4.4	-7.2	-7.1	-6.9
16	91737510	-4.1	-3.7	-6.5	-6.1	-5.2	-5.3	-6.9	-8.1
17	5373219	-4.2	-4.8	-5.9	-5.8	-4.9	-6.6	-6.0	-7.0
18	530729	-3.9	-4.9	-6.6	-6.1	-5.1	-8.0	-6.7	-7.5
19	7311	-4.3	-5.1	-6.6	-6.1	-5.1	-7.7	-6.6	-7.1
20	267716	-5.5	-5.3	-6.3	-6.5	-5.3	-7.8	-7.6	-8.0
21	35960	-4.1	-4.3	-5.6	-5.2	-4.3	-5.9	-5.6	-6.3
22	545303	-5.0	-5.7	-7.8	-6.5	-5.1	-8.2	-3.6	-8.2
23	91719722	-4.1	-5.1	-6.2	-5.9	-4.9	-7.7	-6.7	-7.1
24	3026	-4.1	-4.6	-6.4	-6.4	-4.8	-7.0	-6.2	-7.2
25	96009	-3.9	-4.0	-5.3	-5.5	-4.4	-5.7	-6.4	-6.2
26	91691499	-4.4	-4.6	-5.7	-6.6	-5.2	-6.4	-6.2	-6.8
27	985	-5.0	-4.7	-6.0	-6.2	-4.7	-6.6	-7.0	-6.8

28	7427	-5.9	-5.2	-8.1	-5.6	-4.9	-7.7	-5.8	-6.6
29	17161	-6.8	-8.2	-10.7	-8.4	-6.7	-11.3	-7.4	-9.8
30	64947	-4.6	-4.9	-6.3	-6.1	-47	-6.4	-6.1	-6.5
31	54725318	-4.7	-5.1	-5.6	-6.7	-4.0	-7.7	-6.1	-7.1
32	54018957	-4.3	-4.7	-5.7	-6.0	-4.1	-6.4	-6.4	-6.7
33	637775	-6.9	-7.5	-9.1	-9.3	-7.9	-10.7	-8.5	-9.8
34	101715	-4.4	-4.5	-5.7	-4.9	-4.1	-5.8	-5.9	-5.5
35	5281	-4.3	-4.4	-5.6	-6.6	-5.1	-6.6	-6.5	-7.1
36	9546746	-4.2	-4.6	-4.9	-7.0	-4.9	-8.0	-7.6	-8.1
37	5280435	-6.5	-6.1	-7.9	-7.1	-6.1	-8.0	-6.7	-8.8
38	5280450	-3.5	-4.7	-6.3	-6.5	-4.3	-6.8	-6.6	-7.0
39	5280934	-3.2	-4.6	-6.1	-6.2	-4.3	-7.4	-6.8	-6.5
40	521846	-2.6	-3.6	-2.0	-5.8	-2.9	-7.3	-4.7	-6.6
41	532617	-4.2	-5.4	-5.0	-6.7	-6.1	-7.6	-8.2	-6.2
42	11747713	-4.8	-5.8	-7.6	-7.6	-5.6	-8.0	-6.9	-8.0
43	10494	-6.2	-7.2	-9.1	-6.1	-6.2	-10.2	-7.1	-10.2
44	547838	-3.9	-4.1	-5.2	-5.6	-4.2	-6.0	-6.1	-5.8
45	6230	-5.2	-6.6	-7.0	-8.5	-6.4	-10.7	-8.9	-9.6
46	42956	-3.3	-4.2	-5.5	-5.5	-3.7	-6.6	-6.3	-7.0
47	8343	-5.1	-6.1	-7.0	-6.9	-6.1	-8.8	-8.1	-8.8
48	191964	-6.6	-5.8	-6.6	-7.7	-5.9	-8.5	-7.9	-8.5
49	8089	-3.9	-5.3	-6.7	-6.5	-5.1	-8.0	-7.7	-7.7
50	11008	-3.0	3.9	-6.0	-5.6	-4.0	-6.5	-6.2	-6.6
51	8372	-11.5	-10.5	-13.3	-14.5	-10.6	-15.8	-14.9	-17.1
52	589198	-4.5	-4.5	-5.8	-5.6	-4.5	-6.7	-6.8	-7.3
53	22932	-5.0	-5.4	-6.6	-7.6	-6.0	-8.1	-8.0	-9.1
54	91735525	-3.8	-4.9	-6.5	-5.8	-5.2	-7.1	-6.1	-7.5
55	117981	-5.4	-5.7	-5.9	-7.1	-5.9	-8.7	-8.1	-8.6
56	638072	-4.5	-5.4	-7.0	-6.6	-4.0	-8.0	-7.8	-7.8
57	181087								
58	11002708	-5.3	-7.0	-9.5	-8.5	-6.6	-10.2	-7.8	-10.2
59	290541	-5.8	-6.7	-7.6	-7.8	-6.4	-9.1	-7.5	-10.6
60	91691425	-4.4	-6.7	-2.8	-7.4	-6.0	-6.4	-6.2	-8.9

List of publications

- 1. A research article entitled: Molecular Modeling, and Identification of Flax Microgreens Lignans as Novel of Prostate Cancer Targets Inhibitor" had been published in the *Journal of Applied Biology & Biotechnology*. Indexing: Scopus [Q3].
- 2. A research article entitled: HPTLC Quantification of 4,4'-Methylenebis(2,6-Di-Tert-Butylphenol) in Flax Microgreen Extracts and its Anticancer Potential Against Prostate Cancer" has been communicated for publication to *International Journal of Applied Pharmaceutics*. Indexing: Scopus [Q2]. Status: Accepted.
- 3. A research article entitled: HPTLC Identification and Quantification of 2,5-Di-tert-butyl-1,4-benzoquinone in Flax Microgreen Extracts: Exploring Its Anticancer Potential Against Prostate Cancer" has been communicated for publication to *Journal of Applied Biology & Biotechnology*. Indexing: Scopus [Q3]. Status: under review.

DOI: 10.7324/JABB.2025.205522



Molecular modeling and identification of flax microgreens lignans as novel prostate cancer target inhibitors

Mudassir Lawal^{1,2} , Neeta Raj Sharma³ , Awadhesh Kumar Verma⁴ , Gurmeen Rakhra^{1*}

ARTICLE INFO

Article history: Received on: June 12, 2024 Accepted on: September 04, 2024 Available Online: January 25, 2025

Key words:

ADMET, flax microgreens, lignans, molecular docking, molecular modeling, prostate cancer

ABSTRACT

One of the most common types of cancer is prostate cancer (PCa) and its prevalence rate is increasing in old men of ~70 years. In pharmacotherapy, natural compounds and their structural analogs have been used for cancer treatment. Several studies have demonstrated the therapeutic potential of Linum usitatissimum, commonly known as flax, in treating various cancers. However, the specific mechanisms by which flax-derived compounds act on PCa remain unclear. This study aims to fill this gap by identifying and evaluating the bioactive compounds in flax microgreens. The GCMS analysis was carried out using a Shimadzu (GCMS-TQ8040 NX). The instrument temperature was set from 50°C up to 300°C for 37 minutes to give a 100% total peak area. The molecular docking studies were carried out using AutoDock tools 4.2 version software. The ADMET properties were predicted and analyzed using SWISSADME online (https://www.swissadme.ch/) and ProTox-3.0 online (https://tox.charite.de/protox3/index.php?site) prediction tools. GC-MS analysis identified 58 phytocompounds in the methanolic extracts of flax microgreens. Among these, CID11002708 and CID290541 exhibited the highest binding affinities to PCa target proteins. The ADMET result shows the compounds have low toxicity and specific metabolic characteristics. Taking into account, the results of molecular docking and ADMET evaluation, it can be concluded that CID11002708 and CID290541 hold promise as novel inhibitors for the treatment of PCa. The current results can further be validated via in vitro and in vivo studies.

Department of Biochemistry, School of Bioengineering and Biosciences, Lovely Professional University, Phagwara, India.

Department of Biochemistry and Molecular Biology, Federal University Dutsin-Ma, Katsina, Nigeria.

³Department of Biotechnology, School of Bioengineering and Biosciences, Lovely Professional University, Phagwara, India.

Department of Bioinformatics, School of Bioengineering and Biosciences, Lovely Professional University, Phagwara, India.



HOME / ARCHIVES / ARTICLES IN PRESS DUL-AUG 2025 / Original Article(s)

HPTLC QUANTIFICATION OF 4,4'-METHYLENEBIS(2,6-DI-TERT-BUTYLPHENOL) IN FLAX MICROGREEN EXTRACTS AND ITS ANTICANCER POTENTIAL AGAINST PROSTATE CANC

MUDASSIR LAWAL

Department of Biochemistry, School of Bioengineering and Biosciences, Lovely Professional University, Phagwara, Punjab, India. Department of Biochemistry and Molecular Biology, Federal University Dutsin-Ma, Katsina-Nigeria

NEETA RAJ SHARMA

Department of Biotechnology, School of Bioengineering and Biosciences, Lovely Professional University, Phagwara, Punjab, India

AWADHESH KUMAR VERMA

Department of Bioinformatics, School of Bioengineering and Biosciences, Lovely Professional University, Phagwara, Punjab, India



IBRAHIM HAMZA KANKIA

Department of Biochemistry, Faculty of Natural and Applied Sciences, Umaru Musa Yar'adua University, Katsina-Nigeria https://lineary.com/doi/10.000-0001-7474-2247

VETRISELVAN SUBRAMANIYAN

Department of Medical Sciences, School of Medical and Life Sciences Sunway University, No. 5, Jalan Universiti, Bandar Sunway. 47500 Selangor Darul Ehsan Malaysia

CUDMEEN DAKHDA

Department of Blochemistry, School of Bloengineering and Blosciences, Lovely Professional University, Phagwara, Punjab, India

DOI: https://doi.org/10.22159/ijap.2025v17i4.53939

PUBLISHED

03-05-2025

HOW TO CITE

LAWAL, M., SHARMA, N. R., VERMA, A.
K., KANGA, I. H., SUBRAMANIYAN, V., &
RAMHRA, G. (2025). HPTLC
GUANTIFICATION OF 4,4"METHYLENBENS(2,6"-OI-TERTBUTYLPHENOL) IN FLAX MICROGREEI
EXTRACTS AND ITS ANTICANDER
POTENTIAL AGAINST PROSTATE
CANCER. International Journal of Applice
Pharmaceutics, 17(4).
https://doi.org/10.22159/jap.2029v1714.53
939

More Citation Formats

**

More Citation Formats

ISSUE

Go

5/6/25, 12:34 PM HPTLC QUANTIFICATION OF 4.4"-METHYLENEBIS(2,6-DI-TERT-BUTYLPHENOL) IN FLAX MICROGREEN EXTRACTS AND ITS ANTICANCER POTENTIAL AGAINST PROSTAT...

Keywords: ADMET, Antioxidants, Anti-prostate cancer, Flax microgreens, HPTLC, Molecular docking

ABSTRACT

Objective: This research aimed to evaluate the antioxidant activity of methanolic extract of flax microgreens (MEFM), to identify and quantify 4.4'-Methylenebis (2.6-Di-tert-butylphenol) [4.4'-M(2.6-DTBP)] using GC-MS and HPTLC, and assess its inhibitory activity against prostate cancer.

Methods: In vitro antioxidant activity was determined by 2,2-Diphenyl-2-picryl-hydrazyl (DPPH) scavenging activity. 4,4'-M(2,8-DTBP) was identified and quantified by Gas Chromatography-Mass Spectrometry (GC-MS) and High Performance Thin Layer Chromatography (HPTLC) analysis. The docking simulation had been carried out in PyRx 0.8 software. Toxicity studies were performed using ADMETlab 3.0 and ProTox 3.0 prediction tools, respectively. The cytotoxic effects and induction of apoptotic cell death by MEFM and 4,4'-M(2,8-DTBP) on PC-3 cell lines were assessed by MTT(3-(4,5-dimethylthiazol-2-yl)-2,5-diphenyltetrazolium bromide) and annexin V apoptosis assays, respectively.

Results: The HPTLC fingerprint confirmed the presence of 4,4'-M(2,6-DTBP) in the MEFM and indicated its existence in high content. 4,4'-M(2,6-DTBP) exhibited the highest binding energies (-17.1 kcal/mol) and favorable interactions against prostate cancer target proteins. The Absorption, Distribution, Metabolism, Excretion, and Toxicity (ADMET) and toxicity prediction studies revealed that this 4,4'-M(2,6-DTBP) compound had low toxicity and distinct metabolic properties. The MEFM showed strong growth inhibition against PC-3 (IC₅₀: 377.5 µg/ml), whereas 4,4'-M(2,6-DTBP) exhibited weak growth inhibition (IC₅₀: 2324.78 µg/ml). The annexin V assay revealed that the MEFM and 4,4'-M(2,6-DTBP) significantly increased total apoptosis to 41.03% and 22.86%, respectively. In early apoptotic cells, the MEFM and 4,4'-M(2,6-DTBP) caused 40.9% and 19.5% cell death, while in late apoptotic cells, cell death was found to be 0.13% and 3.36%, respectively.

Conclusion: The extract and its bioactive compound demonstrate anticancer potential, but in vivo studies are required to further evaluate efficacy, metabolism, and toxicity in a living system.

Articles In Press [Jul-Aug 2025]
SECTION
Original Article(s)

Copyright (c) 2025 MUDASSIR LAW NEETA RAJ SHARMA, AWADHESH KUMAR VERMA, IBRAHIM HAMZA KANKIA, VETRISELVAN SUBRAMANIYAN, GURMEEN RAKI-



This work is licensed under a <u>Creativ</u> <u>Commons Attribution 4.0 Internationa</u> <u>License</u>.



List of conferences attended

- Certificate of presentation on titled "UV-Vis quantification of 4, 4'-Methylenebis (2,6-DI-tert-butylphenol) from flax microgreens and its inhibitory activity against 5α-Reductase enzyme" International Conference on Current Trends in Toxicology & 43rd Annual Meeting of the Society of Toxicology (ICCTT 2024), India.
- Certificate of oral presentation on titled "GC-MS profile of flax microgreens and molecular identification of its lignans as novel inhibitor of target proteins in prostate cancer" at International Conference on "Recent Advances in Fundamental and Applied Sciences" (RAFAS-2024) funded by SERB (DST, Govt. of India).
- Certificate of participation of the "4th international conference on Recent Advances in Bio-energy Research" (ICRABR-2023) organized by Sardar Swaran Singh National Institute of Bio-energy, Kapurthala, Punjab, India.







List of workshops attended

- 1. Certificate of participation in the one-day Online International Workshop on "RESEARCH METHODOLOGY AND SCIENTIFIC WRITING" held virtually on Wednesday, February 19th, 2025 by Maryam Abacha American University of Nigeria.
- 2. Certificate of learning in the short course on "BIOINFORMATICS COURSE 201" organized by Genomac Institute Inc. I USA Incorporated. October 12, 2024.
- 3. Certificate of participation in the Online International Workshop on "RESEARCH INFORMATICS: A MODULE OF RESEARCH METHODOLOGY" hosted by Maryam Abacha American University of Nigeria. 09 SEPTEMBER 2024.
- 4. Certificate of participation in the one-day Online International Workshop on "ARTICLE PUBLICATION IN REPUTABLE JOURNALS" held virtually on Thursday, April 4th, 2024 by Maryam Abacha American University of Nigeria.









Certificate of Participation

This certificate is presented to

Mudassir Lawal

For participation in the one-day online international workshop on Article Publication in Reputable Journals

> held virtually on Thursday, April 4th, 2024 **by** Maryam Abacha American University of Nigeria

Dr. Habib Awais Abubakar Vice President Administration, MAAUN



Prof (Dr.) Mohammad lerar

Prof. (Dr.) Mohammad Israr The President of MAAUN

Ethical approval certificate



Dutsinma Road, P.M.B 2218 Katsina, Nigeria Tel: +2348066225056, +2347065069482 Website: http://www.umyu.edu.ng

Date: 5th November, 2024

Dear Mudassir

Ethical Approval Letter

We are pleased to certify that the research titled; IDENTIFICATION AND CHARACTERIZATION OF BIOACTIVE COMPOUND FROM FLAX MICROGREENS AND EVALUATION OF ITS PROTECTIVE EFFECT AGAINST TESTOSTERONE-INDUCED PROSTATE CANCER has been approved by UMYU Committee on Animal Use and Care (UMYUCAUC) with approval number: UMYUCAUC/2024/49.

To ensure a seamless experience during the research, we kindly request the following information from you:

Confirmation of Research Work: Please confirm when you are available to start the research work

Requirements: Please inform us of any specific equipment or technical requirements you may need for your research work. We will make every effort to accommodate your requests, ensuring that your research work is carried out effectively.

Should you have any questions or require further assistance, please do not hesitate to contact Dr Ibrahim Hamza Kankia, +2348066225056, email: ibrahim.hamza@umyu.edu.ng.

Thank you

Sincerely,

Dr Ibrahim Hamza Kankia Chairman, Laboratory Committee +2348066225056

Certificate of authentication of collected plant



KEBBI STATE UNIVERSITY OF SCIENCE AND TECHNOLOGY ALIERO FACULTY OF LIFE SCIENCES

DEPARTMENT OF PLANT SCIENCE AND BIOTECHNOLOGY

NO: F (VOUCHER-SPECIMEN-KSUSTA/PSB/11/VOUCHER NO: 657)

DATE: 2-7-2024

VOUCHER-SPECIMEN & IDENTIFICATION CERTIFICATE

This is to certify that **Dr. Gurmeen Rakhra**, a faculty in the department of Biochemistry, School of Pioengineering and Biosciences, Lovely Professional University, Phagwara, Punjab, 144001, India submitted the specimen in our PBS herbarium Kebbi State University of Science and Technology Aliero. The specimen has been identified by undersigned on the basis of morphological characters. The following voucher specimen was issued below:

S/N	species names	Family	Date of collection	Locality	Voucher specimen number
01.	Linum usitatissimum	Linaceae	14/11/2023	Hi-Tech Polyhouse, Lovely Professional University (LPU) Phagwara, Punjab- India	KSUSTA/PSB/H/Voucher No: 657

Prof. Dharmendra Singh

HOD

PSB KSUSTA Part State Niveria